BLACK CARBON STABILITY IN SOIL

A Dissertation

Presented to the Faculty of the Graduate School

of Cornell University

In Partial Fulfillment of the Requirements for the Degree of

Doctor of Philosophy

by

Binh Thanh Nguyen

January 2009

© 2009 Binh Thanh Nguyen

BLACK CARBON STABILITY IN SOIL

Binh Thanh Nguyen, Ph. D.

Cornell University 2009

Black carbon (BC) is the residue from incomplete combustion of biomass and is an important soil C pool. Its role, as a soil C pool and as a potential approach to actively sequestering atmospheric CO_2, greatly depends on its stability, which is likely controlled by environmental conditions, in addition to its intrinsic chemical properties. This dissertation has three research chapters, investigating changes in quantity and quality of BC (i) over decadal time period in cultivated soil; (ii) over an annual time scale as affected by water regimes, or (iii) temperature.

The first chapter investigates long term BC dynamics in cultivated soil, which had been converted to maize cultivation for 100 years. Within the first 30 year since deposition to soil, BC concentrations decreased rapidly, and reached a steady state. Oxidation of BC occurred during the same period of time, which was restricted to its surfaces. The second chapter quantifies BC stability under varying water regimes. Four BC types, produced by charring corn residue or oak wood at either 350 or 600°C, were incubated at 30°C under aerobic, waterlogged and alternating aerobic-waterlogged conditions. BC mineralization, 6-21% for the first year, was significantly greater under aerobic and alternating aerobic-waterlogged conditions than waterlogged conditions. However, these effects of water regime significantly depended on the BC type. BC produced from corn at 350°C showed the greatest C loss and change in properties during aerobic condition, whereas BC produced from oak at 600°C mineralized to a much lower extent during the 1-year incubation. The third chapter focuses on temperature sensitivity of decomposition of the aforementioned four BC materials. In response to increase in incubation temperature, the more stable BC types,

such as oak-BC produced at 600°C, were more sensitive to decomposition than the more labile materials, such as corn-BC formed at 350°C. The temperature coefficient (Q_{10}) decreased with increasing incubation temperature, and ranged from 1.01-5.79.

Mineralization of BC in all three studies were greatly coupled with changes in BC quality, such as molecular chemical functional group chemistry, OH, C=O and aliphatic C-H, and closely related to its initial properties, such as nano- and micro-structure as well as mineral content.

BIOGRAPHICAL SKETCH

Binh Thanh Nguyen was born in Quang Binh Province, a central, coastal region of Vietnam in 1972. He was the eldest in a family of four children, 2 brothers and 2 sisters. His father was an accountant for many years before retiring and his mother is a farmer.

In 1991, he was admitted to Hue University of Agriculture and Forestry to do his bachelors degree in agricultural engineering, for four and half years. After graduation he was offered a research assistant position in the department of Agro-Chemistry and Soil Science at the Rubber Research Institute of Vietnam (RRIV). He participated in a number of projects, focusing on soil conservation and landuse classification as well as fertilizer trials on rubber trees, targeting yield performance of the plant. The institute is unique in Vietnam, performing most research on rubber trees, which is planted mainly in South-East regions.

In 2002, he was awarded a scholarship by the government of Vietnam, known as MOET 322, to do his master program of Soil Conservation and Management at the University of Adelaide – South Australia from January 2003 to August 2004, and earned a MS degree by the end of course period. During this program, he received support from the RRIV and thus was offered a research position at the Institute upon graduation.

In August 2005, he was awarded another scholarship, from the Vietnam Education Foundation (VEF) to pursue a Ph.D. program at Cornell University. Additionally, he also received financial support by the Department of Crop and Soil Sciences – Cornell University and his major advisor, Associate Professor, J. Lehmann for the program.

ACKNOWLEDGMENTS

Firstly, I would like to extend special thanks to my committee, Associate Professor Johannes Lehmann, Professor Susan Riha, and Professor Timothy James Fahey for their invaluable support and instruction during my study. Without the brilliant recommended and sometimes challenging ideas from Dr. Lehmann, I would not have been able to complete this dissertation. I really appreciated what Dr. Lehmann did for me during my time at Cornell University.

I also thank the Chairs of the Department of Crop and Soil Sciences, Professor Stephen Daniel DeGloria and Professor Harold Mathijs Van Es for admitting me to this program and funding from my third year.

I am grateful to my sponsor, Vietnam Education Foundation (VEF) to fully support my first two years. This is a great organization supporting Vietnamese students to do post-graduating programs at US universities and I am very lucky to be a member of this community. Grateful acknowledgement is also given to the Wu Fellowship and Coupled Natural and Human Systems Program of the Biocomplexity Initiative of the NSF under grant BCS-0215890 for financial support.

I have been lucky to be able to work in a large group with diverse and helpful people at the Soil Biogeochemistry lab of Dr. Lehmann. I am indeed thankful to colleagues working at this lab and in the Bradfield building for creating such a friendly and academic environment.

Finally I would like to express my deep respect to my parents, my forever love to my daughter and my wife, and thanks to my close friends in Vietnam and in the USA for their unlimited support and sincere encouragement during my study.

TABLE OF CONTENTS

LIST OF FIGURES

LIST OF TABLES

CHAPTER 1

INTRODUCTION

I.1. Why studying the stability of black carbon (BC)

Black carbon (BC) is the residue of incomplete combustion of biomass. Black C has formed throughout history and anywhere on the Earth where fire is occurring. Prone transportation due to its light, porous and flying properties by water erosion and wind blowing makes BC ubiquitously present in all terrestrial and aquatic ecosystems as well as in the atmosphere.

As a pool of soil organic carbon (SOC), BC, due to its recalcitrant properties, increasingly cumulates in soils, accounting for a considerable portion of SOC, up to 30% in some Australian soils (Skjemstad et al., 1996), 35% in Terra Preta –Brazilian Oxisols (Glaser et al., 2000), and 45% in German Chernozemic soils (Schmidt et al., 1999, 2002). Nevertheless, BC eventually decomposes; otherwise global organic C stocks would be converted to BC within 100,000 years (Goldberg, 1985, p43). Beside its molecular chemical and physical properties, environmental conditions are key determinants of its stability or decomposition. For example, in sea sediment, BC may be present for more than ten thousands of years (Masiello and Druffel, 1998), while under tropical, aerobic conditions, BC may have mean residence times of decades to a century (Bird et al., 1999). As a result, BC stability and longevity are controlled by (i) its properties, determined by charring conditions and BC precursor materials; and (ii) exogenous conditions such as human activity, water regime and temperature.

BC bears many important and interesting features, stimulating research as a material in agricultural and environment sciences. On the one hand, BC amendments to soil may help improving soil fertility and crop performance through (a) mitigating soil

acidification and ameliorating aluminum toxicity in acid soil (Glaser el al., 2002), and (b) improving soil nutrient retention (Glaser el al., 2002) as well as increasing nutrient content such as nitrogen, phosphorus, potassium and calcium (Glaser et al., 2001). On the other hand, because of its recalcitrant properties, converting relatively labile plant residues to relatively stable BC may help combating global warming due to active withdrawal of CO_2 from the atmosphere and long-term storage and sequestration in soil.

I.2. Research questions

The two mentioned important features would be without value if BC were to decompose rapidly. BC stability is a function of its properties and environmental conditions such as cultivation, water regime and temperature. In this dissertation, it is, therefore, that BC stability is investigated through three research chapters, with the following research questions:

1. How do BC quality and quantity change over a centennial timescale in cultivated soil?

2. How does BC mineralize and change in properties in response to different water regimes?

3. How sensitive does BC decomposition respond to increasing temperature?

4. Do BC materials differing in quality respond differently to changes in water regime and temperature?

REFERENCES

Bird, M.I., Moyo, C., Veenendaal, E.M., Lloyd, L., Frost, P., 1999. Stability of elemental carbon in a savanna soil. Global Biogeochemical Cycles 13, 923-932.

Glaser, B., Balashov, E., Haumaier, L., Guggenberger, G., Zech, W., 2000. Black carbon in density fractions of anthropogenic soils of the Brazilian Amazon region. Organic Geochemistry 31, 669-678.

Glaser, B., Haumaier, L., Guggenberger, G., Zech, W., 2001. The 'Terra Preta' phenomenon: a model for sustainable agriculture in the humid tropics. Naturwissenschaften 88, 37–41.

Glaser B., Lehmann, J., Zech, W., 2002. Ameliorating physical and chemical properties of highly weathered soils in the tropics with charcoal – a review. Biology and Fertility of Soils 35, 219–230.

Goldberg, E.D., 1985. Black carbon in the environment. Wiley, New York.

Masiello, C.A., Druffel, E.R.M., 1998. Black carbon in deep-sea sediments. Science 280, 1911–1913.

Schmidt, M.W.I., Skjemstad, J.O., Gehrt, E., Kogel-Knabner, I., 1999. Charred organic carbon in German chernozemic soils. European Journal of Soil Science 50, 351-365.

Schmidt, M.W.I., Skjemstad, J.O., Jager, C., 2002. Carbon isotope geochemistry and nanomorphology of soil black carbon: Black Chernozemic soils in central Europe originate from ancient biomass burning. Global Biogeochemical Cycles 16, Art. No.1123.

Skjemstad, J.O., Clarke, P., Taylor, J.A. Oades, J.M., McClure, S.G., 1996. The chemistry and nature of protected carbon in soil. Australian Journal of Soil Research 34, 251-271.

CHAPTER 2

LONG-TERM BLACK CARBON DYNAMICS IN CULTIVATED SOIL[1]

Abstract

Black carbon (BC) is a quantitatively important C pool in the global C cycle due to its relative recalcitrance compared with other C pools. However, mechanisms of BC oxidation and accompanying molecular changes are largely unknown. In this study, the long-term dynamics in quality and quantity of BC were investigated in cultivated soil using X-ray Photoelectron Spectroscopy (XPS), Fourier-Transform Infrared (FTIR) and Nuclear Magnetic Resonance (NMR) techniques. BC particles and changes in BC stocks were obtained from soil collected in fields that were cleared from forest by fire at 8 different times in the past (2, 3, 5, 20, 30, 50, 80 and 100 years before sampling) in western Kenya. BC contents rapidly decreased from 12.7 to 3.8 mg C g^{-1} soil during the first 30 years following deposition, after which they slowly decreased to a steady state at 3.5 mg C g^{-1} soil. BC-derived C losses from the top 0.1 m over 100 years were estimated at 6,000 kg C ha^{-1}. The initial rapid changes in BC stocks resulted in a mean residence time of only around 8.3 years, which was likely a function of both decomposition as well as transport processes. The molecular properties of BC changed more rapidly on surfaces than in the interior of BC particles and more rapidly during the first 30 years than during the following 70 years. The Oc/C ratios (Oc is O bound to C) and carbonyl groups (C=O) increased over the first 10 and 30 years by 133 and 192%, respectively, indicating oxidation was an important process controlling BC quality. Al, Si, polysaccharides, and to a lesser extent Fe were found on BC particle surfaces within the first few years after BC deposition to soil.

[1] Published as: Nguyen, B.T., Lehmann, J., Kinyangi, J., Smernik, R., Riha, S.J., Engelhard, M.H., 2008. Long-term black carbon dynamics in cultivated soil, Biogeochemistry 89, 295-308.

The protection by physical and chemical stabilization was apparently sufficient to not only minimize decomposition below detection between 30 and 100 years after deposition, but also physical export by erosion and vertical transport below 0.1 m.

II.1. Introduction

Black carbon (BC) is a C-rich organic material derived from incomplete combustion of fossil fuels and vegetation and from weathering of graphitic C in rocks (Schmidt and Noack 2000; Koelmans et al. 2006). BC is most likely ubiquitous in terrestrial and aquatic ecosystems as well as in the atmosphere. It is comprised of a continuum of forms, ranging from slightly charred organic material to highly condensed, refractory soot (Masiello 2004). In this study the term BC is used to describe the residual product from incomplete combustion of biomass either by land clearing or natural forest fires.

It is well known that the global C cycle is closely connected to global climate change largely through anthropogenic emissions of carbon dioxide originating from fossil fuel use and land use change (IPCC 2007). An increase in temperature of about 0.8 K was related to increases in carbon dioxide concentrations of 77 ppmv in the last century (Bala et al. 2005). BC may influence global C cycles and climate directly and indirectly. Direct effects involve adsorption of solar radiation by soot aerosols (Jacobson 2001). The indirect effects are the removal of carbon dioxide from rapid biosphere-atmosphere gas exchange through the formation of BC during fires. It remains largely unknown to what extent BC decomposition contributes to carbon dioxide emissions from soils and how recalcitrant this temporary C sink is (Koelmans et al. 2006; Preston and Schmidt 2006).

One of the distinguishing properties of BC is its high stability in the environment relative to other types of organic C substances. It can persist up to 13,900 years in

deep-sea environments (Masiello and Druffel 1998) and was found to have a mean residence time of 10,000 years in soils (Swift 2001). In comparison, typical turnover times of soil organic matter were 6 to 20 years in surface horizons (Torn et al. 2005) and those of fine litter were 1.3 years in natural tropical forests (Weerakkody and Parkinson 2006). Consequently, BC gradually accumulates in soils, relative to other organic substances, and thus becomes a quantitatively important portion of soil organic matter.

However, we also know that BC must eventually decompose as global production and stocks do not match if BC is assumed inert (Schmidt 2004; Schmidt and Noack 2000). Information about turnover times of BC is scarce and most data are available from decomposition experiments over a limited number of years (Preston and Schmidt 2006). Measured decay rates varied significantly between 0.26 to 0.78% C losses over the first 60 days of incubation, largely due to different BC properties (Hamer et al. 2004), and remained below 2% C loss for 120 days of incubation (Baldock and Smernik 2002). Extrapolation from laboratory experiments to natural environments is hampered by inadequate simulation of long-term dynamics (Lehmann 2007) and lack of consideration of all factors affecting BC disappearance such as soil fauna and flora, wetting and drying cycles and leaching. One of the few field experiments reported a disappearance of 47% of biomass-derived BC from savanna fires during 50 years (Bird et al. 1999). Similar to laboratory experiments, however, such field observations are relatively short-term studies compared to the estimated turnover time of up to 10,000 years (Swift 2001; Masiello and Druffel 1998). While some information is available about temporal dynamics of BC stocks in unmanaged ecosystems (Preston and Schmidt 2006), very few studies report results from agricultural soil (Skjemstad et

al. 2001). Therefore, observations of BC dynamics in cultivated soil over several decades to centuries are needed to begin to quantify BC loss processes.

During exposure in soil, BC not only gradually disappears as it mineralizes to CO_2, leaches or erodes as dissolved and particulate organic C, but BC particles are also chemically altered due to surface oxidation and interactions with non-BC (Liang et al. 2006). Brodowski et al. (2005) found that the O/C ratios were higher near the surface than the interior of BC particles in a German Chernozem, suggesting that oxidation of BC had occurred, starting from the surface of the particles. Such surface oxidation can occur over short periods of time and is able to significantly increase cation exchange capacity of BC particles and soils rich in BC within a few months (Cheng et al. 2006). Whether surface oxidation is further increased beyond a period of months or whether interior regions of BC particles are oxidized to the same degree as surfaces over decadal and centennial time scales is not known.

This study investigates changes in BC residence time and quality in cultivated soil over a period of 100 years. We hypothesize that an initial rapid disappearance of BC is followed by lower losses and that surfaces of BC are oxidized rapidly during the first few years, whereas oxidation of entire BC particles is significantly slower.

II.2. Materials and Methods

II.2.a. Study sites

Details of the experimental sites that are part of a larger study were reported by Solomon et al. (2007) and Kimetu et al. (2008). The study sites used in the present work were located in South Nandi (00º 04' 30" N, 34º 58' 34" E), western Kenya, with altitudes ranging from 1600 to 1800 m above sea level, mean annual temperature of

about 19°C and mean annual precipitation of about 2000 mm. Soils were classified as Humic Nitosols (FAO/UNESCO) or Typic Palehumults (USDA), which were extremely deep dark reddish brown soils with friable clay and thick humic topsoils with 45-49% clay, 15-25% silt, and 26-40% sand (Kimetu et al. 2008).

II.2.b. Soil collection and preparation

Slash and burn had been used at the experimental site to convert the native forest to cultivated soils during the past hundred years. Forest trees were cut and burned on site during conversion. After conversion, the soil was plowed to 0.1 - 0.12 m depth for maize (Zea mays L.) cultivation without fertilizer application. Although most of the biomass C was transformed to carbon dioxide during the biomass burning and rapidly released into the atmosphere, a small amount of C was charred and remained in soil as BC after conversion (Forbes et al. 2006). Burning was not practiced on fields following the initial conversion. Therefore, ages of BC correspond to the time since conversion from forest to agriculture, making use of different conversion ages to construct a time series or chronosequence of BC ages (Solomon et al. 2007; Kimetu et al. 2008). A subset of the soil samples from the southern Nandi forest series (Solomon et al. 2007) was selected for this study to examine the long-term BC dynamics.

Table II.1. Basic properties and information of the studied soils

Years since BC deposition	Carbon (%)	Nitrogen (%)	C/N	Bulk density (Mg m^{-3})
0	9.18	0.95	9.69	0.67
2	7.56	0.73	10.32	0.70
3	6.74	0.72	9.30	0.80
5	4.62	0.49	9.42	0.80
20	2.74	0.29	9.53	1.00
30	2.58	0.29	9.00	1.06
50	1.39	0.15	9.18	1.12
80	1.39	0.15	9.27	1.12
100	2.32	0.24	9.85	1.12

Soil sampling and preparation were described in detail by Solomon et al. (2007). In brief, 18 soil samples were collected in 2003 from 18 farmer's fields differing in their conversion ages ranging from 2 to 100 years prior to sample collection, in comparison to forest soil in southern Nandi, Kenya. We selected fields within a 12-km^2 area with similar climate, geology and soil type. Nine 200-cm^3 core sub-samples from the upper 0.1 m of soil were sampled in each field and then combined into one composite soil sample. The samples were then air-dried, sieved (<2 mm) and stored for analysis. The 18 soil samples were pooled into 8 composite samples based on their conversion ages (100, 80, 50, 30, 20, 5, 3, 2 years before sampling) corresponding to 8 ages of BC, in comparison to a forest soil (Table II.1).

II.2.c. BC preparation

BC particles from these 9 soil samples were separately hand-picked for FTIR and XPS analyses using super tweezers (N5, Dumont, Montignez, Switzerland) under a light microscope (303; SMZ-10, Nikon, Japan). BC particle sizes ranged from 5-90 μm. Two size classes of BC particles (<30 and >50 μm) were separated for FTIR scanning. In addition, a fresh BC sample, which was produced by natural combustion of the same native forest biomass, was also collected under field condition for comparison. The fresh BC sample was measured by FTIR 4 weeks after production.

II.2.d. BC quantification

NMR analysis

BC concentrations of bulk soils were estimated from spectra of solid-state ^{13}C Cross Polarization-Magic Angle Spinning Nuclear Magnetic Resonance (^{13}C CP-MAS NMR) using the "molecular mixing model" developed by Nelson and Baldock (2005). In brief, this technique converts distributions of signal across chemical shift regions to distributions of biopolymers (carbohydrate, protein, lignin and aliphatic biopolymers) plus BC and pure carbonyl. In all cases a good fit was achieved, as demonstrated by a small "error" term of 1.1 to 4.3, as defined in Nelson and Baldock (2005).

Prior to NMR analysis, soil samples were treated with 2% HF acid, following the procedure proposed by Skjemstad et al. (1994). Solid-state ^{13}C CP NMR spectra were recorded at a frequency of 50.3 MHz on a Varian Unity 200 spectrometer (Varian Inc., Palo Alto, CA). Samples were packed in a 7-mm-diameter cylindrical zirconia rotor with Kel-F end-caps and spun at 5000±100 Hz in a Doty Scientific MAS probe.

Manual isolation

Approximately 5 g of each soil sample was weighed for hand-picking of BC particles using the same method described for BC preparation above. All soil BC particles, which were visualized under such light microscopy, were collected and then used for C analysis.

II.2.e. FTIR procedure

Fourier Transformation Infrared (FTIR) absorbance spectra were recorded on a Mattson Model 5020 FTIR Spectrometer (Madison, WI) at wave numbers from 400 to 4000 cm^{-1}. KBr pellets were prepared containing 0.3% wt of finely ground BC powder. One hundred scans were averaged with a resolution of 4 cm^{-1} by subtracting values obtained from pure KBr pellets. Carbon chemical functional groups were assigned to wave numbers from FTIR spectra following Solomon et al. (2007). Wave numbers were assigned as follows: 3370 cm^{-1} to hydroxyl (O-H) groups of phenols with traces of amine (N-H), 2920 – 2853 cm^{-1} to aliphatic-C (CH_3 and CH_2), 1700 cm^{-1} to carbonyl-C and ketonic-C (C=O), 1642 cm^{-1} to aromatic-C (C=C) vibrations and to a smaller extent to C=O stretching in quinones and ketonic acids, 1389 cm^{-1} to aliphatic deformation of CH_2 or CH_3 groups, and 1036 cm^{-1} to C-O stretching vibrations of polysaccharides.

Each BC sample was analyzed in duplicate, and the results were averaged. Relative proportions (%) of C chemical species, such as O-H, C-H, C=O, C=C and C-O were obtained from corresponding spectrum intensities, which were measured by establishing individual base lines for each peak position. Using Omnic software, version 7.2 (Thermo Electron Corporation, 1992-2005) we located wavenumbers associated with detected peaks assigned to the C chemical species listed above after

base line correction and normalization. Base lines were drawn as follows: 3747-2975 cm^{-1} for O-H, 2991-2769 cm^{-1} for C-H vibration at 2920-2853 cm^{-1}, 2735-1670 cm^{-1} for C=O, 1733-500 cm^{-1} for C=O, 1488-1348 cm^{-1} for C-H vibration at 1389 cm^{-1} and 1315-946 cm^{-1} for C-O.

II.2.f. X-ray photoelectron spectroscopy

X-ray Photoelectron Spectroscopy (XPS) was used to characterize surfaces of BC particles in comparison to the properties of the interior of BC particles. Both intact BC particles for determining surface properties and finely ground powder for bulk properties of the same BC sample were analyzed by XPS. The maximum depth that XPS can probe is about 10 nm, allowing it to distinguish between surface and bulk properties using the analysis scheme described here. BC samples of both intact and ground powder were mounted onto Scotch brand double-sided tape and placed onto specifically designed samples holders for XPS analysis. Care was taken to mount a uniform and densely packed continuous layer of particles. The sample holder was then placed into the XPS vacuum introduction system and pumped to $<1x10^{-6}$ Torr using a turbomolecular pumping system prior to introduction into the main ultra high vacuum system. The main vacuum system pressure is maintained at $<5x10^{-9}$ Torr during analysis and pumped using a series of sputter ion pumps.

XPS measurements were performed using a Physical Electronics Quantum 2000 Scanning ESCA Microprobe (Physical Electronics, Chanhassen, MN, USA, a divison of ULVAC PHI). This system uses a focused monochromatic Al Kα X-ray (1486.7 eV) source and a spherical section analyzer. The instrument has a 16-element multichannel detector. The X-ray beam used was a 100 W, 100 μm diameter beam that was rastered over a 1.4 mm by 0.2 mm rectangle on the sample. The X-ray beam is

incident normal to the sample and the photoelectron detector was at 45° off-normal. Wide scan data were collected using a pass energy of 117.4 eV. Narrow scan or high energy resolution spectra of C1s, O1s, Fe2p, Al2p and Si2p were collected using a pass energy of 46.95 eV.

II.2.g. Quantification of elemental proportions and C species from XPS spectra

XPS spectra were deconvoluted to separately identify C-bonded O species and different C forms. Deconvolution was accomplished with the non-linear least squares curve fitting program XPSPEAK Version 4.1. The procedure was described in detail by Cheng et al. (2006). C1s binding energy levels were assigned as follows: at 284.6 eV to C-C, C=C, and C-H bonds, at 286.2 eV to C–O, at 287.6 eV to C=O, and at 289.1 eV to COO. Oxygen bonded to C (Oc) was computed using the sum of all organic O species. Elemental contents are given as relative proportions of all five investigated elements (C, O, Si, Al, Fe) and contents of C species were reported as relative proportions of all four deconvoluted C species.

II.2.h. Statistical Analyses

Dynamics of BC stocks, C species obtained by FTIR and elemental proportion recorded by XPS as a function of time (years) after BC deposition, were calculated using a first order kinetic model with 3 parameters $f = Y_0 + ae^{-bt}$ and $f = Y_0 + a(1-e^{-bt})$, where f is the BC content at time t (year), Y_o is the BC content at time zero, a is a constant and b is a reaction rate constant, applied for decay and rise observations, respectively. Linear regression was conducted to test the correlation coefficients between BC stocks and elemental contents. Statistical analyses were done with Sigma Plot 8.0 and Microsoft Excel.

II.3. Results

II.3.a. Dynamics of BC stocks over 100 years of cultivation

BC entered these soils both from fires predating land conversion and from the burning that occurred when land was converted to agriculture. Irrespective of the origin of the BC, BC concentrations per unit soil mass decreased rapidly to 30% of their initial contents during the first 30 years as estimated by NMR, while by manual quantification, BC stocks decreased to 16% of their initial contents during the first 5 years (Fig. II.1). Corresponding BC stock losses per unit area were 60 and 89% of their initial stocks for NMR and manual quantification, respectively (Figs. II.1E and II.1F). The stocks were calculated based on BC contents and bulk density in the top 0.1 m layer. Beyond 30 years, BC stocks leveled off close to a steady state. BC losses after 100 years totaled about 6000 kg C ha^{-1} to a depth of 0.1 m determined by NMR quantification. Macro BC particles, whose sizes, as defined here, were greater than 50 μm, were not observed beyond 30 years. The proportion of BC as a fraction of SOC showed a weak ($P>0.05$) trend to increase over time since deposition (Figs. II.1C and II.1D).

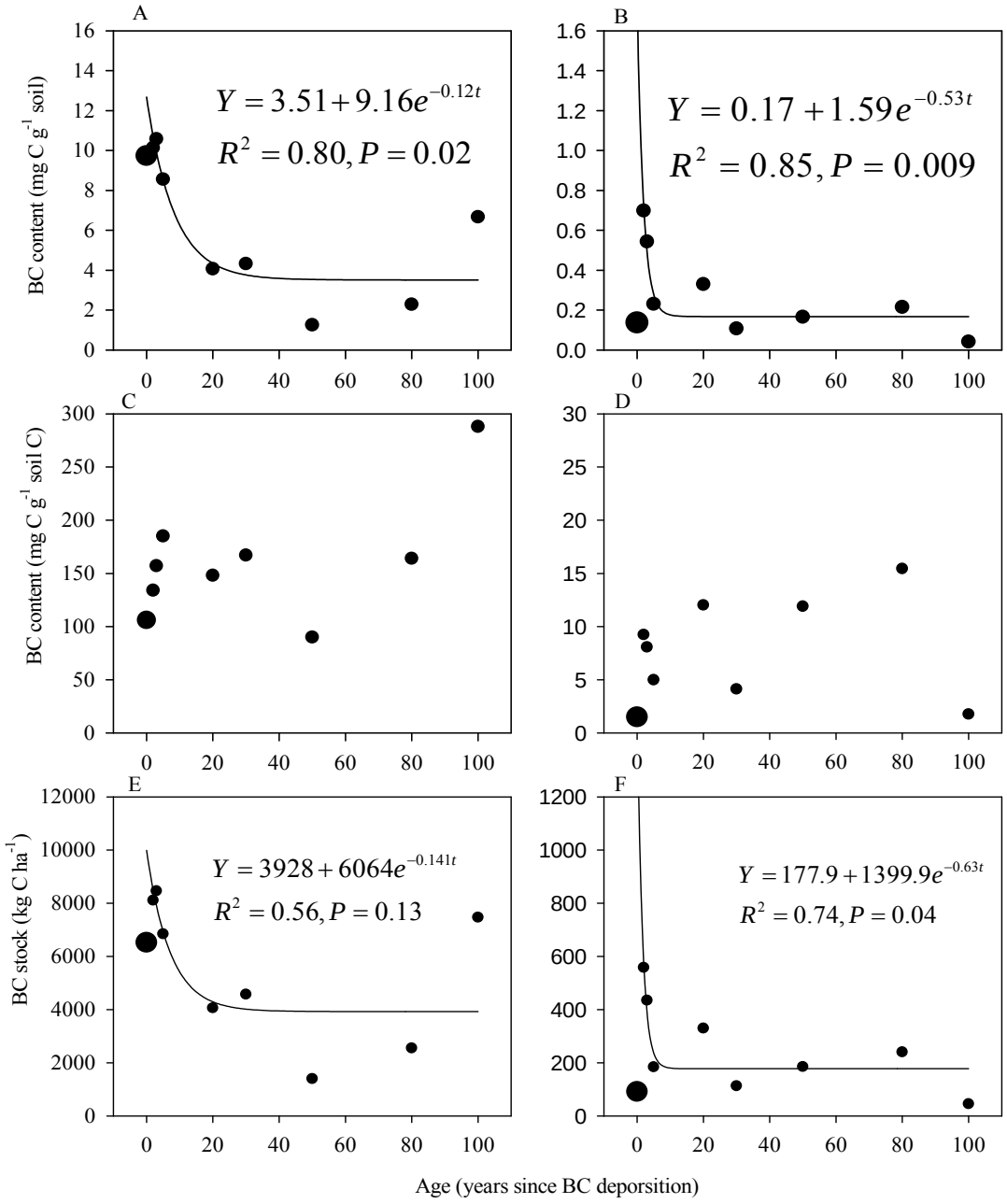

Figure II.1. Long-term dynamics of BC contents and stocks determined by NMR (A, C, E) and by manual (B, D, F) quantification over 100 years. The large circles denote BC contents of forest soil. First order kinetics were fitted, based on BC contents and stocks derived from 8 cultivated soil samples. BC stocks were calculated for a soil depth of 0.1 m

II.3.b. BC properties by XPS investigation

Carbon and oxygen contents of isolated BC particles

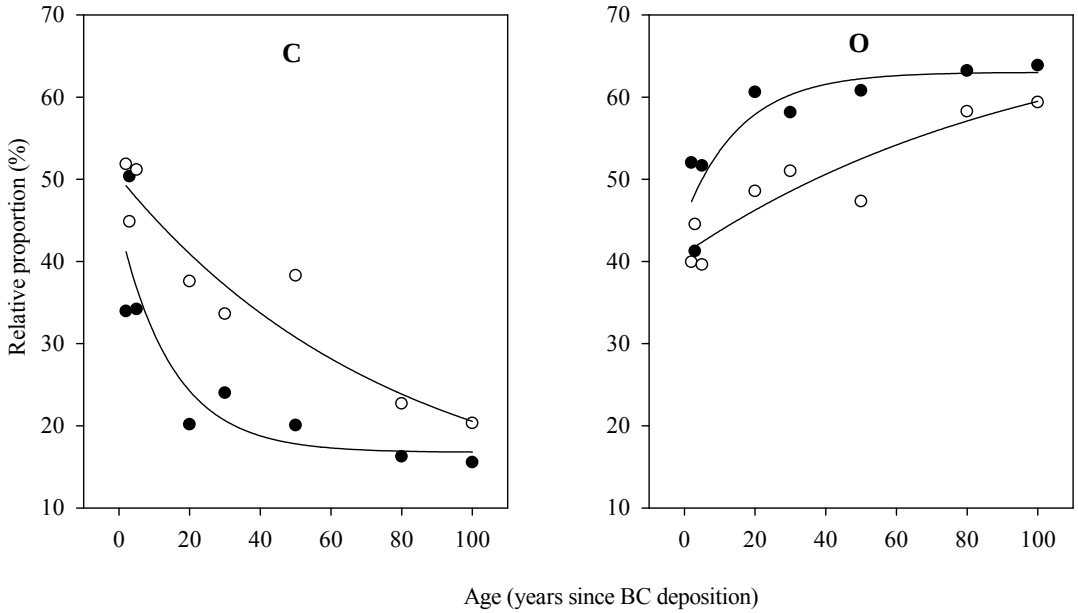

Figure II.2. Quantitative dynamics of O (including mineral and organic O) and C of BC surfaces and entire BC particles by XPS over 100 years in cultivated soil. Solid black circles are the observations of surfaces of BC particles, while open circles are observations of bulk properties of BC particles

Carbon contents, recorded for BC surfaces and for entire particles, decreased from 44.6 to 18.8% and from 51.1 to 34.2%, respectively, during the first 40 years since conversion (Fig. II.2). In contrast, total O contents rapidly increased from 45.2 to 61.5% on BC surfaces and from 40.9 to 50.6% in entire particles during the same period of time. Surface properties of both C and O changed more rapidly than those of bulk properties. Beyond 40 years following conversion, C and O proportions of bulk properties continued to change, while those of surface properties leveled off at around 18.8% for C and 61.5% for O after the initially rapid change in the first 40 years.

Consequently, the largest difference between bulk and surface properties with respect to C and O contents was observed in the period of 20 to 40 years following conversion. In comparison, the elemental contents collected 3 years after BC deposition were similar between surface and bulk properties. After 100 years, the C contents of the entire BC particles (22%) approached the C contents of BC surfaces (19%). Correspondingly, the O contents were still slightly higher on BC surfaces (63%) than in the entire particle (58%) after 100 years. To mathematically quantify changes in elemental contents of BC, a first order kinetic model was applied to the XPS data (Table II.2). The rate of change (b) for O and C contents on BC surfaces was 6 times higher than the rate for the entire particles.

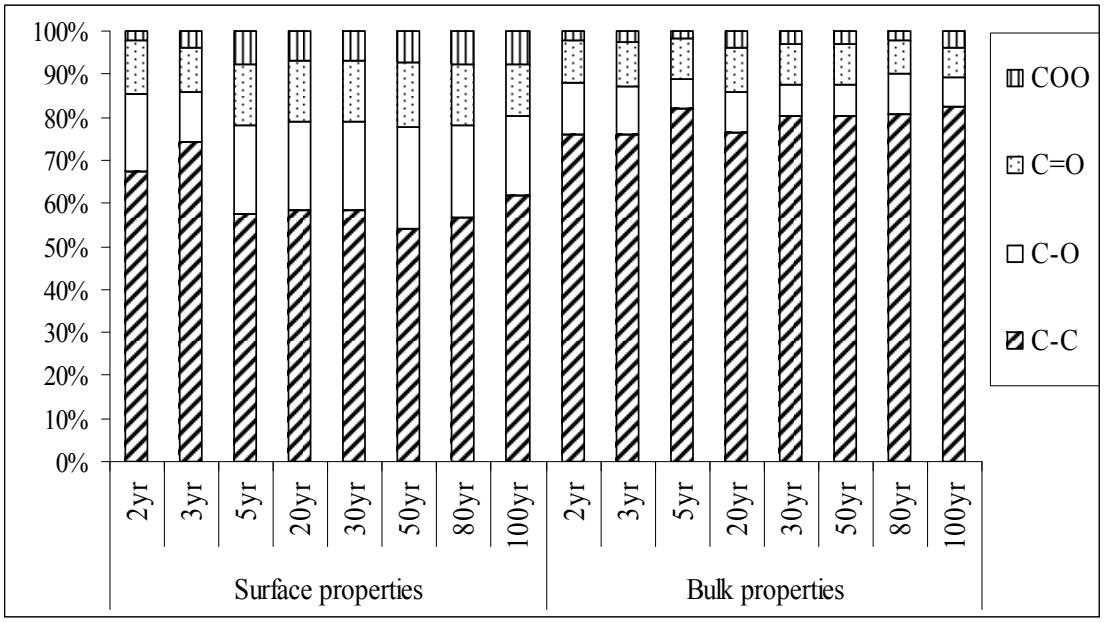

Figure II.3. Carbon chemical species from XPS spectra of BC surfaces and entire BC particles, quantified by deconvolution of XPS spectra

Surfaces of BC contained more oxidized functional groups than entire particles, most of which were C-O and C=O groups (Fig. II.3). Carboxyl C on BC surfaces (COO) increased rapidly within the first 5 years, in contrast to entire BC particles. Total

oxidized functional groups increased over time on BC surfaces, but remained constant for entire BC particles. Similar trends were observed when calculating O/C ratios for O bound to C using the deconvolution results (Fig. II.4). These Oc/C ratios of BC surfaces increased rapidly in the first five years since deposition and were higher than those recorded for entire particles, which showed no change in their Oc/C ratios over time.

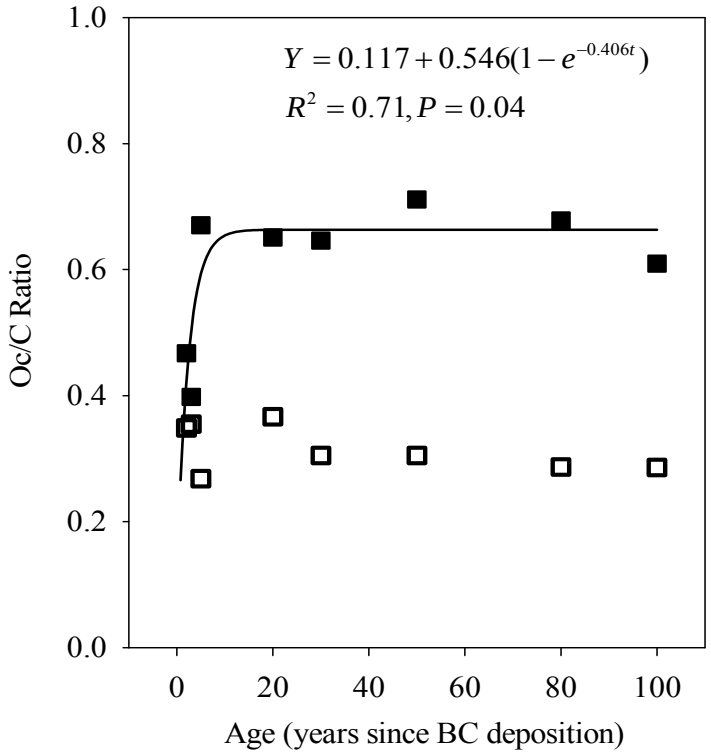

Figure II.4. Oc/C ratios of surface and entire BC particles based on deconvolution results (only O bound to C, denoted by Oc). Solid black squares were the observations of BC surfaces and open squares those of entire BC particles

Table II.2. Model parameters of quantified elements on BC surfaces and in entire BC particles as a function of time (years) since deposition. A first order kinetic model was fitted. A decay curve of $f = Y_0 + ae^{-bt}$ was applied for C and a rise curve of $f = Y_0 + a(1 - e^{-bt})$ was applied for O, Al, Si and Fe.

Elements	Properties of	b	a	Y_0	R^2	P
C	Surface	0.0657	27.8	16.8	0.79	0.020
	Bulk	0.0129	41.9	9.2	0.90	0.003
O	Surface	0.0622	17.8	45.2	0.79	0.02
	Bulk	0.0100	29.3	40.9	0.88	0.005
Al	Surface	0.1279	4.2	3.7	0.73	0.04
	Bulk	0.0489	3.5	3.3	0.82	0.01
Si	Surface	0.0636	4.9	5.5	0.79	0.02
	Bulk	0.0254	5.4	4.2	0.93	0.001
Fe	Surface	0.0095	2.6	0.7	0.87	0.006
	Bulk	0.0029	8.9	0.9	0.95	0.0006

II.3.c. Aluminum, iron and silicon of isolated BC particles

The dynamics of Al and Si on BC surfaces and entire particles over 100 years were similar to that of O, and increased with time. The increases were more rapid on surfaces than in the entire particles. 30 years following deposition, Al contents were about 7.8% for surfaces and 6% for the entire particles, while Si contents were 9.7% for surfaces and 7.1% for the entire particles (Fig. II.5). Beyond 30 years, Al and Si

contents of the entire particle continued to increase, while those of BC surfaces leveled off. Elemental contents of Al and Si of the entire particles approached those of BC surfaces after 100 years, yet remained slightly lower. Fe contents were generally low (below 3%) compared to the other investigated elements (Fig. II.5). Fe contents in both bulk and surface properties slightly and constantly increased over the entire period of 100 years.

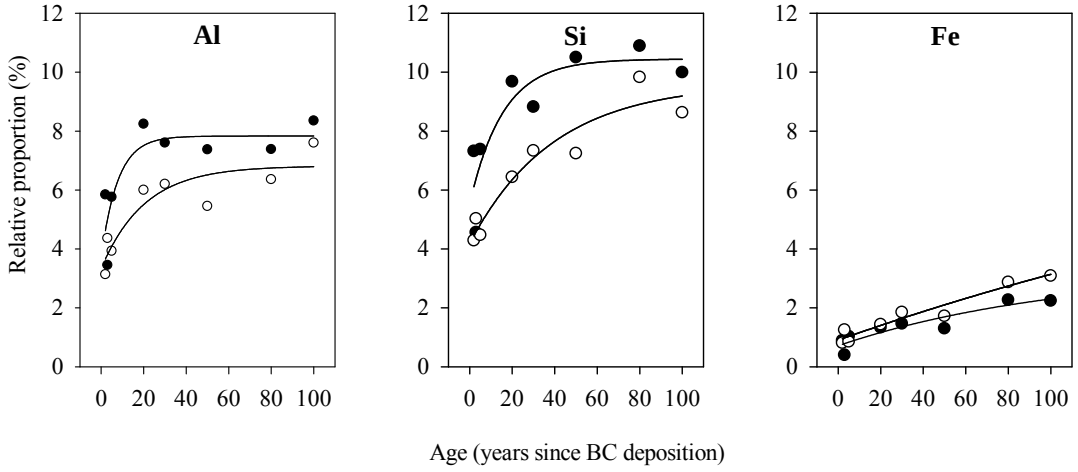

Figure II.5. Dynamics of Al, Fe and Si on BC surfaces (filled circles) and in entire BC particles (open circles) over 100 years

Similar to C and O, the rate of change (b) for BC surfaces was also higher for Al, Si and Fe than the rate for the entire particles, albeit only by a factor of three (Table II.2). This result again indicated that changes in elemental contents of surface properties were faster than those of the entire particles.

II.3.d. Carbon chemical speciation of isolated BC particles by FTIR analysis

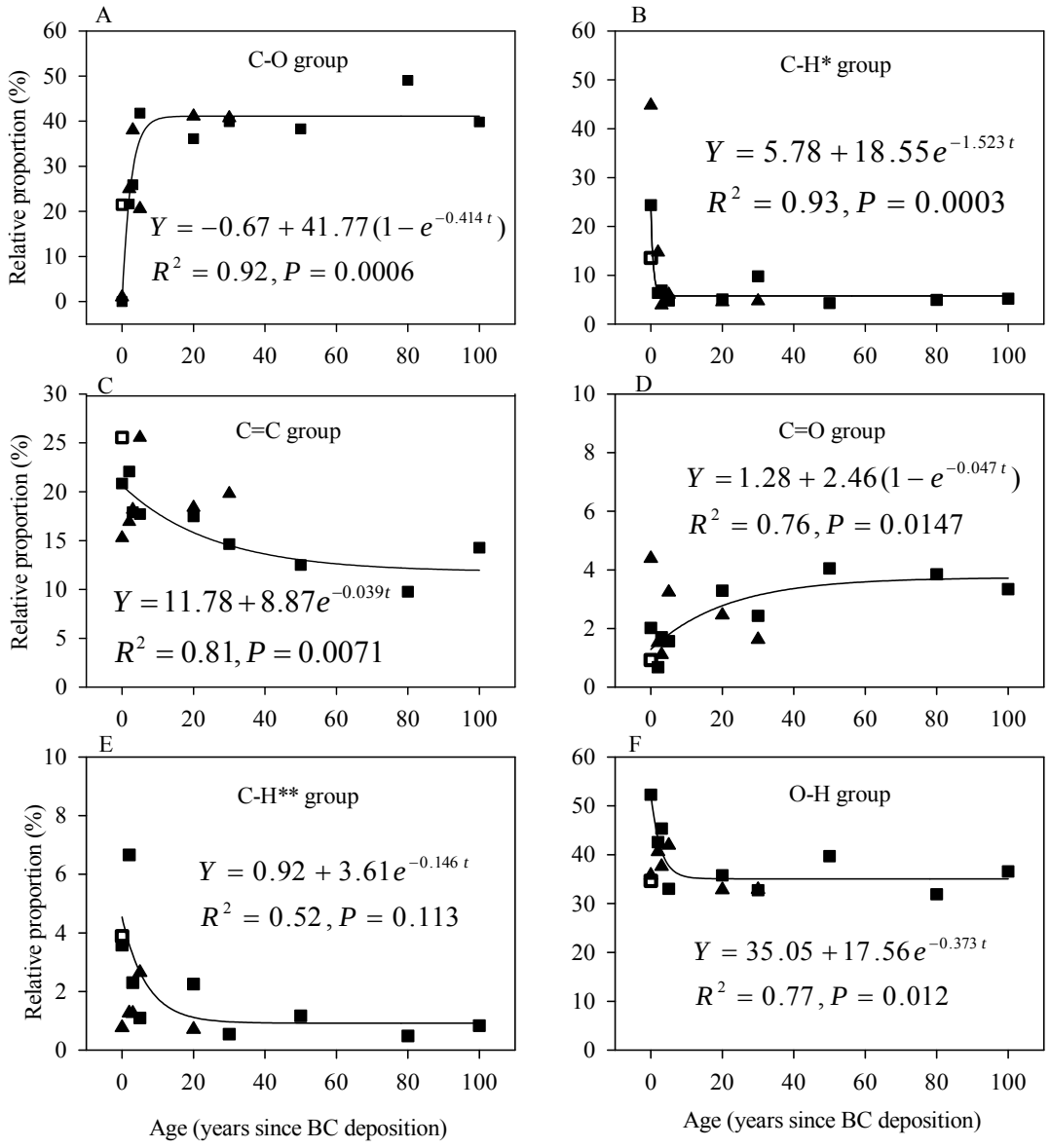

Figure II.6. Dynamics of C functional groups characterized by FTIR of micro-particle (solid squares) and macro-particle BC (solid triangles). The curves were fitted, based only on spectrum intensities of micro-particle BC samples from 8 cultivated soil samples and the fresh BC sample. The open square denotes the observation of forest soil BC. (*) aliphatic C-H vibrating at 1389 cm^{-1}. (**) C-H of asymmetric and symmetric CH_3 and CH_2 groups vibrating at 2910 cm^{-1}

The relative proportions of aromatic groups (C=C) detected at 1642 cm^{-1}, aliphatic C-H at 1389 cm^{-1} and 2920 cm^{-1} and hydroxyl group (O-H) at 3370 cm^{-1} decreased, while C-O at 1036 cm^{-1} and carbonyl groups (C=O) at 1700 cm^{-1} rose over 100 years (Fig. II.6). Of the six C chemical species, the relative proportion of aliphatic C-H at 1389 cm^{-1} decreased the most from 24.3 to 5.8% during the first 5 years and remained at this proportion, while aliphatic C-H groups vibrating at 2920 cm^{-1} decreased more slowly to a very low content of 1.1% after 20 years. O-H of phenols decreased to 35.5% while C-O group of polysaccharides increased rapidly to 40.4% during the first 10 years. Carbonyl changed at a slower rate towards a steady state from 1.3 to 3.7% and aromatic groups from 20.7 to 12.0% during the first 90 years after BC deposition. Chemical C species changed at a similar rate irrespective of the size of the BC particles, whether small (<30 μm) or large (50-2000 μm) (Fig. II.6).

II.4. Discussion

II.4.a. BC production

Based on NMR quantification, and the first order kinetic model (Fig. II.1E), BC stocks at deposition were estimated to be approximately 10,000 kg C ha^{-1}, compared to 6500 kg C ha^{-1} at the forest site. The difference of 3500 kg C ha^{-1} of BC can be interpreted as BC residues derived from incomplete combustion of aboveground forest biomass during forest conversion. Aboveground C stocks in similar East African highland forests were reported to be about 330 ± 65 Mg C ha^{-1} (Glenday 2006). Consequently, an estimated 0.9 to 1.3% of the initial forest C was converted to BC and deposited to soil. This is in good agreement with other studies. Preston and Schmidt (2006) reported a BC production of 1-3% of biomass C by combustion. Forbes et al. (2006) documented average proportions of 0.7 to 2.9% of the initial biomass C that remained

after fires in tropical forests, and Schmidt and Noack (2000) proposed a maximum conversion rate of 1.8 ± 0.2% when burning efficiently.

II.4.b. BC losses from cultivated topsoil over 100 years

BC contents were found to lie in the range of 1 – 11 mg C g^{-1} soil or 10 - 29% of total organic C by NMR and from 0.1 to 0.7 mg C g^{-1} soil or 0.15-1.54% of total organic C by manual quantification (Figs. II.1A, II.1B, II.1C and II.1D). These results were comparable to other studies. In agricultural soils in the US, Skjemstad et al. (2002) showed soil BC contents ranging from 1.8 to 13.6 mg C g^{-1} soil or 10 - 35% of total organic C using the UV-NMR method which captures a similar range of BC forms as the NMR method used here. In Siberian Scots pine forests, Czimczik et al. (2003) found mean BC concentrations of 4.0 and 13.5 mg g^{-1} soil for unburned and burned sites, respectively, using a molecular marker method for BC quantification. Manual quantification commonly underestimates BC contents (Forbes et al. 2006), because small particles cannot be identified and removed under a light microscope. Consequently, in this study manual quantification resulted in 93-95% lower estimates of BC contents than NMR quantification.

Soil BC contents and stocks decreased rapidly in the first 30 years following conversion and leveled off afterwards (Figs. II.1A, II.1B, II.1E, and II.1F). Such a dynamic was also reported by Gavin et al. (2003), who showed an exponential decrease in BC mass with increasing time since the last forest fire. In our study, the dynamics of BC contents could be separated into two phases of different disappearance rates. The first phase of 30 years is characterized by a rapid loss of BC by 70% from the topsoil. The second phase of the last 70 years had a slower loss rate,

where BC contents decreased very slowly to gradually approach the steady state at 3.5 mg C g^{-1} soil or 3,900 kg C ha^{-1} determined by NMR quantification.

The losses observed in this study can be explained by both a decomposition of BC to CO_2 as well as by a physical export below the sampled soil horizon or laterally by erosion. Erosion losses are presumed to be low in the present experiment, since flat landscape positions were selected to minimize lateral soil export. Long-term losses by erosion or vertical transport were low since BC stocks did not decrease beyond 20 years. Shortly after the fire event, however, a certain proportion of BC was likely lost by transport from the topsoil due to low interaction with the mineral matter. Enrichment of BC in subsurface horizons of anthropogenic soils have been reported by Glaser et al. (2000) and Schmidt et al. (1999), although it is not clear whether this was a result of bioturbation, illuviation or direct BC deposition to the subsurface horizon. Dai et al. (2005) concluded that the proportion of BC to total SOM increases with soil depth. They proposed a mechanism of mass movement of BC with clay and silt and accumulation in deeper soil horizons. Relocation of BC to deeper horizons was also one of the reasons that Czimczik et al. (2003) proposed to explain the low topsoil contents of BC in their study and export of BC from watersheds in dissolved form has been found at multiple locations (Hockaday et al. 2007; Guggenberger et al. 2008).

The combination of decomposition and lateral as well as vertical export below a depth of 0.1 m during the first years after BC deposition explains the short mean residence time of 8.3 years, calculated from the inverse of the rate of disappearance (Fig. II.1A). This mean residence time is much shorter than estimates from ^{14}C ages of 2400 to 13,900 years in ocean sediments (Masiello and Druffel 1998), 5,000 years in soils (Skjemstad et al. 1998), half life of 6,623 years in a coastal temperate rain forest of

western Vancouver (calculated by Preston and Schmidt 2006 from Gavin et al. 2003), and of decades to centuries of BC from grass fires in well-aerated tropical savanna soil in Zimbabwe (Bird et al. 1999).

In addition to a physical redistribution within the landscape, the initial phase of rapid BC losses may be the result of rapid mineralization of an easily degradable portion of BC material, which could be decomposed by biotic and abiotic mechanisms. Biotic mechanisms primarily include the activity of heterotrophic soil microorganisms (Hamer et al. 2004), and plant root activities, while abiotic mechanism such as chemical oxidative reactions may also be involved (Middelburg et al. 1999).

Despite the possibility of a rapid mineralization of the labile fraction of BC, decomposition of BC appeared to be slower than decomposition of other C. Another study performed on the same samples described here (Solomon et al. 2007) showed a rapid depletion of 46 to 73% SOC within the first 4 years following conversion. In the current study, we observed a 33% slower change in total BC contents (with a rate of 0.12 $year^{-1}$, Fig. II.1A) than a change in total C remaining (with a rate of 0.16 $year^{-1}$; from Solomon et al. (2007)). Therefore, BC was conserved to a greater extent than other C in the studied soils. Enrichment of BC as a fraction of total organic C with increasing time of continuous cultivation was also found by Skjemstad et al. (2001) in Australia. Similarly, the proportion of BC increased with increasing oxidation over time in marine sediments (Middelburg et al. 1999).

Following the first phase of around 30 years, most of the remaining BC material may have undergone two processes apart from physical export: (a) the labile portion of the BC continuum may have decomposed (Hamer et al. 2004), leaving a BC material behind that is more recalcitrant to decomposition (Bird et al. 1999); and (b) BC

material was likely incorporated into the soil matrix, and thus was physically protected within aggregates (Brodowski et al. 2006) or even by interactions with mineral surfaces. Furthermore, the initially large BC particles may have broken down into small particles by physical pressure derived from agricultural operations, such as plowing, or by earthworm activity, which ingest BC and defecate casts containing small BC fragments (Ponge et al. 2006). The physical breakdown is confirmed by the ratio of BC contents determined by NMR and manual quantification. According to the first order kinetic model, BC stocks determined by NMR were about 7 times higher than those obtained by manual quantification shortly after BC deposition, but were 23 times higher than those obtained by manual quantification after 30 years. This means during the first 30 years, a large amount of BC particles was broken down into particles <5 μm, which could not be identified under the light microscope. In fact we did not recognize any BC particles > 50 μm under the light microscope in soil samples after more than 30 years. The small, broken BC particles, which were more likely to be encapsulated by adsorption to soil components (Krull et al. 2003), further facilitated physical protection of BC materials. This argument is also supported by the fact that elemental Al, Si and Fe were increasingly found on BC surfaces over the course of 100 years (Fig. II.5). As a result, less BC material would be available for decomposition, and thus much slower BC losses were observed beyond the first 30 years. The protection by physical and chemical stabilization was apparently sufficient to minimize either decomposition or physical export by erosion and vertical transport below 0.1 m or both beyond 30 years.

II.4.c. Changes in BC oxidation

The much more rapid oxidation of surfaces exemplified by greater Oc/C ratios of the BC surfaces than of the interior of BC particles (Fig. II.4) is in agreement with other

studies. Brodowski et al. (2005) also observed an increasing O/C ratio from interior to exterior by SEM-EDX. Cheng et al. (2006) concluded from an incubation experiment that oxidation started at surfaces of BC particles. They further stated that the interior of BC particles would be gradually oxidized with long BC exposure in soil. However, our data show that even after 100 years, the Oc/C ratios of the entire BC particle did not increase (Fig. II.4). Oc/C ratios of BC surfaces increased rapidly during the first 5 years and then leveled off at a high level of O, while that of bulk properties was lower and stable during 100 years since BC deposition (Figs. II.3 and II.4). Oxidation increased apparently following an exponential behavior and started from surfaces of particles.

The Oc/C ratios determined by deconvolution of XPS spectra of BC surfaces in our study ranging from 0.4 to 0.7 are higher than the threshold of 0.33 that was proposed to distinguish BC from non-BC by Brodowski et al. (2005), while those of entire BC particles, ranging from 0.27 to 0.37 are comparable to such a ratio. Discounting surface oxidation and adsorption of non-BC, our results suggest an Oc/C ratio of 0.3 for fire-derived and aged BC obtained from soils including only O bonded to C (from deconvolution of XPS data), which agrees well with results from 11 sites in the Eastern U.S. (Cheng et al. 2008).

II.4.d. Molecular changes of BC

Changes in BC properties were also observed in the functional group composition of C-O, C-H, C=C, C=O and O-H (Fig. II.6). Within the first 20 years, aliphatic C-H groups rapidly decreased to a very low proportion, below 1% for C-H vibrating at around 2920 cm^{-1} and below 6% for C-H vibrating at 1389 cm^{-1}. Cheng et al. (2006) also observed a significant decrease in intensity of aliphatic groups vibrating around

2900 cm^{-1} after 4 months of incubation of BC at 30 and 70°C. Cody and Alexander (2005) explained their observations of a selective loss of aliphatic groups to chemical oxidation reactions, which transformed aliphatic groups to either CO groups or soluble organic acids and CO_2. They also pointed out that environmental oxidative potential could be enhanced by the abundance of iron in solution. This argument seems relevant to the present study which showed an increasing abundance of Fe on BC particles.

After 90 years, carbonyl groups (C=O) increased by a factor of 2.8 (from 1.3 to about 3.6%), with a much slower rate of change relative to aliphatic C-H groups. Presumably, this resulted from partial conversion of C-H and/or C=C to C=O, while some BC was completely converted to CO_2 by oxidation. A predominant band at 1036 cm^{-1}, assigned to C-O groups which are mainly derived from polysaccharides of plant litter adsorbed on BC particles, was also observed. Within the first 10 years since conversion the proportion of C-O groups increased dramatically from zero in fresh BC material to almost 41% (Fig. II.6A). Cheng et al. (2006) also observed a distinct band at 1035cm^{-1}, which they attributed to the sorption of organic matter from added manure. The abrupt increase in C-O groups in our study could therefore be a result of sorption of organic matter to BC. Cornelissen et al. (2005) concluded that carbonaceous geosorbents, including BC, could adsorb as much as 10 to 100 times more organic substances than could amorphous organic matter. The third predominant band, assigned to aromatic groups, was observed with a relative proportion of 12% after 90 years. The only slowly decreasing proportion of C=C groups, by 8% over 90 years, was an indication of their high stability and low penetration of oxidation into the BC particles.

Since BC surfaces were highly oxidized as determined by XPS, one could have expected small BC particles to be more oxidized than large particles as determined by

FTIR. However, both small and large BC particles had similar molecular chemical properties. This may be explained by a very thin layer of oxidized C on BC surfaces that is sufficiently masked by bulk analyses as obtained by FTIR and do therefore not reflect differences between those sizes of BC particles investigated here. A preferential leaching loss of less oxidized BC as shown by Leifeld et al. (2007) for soot in comparison to larger char particles is unlikely able to explain the observed increase in oxidation, as only char was sampled here with particle sizes that are much larger than condensation products from combustion.

II.4.e. Interactions of BC with soil mineral matter

Si and Al quickly associated with BC surfaces (Fig. II.5) in the first 30 years, followed by slow rates, with which Al and Si contents approached a steady state. Unlike Al and Si, Fe contents were similar both on BC surfaces and in entire particles, and increased only slightly over time. These dynamics of interaction between mineral elements and BC could be interpreted as evidence for BC encapsulation, and thus physical protection by soil mineral adsorption. Similarly, Brodowsky et al. (2006) found a large proportion of BC protected within aggregates. This indicates that soil mineral adsorption may play an important role in slowing down BC losses both by decomposition as well as by physical export in the second phase after 30 years as argued above.

II.4.f. BC surface oxidation and sorption

There were at least two processes causing the BC dynamics in the soils described here: oxidation and non-BC sorption. These two mechanisms developed proportionally and rapidly in the first few years since BC deposition. The increases in elemental O and carbonyl groups (Figs. II.2 and II.6) with time are indicators of oxidation of BC, the

rate of which decreased over time. The Oc/C ratios of BC surfaces were found to be higher than those of entire BC particles (Fig. II.4), confirming our hypothesis that BC particles were oxidized, beginning from the outside of particles. This is in agreement with other authors (Brodowski et al. 2005; Lehmann et al. 2005; Cheng et al. 2006). Kawamoto et al. (2006) observed an increase in O/C ratios of BC after treatment with ozone occurring on the edges of hexagonal C layers. Liang et al. (2006) showed a dramatic increase in O/C ratios from interior (0.01–0.02) to surfaces (0.09–0.19) of BC particles using a microprobe, indicating a higher level of oxidation on the surface than in the interior of BC particles.

Oxidation may either mineralize BC to CO_2 or change the BC into other organic C forms containing more O. In either case, we found a significant negative correlation, -0.78 and -0.79 ($P<0.001$), between surface Oc/C ratios and both BC stocks or C of BC surfaces, respectively, suggesting that oxidative degradation was likely one of the most important processes controlling BC stock dynamics. We also found that absolute correlation coefficients between BC stocks and elemental contents were higher for BC surfaces than for entire particles, indicating that dynamics of BC stocks were related to oxidation dynamics on surfaces of BC particles. As a result of increasing oxidation, charge density of BC particles likely increased, resulting in more polar non-BC substances to be adsorbed to surfaces of BC particles (Liang et al. 2006; Cheng et al. 2006). Consequently, elemental contents of O on BC surfaces and thus surface oxidation likely derived from both oxidized BC materials and non-BC adsorbed organic materials. Compared to the ratio found here for entire particles of 0.27-0.37 and to the one suggested by Brodowski et al. (2005) of 0.33 for BC, the higher O/C ratios, from 0.4 to 0.7, observed for BC surfaces after 5 years since deposition in our study, also suggest adsorption of non-BC organic materials or oxidation of BC to non-

BC. It can not be fully excluded that preferential leaching or erosion of certain types of BC created the observed dynamics, but is unlikely given the nature of the change. For example, the increasing surface oxidation of BC isolated from the topsoil is unlikely a result of preferential export of unoxidized BC, since mobile BC found in pore water and streams is typically not the least oxidized fraction (Hockaday et al. 2007; Guggenberger et al. 2008).

Adsorption of non-BC materials on BC surfaces could be an important process reducing the oxygen-exposed surface area of BC particles and consequently oxidation potential. The increasing sorption of non-BC organic and inorganic substances on BC materials was suggested by the occurrence of C-O groups indicative of polysaccharides (Fig. II.6A) and by the relative proportion of Al, Si and Fe (Fig. II.5), which rapidly increased during the first few years since BC deposition. Consequently, the increasing adsorption of non-BC materials on surfaces of BC in our study may accelerate physical protection of BC in soil and thus increases protection of BC against oxidation and then decomposition.

II.5. Conclusions

BC stocks decreased rapidly within the first 30 years after deposition and leveled off afterwards. The change in BC stocks likely involved a number of processes, including decomposition, erosion and transport below the depth of observation. Oxidation may degrade BC material, but adsorption of organic and inorganic materials may increase protection of BC against decomposition by reducing air-exposed surface area of BC particles and oxidative degradation. Changes in BC properties over time were found to be highly correlated with BC quantity, indicating that changes in BC quantity and quality occurred concurrently. Oxidation and non-BC adsorption were identified to

control BC dynamics over the hundred years of observation. However, the molecular processes by which non-BC or minerals interacted with BC surfaces remained unclear. Also other soil processes such as an encapsulation of BC by soil particles through aggregation may have contributed to the long-term stability of BC. In addition, physical export played a role but was not quantified separately and warrants further research.

REFERENCES

Bala, G., Caldeira. K., Mirin, A., Wickett, M., Delire, C., 2005. Multicentury changes to the global climate and carbon cycle: Results from a coupled climate and carbon cycle model. Journal of Climate 18, 4531-4544.

Baldock, J.A., Smernik, R.J., 2002. Chemical composition and bioavailability of thermally, altered Pinus resinosa (Red Pine) wood. Organic Geochemistry 33, 1093-1109.

Bird, M.I., Moyo, C., Veenendaal, E.M., Lloyd, L., Frost, P., 1999. Stability of elemental carbon in a savanna soil. Global Biogeochem Cycles 13, 923-932.

Brodowski, S., Amelung, W., Haumaier, L., Abetz, C., Zech, W., 2005. Morphological and chemical properties of black carbon in physical soil fractions as revealed by scanning electron microscopy and energy-dispersive X-ray spectroscopy. Geoderma 128, 116– 129.

Brodowski, S., John, B., Flessa, H., Amelung, W., 2006. Aggregate-occluded black carbon in soil. European Journal of Soil Science 57, 539-546.

Cheng, C.H., Lehmann, J., Thies, J.E., Burton, S.D., Engelhard, M.H., 2006. Oxidation of black carbon by biotic and abiotic processes. Organic Geochemistry 37, 1477-1488.

Cheng, C.H., Lehmann, J., Engelhard, M.H., 2008. Natural oxidation of black carbon in soils: Changes in molecular form and surface charge along a climosequence. Geochim Cosmochim Acta 72, 1598-1610.

Cody, G.D., Alexander, C.M.O., 2005. NMR studies of chemical structural variation of insoluble organic matter from different carbonaceous chondrite groups. Geochim Cosmochim Acta 69, 1085-1097.

Cornelissen, G., Gustafsson, O., Bucheli, T.D., Jonker, M.T.O., Koelmans, A.A., Van Noort, P.C.M., 2005. Extensive sorption of organic compounds to black carbon, coal, and kerogen in sediments and soils: Mechanisms and consequences for distribution, bioaccumulation, and biodegradation. Environmental Science & Technology 39, 6881-6895.

Czimczik, C.I., Preston, C.M., Schmidt, M.W.I., Schulze, E.D., 2003. How surface fire in Siberian Scots pine forests affects soil organic carbon in the forest floor: Stocks, molecular structure, and conversion to black carbon (charcoal). Global Biogeochem Cycles 17, 1020.

Dai, X., Boutton, T.W., Glaser, B., Ansley, R.J., Zech, W. 2005. Black carbon in a temperate mixed-grass savanna. Soil Biology & Biochemistry 37, 1879–1881.

Forbes, M.S., Raison, R.J., Skjemstad, J.O., 2006. Formation, transformation and transport of black carbon (charcoal) in terrestrial and aquatic ecosystems. Science of the Total Environment 370, 190-206.

Gavin. D.G., Brubaker, L.B., Lertzman, K.P., 2003. Holocene fire history of a coastal temperate rain forest based on soil charcoal radiocarbon dates. Ecology 84, 186–201.

Glaser, B., Balashov, E., Haumaier, L., Guggenberger, G., Zech, W. 2000. Black carbon in density fractions of anthropogenic soils of the Brazilian Amazon region. Organic Geochemistry 31, 669-678.

Glenday, J., 2006. Carbon storage and emissions offset potential in an East African tropical rainforest. Forest Ecology and Management 235, 72-83.

Guggenberger, G., Rodionov, A., Shibistova, O., Grabe, M., Kasansky, O.A., Fuchs, H., Mikheyeva, N., Zrazhevskaya, G., Flessa, H., 2008. Storage and mobility of black carbon in permafrost soils of the forest tundra ecotone in Northern Siberia. Global Change Biology 14, 1367-1381.

Hamer, U., Marschner, B., Brodowski, S., Amelung, W., 2004. Interactive priming of black carbon and glucose mineralization. Organic Geochemistry 35, 823–830.

Hockaday, WC., Grannas, A.M., Kim, S., Hatcher, P.G., 2007. The transformation and mobility of charcoal in a fire-impacted watershed. Geochim Cosmochim Acta 71, 3432-3445.

IPCC, 2007. Climate change 2007: the physical science basis. contribution of Working Group I to the Fourth Assessment Report of the Intergovernmental Panel on Climate Change. Cambridge Univ Press, Cambridge, UK.

Jacobson, M.Z., 2001. Strong radiative heating due to the mixing state of black carbon in atmospheric aerosols. Nature 409, 695.

Kawamoto, K., Ishimaru, K., Imamura, Y., 2005. Reactivity of wood charcoal with ozone. Journal of Wood Science 51, 66-72.

Kimetu, J.M,, Lehmann, J., Ngoze, S.O., Mugendi, D.N., Kinyangi, J.M., Riha, S., Verchot, L., Recha, J.W., Pell, A.N., 2008. Reversibility of soil productivity decline with organic matter of differing quality along a degradation gradient. Ecosystems 11, 726-739.

Koelmans, A.A., Jonker, M.T.O., Cornelissen, G., Bucheli, T.D., Van Noort, P.C.M., Gustafsson, O.R., 2006. Black carbon: The reverse of its dark side. Chemosphere 63, 365–377.

Krull, E.S., Baldock, J.A., Skjemstad, J.O., 2003. Importance of mechanisms and processes of the stabilization of soil organic matter for modeling carbon turnover. Functional Plant Biololy 30, 207-222.

Lehmann, J., Liang, B., Solomon, D., Lerotic, M., Luizão, F., Kinyangi, F., Schäfer, T., Wirick, S., Jacobsen, C., 2005. Near-edge X-ray absorption fine structure (NEXAFS) spectroscopy for mapping nano-scale distribution of organic carbon forms in soil: application to black carbon particles. Global Biogeochem Cycles 19, GB1013.

Lehmann, J., 2007. Bio-energy in the black. Frontiers in Ecology and the Environment 5, 381-387.

Leifeld, J., Fenner, S., Müller, M., 2007. Mobility of black carbon in drained peatland soils. Biogeosciences 4, 425-432.

Liang, B., Lehmann, J., Solomon, D., Kinyangi, J., Grossman, J., O'Neill, B., Skjemstad, J.O., Thies. J., Luizão, F.J., Petersen, J., Neves, E.G., 2006. Black carbon increases cation exchange capacity in soils, Soil Science Society of America Journal 70, 1719-1730.

Masiello, C.A., Druffel, E.R.M., 1998. Black carbon in deep-sea sediments. Science 280, 1911-1913.

Masiello, C.A., 2004. New directions in black carbon organic geochemistry. Marine Chemistry 92, 201-213.

Middelburg, J.J., Nieuwenhuize, J., Breugel, P.V., 1999. Black carbon in marine sediments. Marine Chemistry 65, 245–252.

Nelson, P.N., Baldock, J., 2005. Estimating the molecular composition of a diverse range of natural organic materials from solid-state ^{13}C NMR and elemental analyses. Biogeochemistry 72, 1–34.

Ponge, J.F., Topoliantz, S., Ballof, S., Rossi, J.P., Lavelle, P., Betsch, J.M., Gaucher, P., 2006. Ingestion of charcoal by the Amazonian earthworm Pontoscolex corethrurus: A potential for tropical soil fertility. Soil Biology & Biochemistry 38, 2008-2009.

Preston, C.M., Schmidt, M.W.I., 2006. Black (pyrogenic) carbon: a synthesis of current knowledge and uncertainties with special consideration of boreal regions. Biogeosciences 3, 397-420.

Schmidt, M.W.I., Skjemstad, J.O., Gehrt, E., Kögel-Knabner, I., 1999. Charred organic carbon in German chernozemic soils. European Journal of Soil Science 50, 351-365.

Schmidt, M.W.I., Noack, A.G., 2000. Black carbon in soils and sediments: Analysis, distribution, implications, and current challenges. Global Biogeochemical Cycles 14, 777-793.

Schmidt, M.W.I., 2004. Carbon budget in the black. Nature 427, 305-307.

Skjemstad, J.O., Clarke, P., Taylor, J.A., Oades, J.M., Newman, R.H., 1994. The Removal of Magnetic-Materials from Surface Soils - a Solid-State C-13 Cp/Mas Nmr-Study. Australian Journal of Soil Research 32, 1215-1229.

Skjemstad, J.O., Janik, L.J., Taylor, J.A., 1998. Non-living soil organic matter: what do we know about it? Australian Journal of Experimental Agriculture 38, 667-680.

Skjemstad, J.O., Taylor, J.A., Smernik, R.J., 1999. Estimation of charcoal (char) in soils. Communications in Soil Science and Plant Analysis 30, 2283-2298.

Skjemstad, J.O., Dalal, R.C., Janik, L.J., McGowan, J.A., 2001. Changes in chemical nature of soil organic carbon in Vertisols under wheat in south-eastern Queensland. Australian Journal of Soil Research 39, 343-359.

Skjemstad, J.O., Reicosky, D.C., Wilts, A.R., McGowan, J.A., 2002. Charcoal carbon in US agricultural soils. Soil Science Society of America Journal 66, 1249-1255.

Solomon, D., Lehmann, J., Kinyangi, J., Amelung, W., Lobe, I., Pell, A., Riha, S., Ngoze, S., Verchot, L., Mbugua, D., Skjemstad, J.O., Schäfer, T., 2007. Long-term impacts of anthropogenic perturbations on dynamics and speciation of organic carbon in tropical forest and subtropical grassland ecosystems. Global Change Biollogy 13, 511-530.

Swift, R.S., 2001. Sequestration of carbon by soil. Soil Science 166, 858–871.

Torn, M.S., Vitousek, P.M., Trumbore, S.E., 2005. The influence of nutrient availability on soil organic matter turnover estimated by incubations and radiocarbon modeling. Ecosystems 4, 352-372.

Weerakkody, J., Parkinson, D., 2006. Input, accumulation and turnover of organic matter, nitrogen and phosphorus in surface organic layers of an upper montane rainforest in Sri Lanka. Pedobiologia 50, 377-383.

CHAPTER 3

BLACK CARBON STABILITY UNDER VARYING WATER REGIMES

Abstract

The stability of biomass-derived black carbon (BC) or biochar as a slow cycling pool in the global C cycles is an important property, and is likely governed by environmental conditions. This study investigated the effects of water regimes (aerobic, waterlogged and alternating aerobic-waterlogged conditions) and differences in BC materials, produced by carbonizing corn residues and oak wood at two temperatures (350°C and 600°C) on BC degradation at 30°C over one year in a full factorial experiment. Effects of water regimes on C loss and potential cation exchange capacity (CECp at pH7) significantly depended on biomass types. Corn BC both mineralized (16% C loss for the first year) and oxidized (1000 mmole(+) kg C^{-1}) significantly faster under aerobic conditions than other water regimes, whereas oak BC mineralized most rapidly (12%) under alternating aerobic-waterlogged conditions with similar oxidation irrespective of water regime. During one year of waterlogged incubation, the O/C ratios did not significantly ($P>0.05$) increase even though BC was mineralized by 9% and CECp increased by 170 mmole(+) kg C^{-1}, in contrast to aerobic and alternating aerobic-waterlogged conditions. While mineralization and oxidation significantly decreased at higher charring temperature for corn, no difference was observed for oak ($P>0.05$). Aerobic and alternating conditions increased carboxylic and OH functional groups, while they decreased aliphatic groups. The pH increased by about one unit for corn-BC, but decreased by 0.2 units for oak-BC, indicating strong mineral dissolution of corn-BC. Carbon loss strongly correlated with changes in O/C ratios of both corn BC and oak BC, indicating that BC oxidation was most likely the major mechanism controlling BC stability. However, under

waterlogged conditions, additional mechanism may govern BC degradation and require further investigation.

III.1. Introduction

Black carbon (BC) is a general term used to describe products derived from incomplete combustion of vegetation and fossil fuels (Schmidt and Noack, 2000). It is a continuum of C forms rather than a particular compound. BC can form through two different pathways of either recondensation of volatiles forming graphitized soot-BC or of incomplete combustion leaving behind solid residues (Schmidt and Noack, 2000). This study focused on the product derived from the latter process.

BC constitutes a considerable proportion of soil organic C (SOC), being as much as 30% in some Australian soils (Skjemstad et al., 1996), up to 35% in Terra Preta – Brazilian Oxisols (Glaser et al., 2000) and up to 45% in German Chernozemic soils (Schmidt et al., 1999, 2002). Since estimates of the annual global production of BC, 0.04-0.19 $\times$ 10^{15}g (Kuhlbusch, 1998), are much lower than global net primary production, 56 $\times$ 10^{15}g C (Zhao et al., 2005), BC must be much more stable relative to other soil organic matter forms. Therefore, BC is assumed to have long mean residence time of possibly up to 10,000 years in soils (Swift, 2001). As a result, BC may play a considerable role in sequestering C, and thus merits studying in the light of recently reported global warming due to increasing carbon dioxide concentration in the atmosphere.

Even though BC appears to be relatively stable, it must eventually mineralize. Otherwise, global organic C stocks would be converted to BC on Earth's surface within 100,000 years (Goldberg, 1985, p43). Glaser et al. (2002) concluded that BC was decomposable but its turnover was much slower than that of other soil organic

substances. Slow BC decomposition in soils and sediments occurs through (i) microbial degradation (Shneour, 1966; Baldock and Smernik, 2002; Hamer et al., 2004) and (ii) abiotic oxidation (Cheng et al., 2006; Cohen-Ofri et al., 2006). O/C ratios (Brodowski et al., 2005; Liang et al., 2006) and carboxyl functional groups (Lehmann et al., 2005; Liang et al., 2006) were higher on surfaces of BC particles than in their interior. Hamer et al. (2004) suggested that some microbes were able to use BC as the sole C source. Moreover, Hofrichter et al. (1999) concluded that an enzyme, manganese peroxidase, released from ligninolytic basidiomycetes, a wood and leaf litter-decaying fungi, was able to decompose brown coal, indicating that BC could be degraded by microbes.

BC was found to persist in marine sediments for 13,900 years (Masiello and Druffel, 1998), while was estimated to have mean residence times of only decades to one century in well-aerated, tropical soil (Bird et al., 1999), indicating that water regimes may play an important role in BC degradation. Soil normally undergoes alternating drying and rewetting following seasonal weather changes or during cycles of rain events and dry spells, resulting in natural alternation of aerobic and waterlogged conditions. The cycles of drying and rewetting have been reported to influence SOM decomposition (Soerensen, 1974), nutrient availability (Birch, 1958; Halverson et al., 2000; Nguyen and Marschner, 2005) and microbial activity (Gestel et al., 1993). Similarly, the alternation of aerobic and waterlogged conditions may affect BC degradation to a greater extent than any single, constant phase. However, such effects have not yet been reported.

In addition to environmental conditions, BC degradation may also be determined by its quality, mainly as a result of charring temperature and the type of biomass. Based on BC characterization using infrared spectroscopy and thermogravimetry, Labbe et

al. (2006) concluded that BC properties were determined by both plant species and carbonization temperatures. Hamer et al. (2004) reported that BC derived from corn stover and rye was mineralized more rapidly than those derived from wood, indicating the importance of plant materials. In addition, increasing the charring temperature up to 350°C decreased BC mineralization over 120 days of incubation (Baldock and Smernik, 2002). Whether different types of BC as a function of both charring temperature and biomass type respond differently to both aerobic and waterlogged environments, has not been reported.

Therefore, the current study was conducted to address these knowledge gaps by investigating the response of different BC materials to varying water regimes. We hypothesized that (i) BC decomposition and oxidation are slower under waterlogged than aerobic and alternating waterlogged-aerobic conditions; (ii) BC materials higher in mineral content (as a function of biomass type) and are less stable than materials lower in mineral content.

III.2. Materials and methods

III.2.a. BC preparation

Corn stover residue (*Zea mays* L.) and oak shavings (*Quercus* ssp.) were carbonized at two temperature levels, 350 and 600°C, to produce 4 BC materials (corn-350-BC, corn-600-BC, oak-350-BC and oak-600-BC) using slow pyrolysis (Daisy Reactor, Best Energies, Inc., Cashton, WI, USA). We used the BC produced at these temperatures because they constitute the lowest and highest temperatures that are conventionally used in slow pyrolysis (Brown, 2009) and maximum temperatures typically observed in fires under natural conditions (Gibson et al., 1990). The reactor was fitted with paddles for thorough mixing the feedstock to ensure homogenous

charring. Approximately 3 kg of feedstock were manually placed into the main chamber, which was thoroughly purged with N_2 (with the mixer running). The pre-dried material (<10% moisture) was isothermically charred for 80 – 90 minutes, including rising temperature to the target with a few degrees per minute and holding at final temperature for 15-20 minutes. After completion of the pyrolysis, the propane was turned off and the main chamber was allowed to cool before scooping the BC under N_2 purge for use. We then slightly ground the BC to pass 2 consecutive 2-mm and 0.5-mm sieves and BC particles remaining on the 0.5-mm sieve were collected into separate plastic bags and stored in a desiccator for the incubation experiment. Initial properties of the BC are shown in Table III.1.

III.2.b. Water holding capacity

A mixture of 19 g of pure, white sand (Sigma Aldrich No. 274739, -50 +70 mesh ; ignited at 500°C for 24 hours) and 1 g of BC material were weighed on a funnel covered with Whatman No.1 filter paper. The BC-sand mixture was mixed well and saturated with distilled water. After free draining until no additional water loss was recorded, the water content was determined by taking the difference in weight of the filter paper and BC-sand mixture before and after oven drying at 105°C for 24 hours. In addition a Whatman filter paper-covered funnel without any sand and BC was also prepared as a control. Water content held by the filter paper was subtracted. The measured water holding capacity of the BC-sand mixtures was: 44% for corn-350-BC, 42% for corn-600-BC, 40% for oak-350-BC and 34 % for oak-600-BC.

Table III.1. Initial properties of BC materials

Biomass types	Charring temp. (°C)	Elemental content (%)											C/N	O/C	H/C	CECp[a]	pH[b]
		C	N	O	H	K	Ca	Fe	Si	Mn	Others	Sum					
Corn residue	350	67.5	0.9	25.1	4.74	1.04	0.27	0.05	0.02	0.006	0.50	100.2	73	0.37	0.07	610	5.88
	600	79.0	0.92	16.3	2.52	0.67	0.31	0.08	0.03	0.008	0.49	100.3	86	0.21	0.03	215	6.71
Oak wood	350	75.9	0.10	19.6	4.27	0.11	0.07	0.003	0.02	0.000	0.03	100.1	759	0.26	0.06	131	4.84
	600	88.4	0.12	9.0	2.13	0.22	0.09	0.13	0.01	0.004	0.06	100.2	737	0.10	0.02	89	4.91

[a]CECp = Potential Cation Exchange Capacity in mmole(+)kgC^{-1}

[b]pH in 1:20 w:v water

III.2.c. Microbial and nutrient solution

We extracted 2 L of microbial solution from a surface soil sample (0 – 0.2 m) taken from a site of a historical charcoal blast furnace in Cartersville, Georgia, that was used by Cheng et al. (2008a). The soil sample had high BC contents, which was the remnant of wood charcoal, deposited to the soil between the 1830s and 1864 during the operation of a blast furnace for iron production. We expected the soil microbial community to be well adapted to the presence of BC after a long-term exposure to this BC-rich environment. As the soil sample had been stored at 5°C after sampling, it was incubated at 30°C for 2 weeks to activate the microbial community. The microbial extraction was done by adding 25 g of the soil to 2 L of distilled water, slightly shaking for 30 minutes and filtering through a Whatman No.1 filter paper. Nutrients were added to the solution to give 4 mM NH_4NO_3, 4 mM $CaCl_2$, 2 mM KH_2PO_4, 1 mM K_2SO_4, 1 mM $MgSO_4$, 25 μM $MnSO_4$, 2 μM $ZnSO_4$, 0.5 μM $CuSO_4$, and 0.5 μM Na_2MoO_4 (Cheng et al., 2006). The amounts of added nutrients (N, K, Ca, Fe), as a proportion of those contained in BC materials are shown in Table III.2.

Table III.2. Proportion (%) of added nutrients to those in BC materials

Biomass type	Charring temperature (°C)	N	K	Ca	Fe
Corn residue	350	0.56	0.60	2.37	0.009
	600	0.56	0.93	2.07	0.006
Oak wood	350	5.34	5.67	9.14	0.149
	600	4.48	2.84	7.11	0.003

III.2.d. Experimental design

A completely randomized factorial experiment with 8 replicates and 3 factors was set up. About 19 g of pure sand was weighed into 60-mL glass bottles, to which 1 g of ground BC material was added. The bottles received 2 mL of microbial nutrient solution and were incubated in a 30°C-controlled room. No further nutrients were added during incubation. Carbon concentrations in the 1:19 BC:sand mixtures were as follows: 3.38% for corn-350-BC and 3.98% for corn-600-BC, 3.82% for oak-350-BC and 4.45% for oak-600-BC.

At the beginning of the experiment, we initiated three different water regimes: (a) Constantly aerobic conditions, here defined as 60% of water holding capacity. The mixture in the bottles was brought to 60% of water holding capacity with deionised water, and kept constant during incubation. (b) Constantly waterlogged conditions, here defined as submerged in water. The mixture in the bottles was fully submerged in deionized water, and kept constant during incubation. The water level was about 20 – 30 mm higher than the level of the BC-sand mixture. (c) Alternating aerobic-waterlogged conditions. The water regime in the mixture was subjected to periodical change from aerobic to waterlogged conditions. We started with the waterlogged phase by adding distilled water to the bottles to about 150% of water holding capacity which led to submerged conditions. The waterlogged phase continued for about 7-9 days and water in the bottles was then allowed to rapidly evaporate, leading to the aerobic phase. After 2 weeks, when water contents decreased to approximately 30-40% of water holding capacity, we began a new cycle by re-submerging the mixture and adjusting to 150% water holding capacity. These cycles were repeated continuously for one year.

For improving the accuracy of the water maintenance, we placed 8 bottles of the same water treatment in a plastic tray, which was partially covered with aluminum foil. Distilled water was added to the trays. We covered the trays containing incubations under alternating aerobic-waterlogged conditions to accelerate water evaporation to reach aerobic condition within 7-9 days. We created 5 small holes in the covered aluminum foil of the aerobic and waterlogged treatments for appropriate air exchange. Water status in the plastic trays and of the mixture in bottles was monitored weekly by weighing and adding an appropriate amount of distilled water.

By the end of the one-year incubation, the trays were uncovered for air-drying in a 30°C-controlled room. The BC-sand mixture was remixed well and then dried in an oven at 60°C for 2 days before sampling. About 5 g of mixture in each bottle were taken for BC particle isolation using super tweezers (N5, Dumont, Montignez, Switzerland). Another 5 g of the mixture were sampled and ball milled for total elemental analyses. The last 10 g were used for pH and CECp measurements.

III.2.e. Total elemental analyses

Mineral contents were measured by grinding 2 g of BC material followed by HNO_3 digestion in a closed microwave system for 12 hours. The digest was used for total elemental determination using Inductively Coupled Plasma (ICP) spectrometry (ICP-AES, Spectro CIROS, CCD, Germany). Total C and N were measured by continuous flow isotope ratio mass spectrometry (20-20 mass spectrometer, Sercon, Crewe, UK) after sample combustion to CO_2 and N_2 at 1000°C in an on-line elemental analyzer (PDZEuropa ANCA-GSL, Crewe, UK). The gases were separated on a Carbosieve G column (Supelco, Bellefonte, PA, USA) before introduction to the IRMS. Total N and C were calculated from the integrated total beam energy of the sample in the mass

spectrometer compared to a calibration curve derived from standard samples of known C and N content. Total H was measured by continuous flow TCEA (Thermal Conversion Elemental Analysis) using a Hekatech furnace (1400°C) by reaction with glassy carbon in a molybdenum foil-lined ceramic reaction tube to yield hydrogen (H) gas. Hydrogen was calculated from the integrated total beam energy of the sample in the mass spectrometer compared to a calibration curve derived from standard samples of known H content.

Ash and sand material in percent of the mixture were quantified by combusting 50 mg of ground BC-sand mixture at 630°C in a furnace for 24 hours. Oxygen concentrations were determined by difference from contents of C, N, H and the ash-sand mixture. This method was used by Baldock and Smernik (2002) in a 120-day experiment using a similar BC-sand incubation, although O concentrations quantified by this method may contain small amounts of sulfur, which were not accounted for.

pH in water was measured at a ratio of 1:20 (w/v water). Twenty milliliters of distilled water were added to 1 g of the BC-sand mixture. After one hour of occasional stirring, pH values were read twice using a pH meter. Potential Cation Exchange Capacity (CECp) was determined by saturating 3.0 g of the BC-sand mixture with 30 mL of 1N ammonium acetate at pH = 7 twice for one hour. The mixture, after ammonium acetate extraction using an extractor, then received 40 mL of 2N KCl to replace the absorbed NH_4^+ cations. The extracted NH_4^+ was quantified using a continuous flow analyzer (Technicon Auto Analyzer, Chauncey, CT, USA) and calculated as CECp.

III.2.f. BC particle characterization

BC particles from 8 replicates were pooled into two composite samples for the characterization of the molecular functional group chemistry using Fourier Transform

Infrared (FTIR) spectroscopy. BC samples were first pH standardized with a pH-7 solution by saturating BC materials with distilled water overnight. We standardized the pH of the BC materials to avoid effects of dissociation of chemical functional groups on spectral properties determined by FTIR (Cheng et al., 2008a). Details of the FTIR technique were described by Cheng et al. (2006). In brief, FTIR spectra were recorded on a Mattson Model 5020 FTIR Spectrometer (Madison, WI) at wavenumbers from 500 to 4000 cm^{-1}. KBr pellets, containing 0.3% wt of finely ground BC powder were prepared and scanned one hundred times. Chemical functional groups of BC were proportionally quantified using FTIR spectra and Omnic 7.2 (Thermo Electron Corporation, 1992-2005). Details of quantification were described by Nguyen et al. (2008).

III.2.g. BC loss

The BC loss over a 1-year period of incubation was estimated by taking the difference in C concentration (%), determined by elemental C analysis after incubation and at the beginning of experiment.

III.2.h. Statistical analyses

Analysis of variance was applied using a completely randomized, factorial design with 8 replicates and 3 experimental factors. Least Significant Difference (LSD) and Student test were used to classify treatments that significantly differed in means from each others. All statistical analyses were done with JMP 6.0 and Sigma plot 9.0.

III.3. Results

III.3.a. BC mineralization

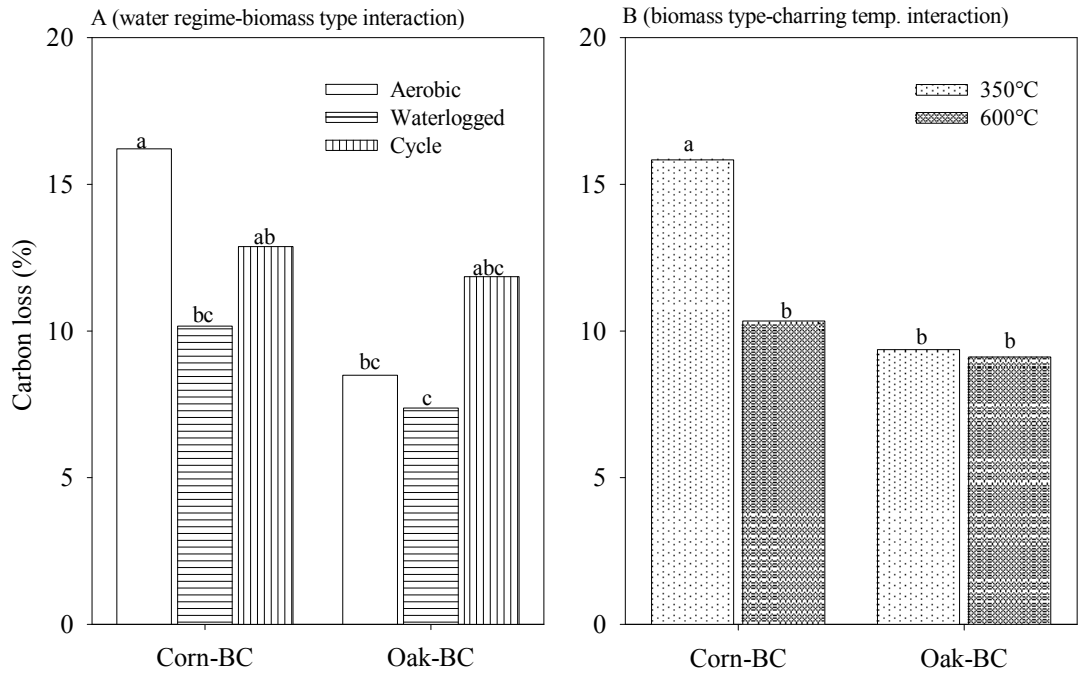

Figure III.1. Carbon loss of BC materials over the first year as influenced by water regime, biomass type and production temperature. Within each graph, bars with the same letter were not significantly different ($P<0.05$). Only significant interaction effects were shown, see appendix Tables III.1 and III.2 for full data.

C loss of BC produced from the two biomass types depended on water regimes (significant interaction between biomass type and water condition at $P<0.05$, Fig. III.1), but did not differ with production temperature. For corn-BC, aerobic conditions resulted in the highest C loss rate (16% for the first year) while for oak-BC the alternating aerobic-waterlogged conditions led to the highest C loss (12% for the first year). The lowest C loss (7-8%) was recorded under waterlogged conditions for both oak- and corn-BC. In addition, C loss of BC produced from the two biomass types

also depended significantly on charring temperature (significant interaction at P<0.05). The production temperature significantly affected mineralization of corn-BC, but it had no effect on mineralization of oak-BC (Fig. III.1).

III.3.b. Oxidation

During incubation, the O/C ratios of all four BC materials increased significantly (P<0.05), unless incubated under continuous waterlogged conditions (Fig. III.2). Only main effects of water regime, biomass type and charring temperature on O/C ratios were significant (Fig. III.2), whereas none of the interactions were significant (P>0.05). Aerobic and alternating conditions resulted in O/C ratios of 0.31 and of 0.30, respectively, significantly higher than ratios under waterlogged conditions of 0.26 (Fig. III.2A). Oxygen contents per unit C were significantly higher in corn-BC than in oak-BC and when BC was produced at 350°C than 600°C (Fig. III.2).

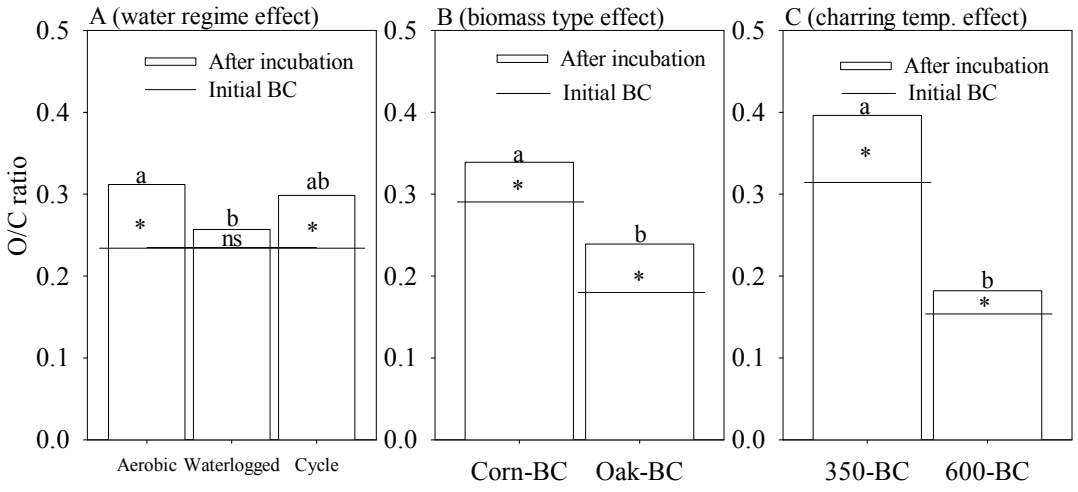

Figure III.2. Changes in O/C ratios of BC materials over the first year as influenced by water regime, biomass type and production temperature. Within each graph, bars with the same letter were not significantly different (P<0.05). * and ns indicate significant

(P<0.05) or not significant (P>0.05) changes in O/C ratios during incubation, and lines indicate initial O/C ratios. Only significant effects were shown, see appendix Tables III.3 and III.4 for full data.

III.3.c. Potential Cation Exchange Capacity (CECp) and pH

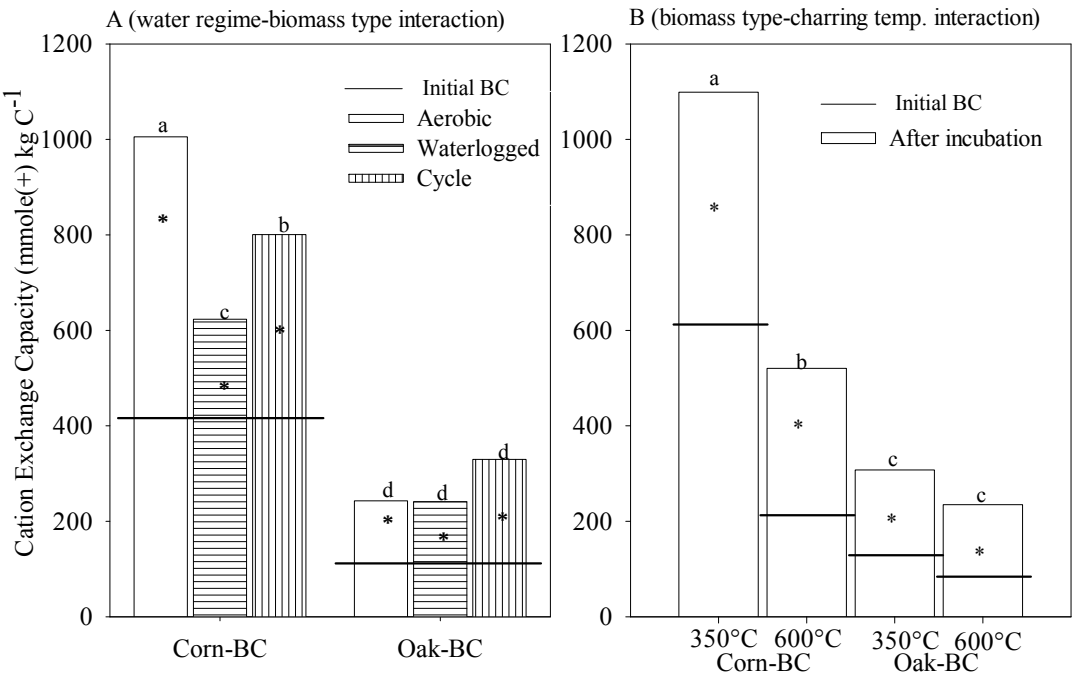

Figure III.3. Changes in CECp of BC materials over the first year as influenced by water regime, biomass type and production temperature. Within each graph, bars with the same letter were not significantly different (P<0.05). * and ns indicate significant (P<0.05) or not significant (P>0.05) changes in CECp during incubation, and lines indicate initial CECp. Only significant interaction effects were shown, see appendix Tables III.5 and III.6 for full data.

After one year CECp doubled irrespective of biomass type or charring temperature. Similar to C loss dynamics, changes in CECp and pH for corn-BC were significantly affected by charring temperature, whereas the charring temperature did not affect

changes for oak-BC. As also seen for C loss, aerobic conditions increased development of CECp the most for corn-BC, whereas for oak-BC this was the case with alternating aerobic-waterlogged conditions.

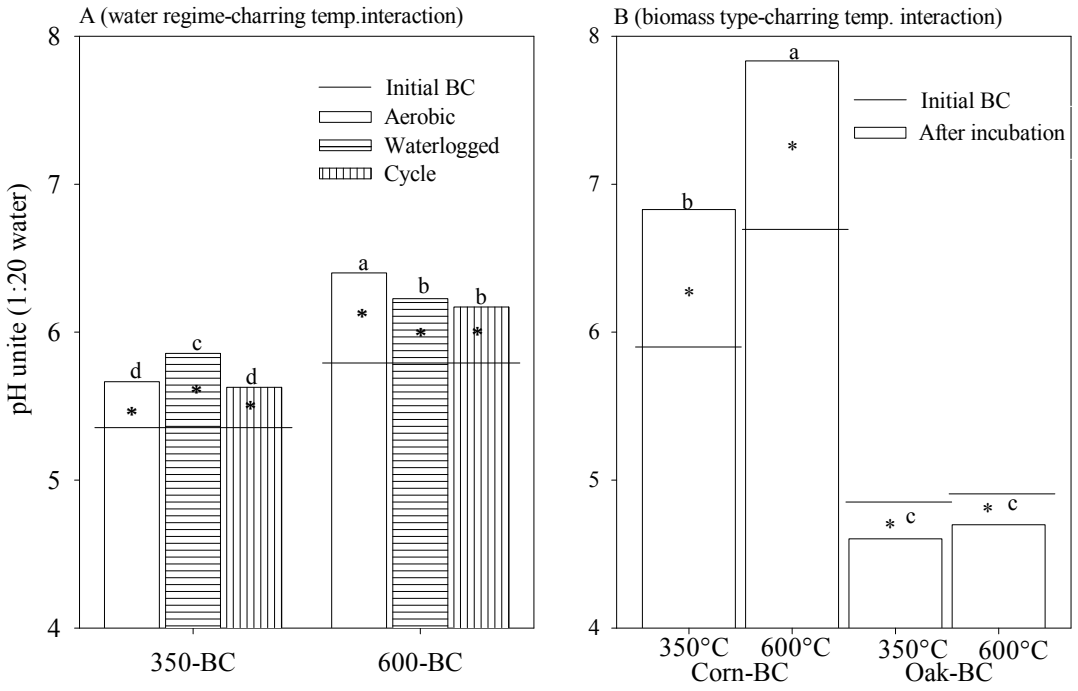

Figure III.4. Changes in pH of BC materials over the first year as influenced by water regime, biomass type and production temperature. Within each graph, bars with the same letter were not significantly different ($P<0.05$). * and ns indicate significant ($P<0.05$) or not significant ($P>0.05$) changes in pH during incubation, and lines indicate initial pH. Only significant interaction effects were shown, see appendix Tables III.7, III.8 for full data.

The pH values of corn-BC were initially 1-1.8 pH units greater than those of oak-BC (Table III.1). During incubation, the pH of corn-BC increased by 0.95 (at 350°C) and 1.12 (at 600°C) pH units, whereas the pH of oak-BC decreased by 0.24-0.21 (at both 350°C and 600°C) pH units (Fig. III.4).

III.3.d. Correlations

In general, C losses were significantly related to O/C ratios and its increment (ΔO/C) for both corn- and oak-BC (Table III.3). The increase in CECp (ΔCECp) was also well related with O/C, ΔO/C and pH for only corn-BC. Changes in pH values (ΔpH) were not correlated with any other parameters for both corn- and oak-BC (Table III.3).

III.3.e. Changes in functional group chemistry

Only small differences between corn-BC and oak-BC were found with respect to the relative proportions of chemical functional groups of OH, vibrating at 3192-3411 cm^{-1}, C=O at 1700 cm^{-1}, C=C at 1595-1630 cm^{-1} and aliphatic groups at 2856-2922 cm^{-1} and at 1430–1440 cm^{-1} (Fig. III.5). Increasing charring temperature, however, decreased proportions of C=O and aliphatic groups while it increased proportions of O-H groups of both corn- and oak – BC. After one year of incubation, both corn- and oak-BC under aerobic and alternating aerobic-waterlogged conditions contained higher proportions of aliphatic forms and O-H groups than under waterlogged conditions. C=O groups of corn-BC also increased to a greater extent under aerobic and alternating conditions than under waterlogged condition, whereas oak-BC showed inconsistent trends between water regimes.

Table III.3. Correlation coefficients between changes in BC properties. * and ns indicated significant (P<0.05) or not significant (P>0.05) relationship, respectively. Δ: change during incubation (obtained by subtraction of initial values from final values)

Index	Corn-BC							Oak-BC						
	C loss	O/C	CEC	pH	ΔO/C	ΔCEC	ΔpH	C loss	O/C	CEC	pH	ΔO/C	ΔCEC	ΔpH
C loss	1.00							1.00						
O/C	0.54*	1.00						0.40*	1.00					
CEC	0.54*	0.60*	1.00					0.09^{ns}	0.19^{ns}	1.00				
pH	-0.40*	-0.64*	-0.67*	1.00				-0.10^{ns}	-0.27^{ns}	-0.07^{ns}	1.00			
ΔO/C	0.48*	0.86*	0.31*	-0.28^{ns}	1.00			0.64*	0.79*	0.02^{ns}	-0.13^{ns}	1.00		
ΔCEC	0.49*	0.33*	0.88*	-0.36*	0.23^{ns}	1.00		0.09^{ns}	0.06^{ns}	0.99*	-0.02^{ns}	-0.03^{ns}	1.00	
ΔpH	-0.26^{ns}	-0.23^{ns}	-0.30^{ns}	0.75*	-0.15^{ns}	-0.25^{ns}	1.00	-0.06^{ns}	-0.09^{ns}	0.03^{ns}	0.97*	-0.04^{ns}	0.04^{ns}	1.00

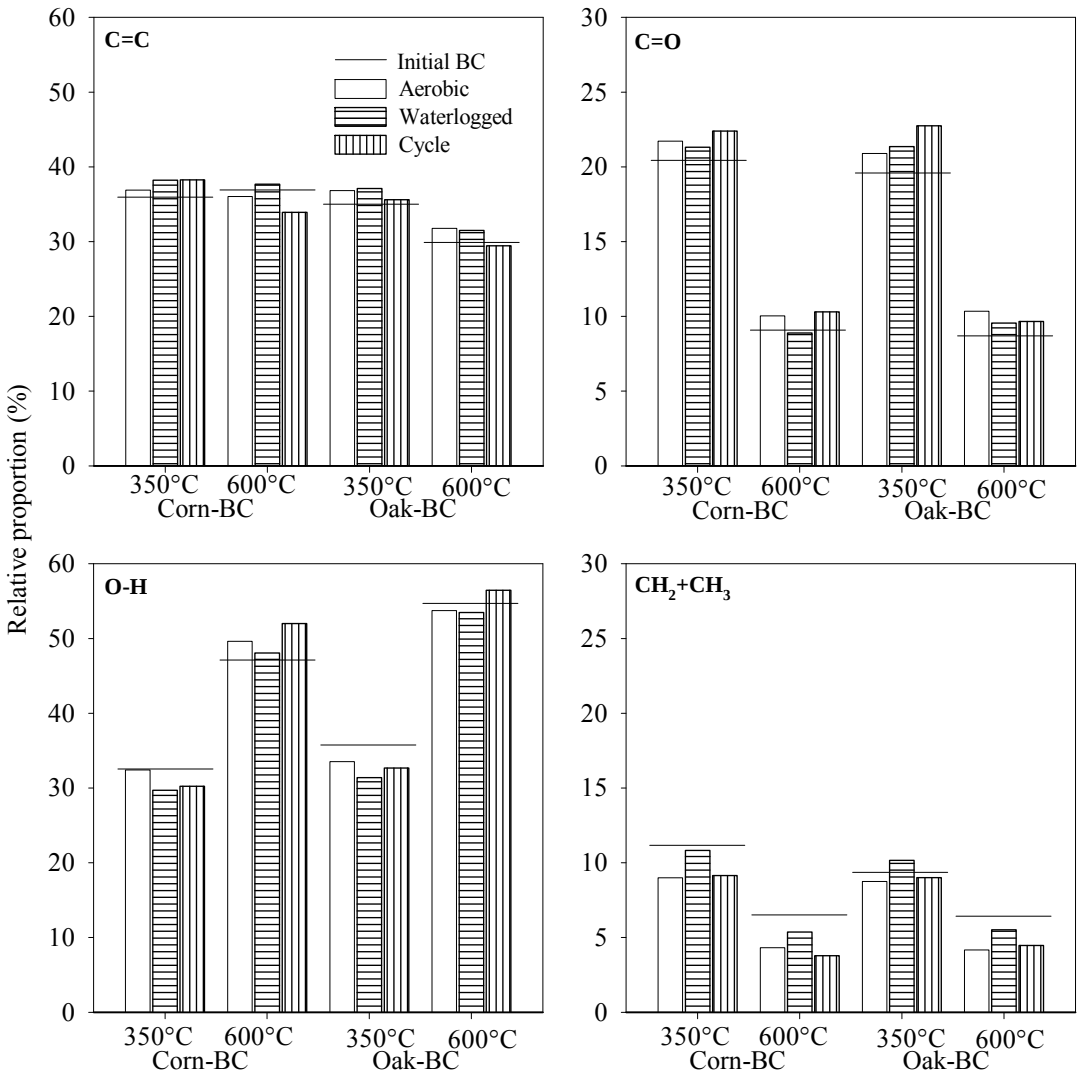

Figure III.5. Relative proportion of chemical functional groups quantified from FTIR spectra. Lines indicate initial proportions.

III.4. Discussion

III.4.a. Effects of production temperature and biomass types on BC properties

Lower O/C and H/C ratios and higher C with increasing production temperature (Table III.1) can be explained by loss of O and H, increased condensation of C

structures (Nishimiya et al., 1998), dominance of aromatic C, and emergence of O-aryl furan-like C (Baldock and Smernik, 2002). Similar increases in C associated with decreases in H and O contents have been described for many different biomass types over the temperature range examined here (Czimczik et al., 2002; Antal and Grønli, 2003; Mochidzuki et al., 2003; Braadbaart et al., 2004; Trompowsky et al., 2005).

The higher C and lower N and mineral contents in oak-BC than in corn-BC are reflective of the chemical properties of oak and corn biomass (Table III.1). Also Antal and Grønli (2003) and Hamer et al. (2004) showed higher C and lower O contents in oak-derived BC than in corn-derived BC. In fact, BC typically reflects the original properties of biomass types. For example, the structures of the original plant tissue were even retained in BC materials formed at low production temperature (Brodowski et al., 2005; Kim and Hanna, 2006).

III.4.b. Effects of water regimes

The more pronounced effects of aerobic than waterlogged conditions on C loss, O/C ratios, and CECp can be explained by the availability of oxygen for both abiotic and biotic oxidation and decomposition, which is well known for soil organic matter (Soerensen, 1974; Morris et al., 2004). However, alternating aerobic–waterlogged conditions typically result in greater mineralization of soil organic matter than constantly aerobic conditions (Birch, 1958; Cabrera et al., 1993; Gestel et al., 1993; Wu and Brookes, 2005). The reason for the often greater mineralization during drying and rewetting lies in destruction of soil structure by breaking down soil aggregates (Chepkwony et al., 2001; Denef et al., 2001), in greater soil nutrient availability (Gestel et al., 1993; Nguyen and Marschner, 2005), in higher microbial activities (Birch, 1958; Gordon et al., 2008), or in the turnover of microbial matter (Gestel et al.,

1991). Yet, aggregate protection of BC may not have occurred in this study, because BC was incubated in a sand medium and aggregates did not form. This is most likely the reason explaining similar effects of aerobic and alternating conditions.

BC-C losses between 6 and 21% during the first year in this study were rapid, compared to estimated mean residence times of BC in the soil environment. Bird et al. (1999) calculated mean residence times of BC ranging from decades to one century in well-aerated tropical soils, while other authors, Swift (2001), Skjemstad et al. (1998), Schmidt et al. (2002) estimated it to exceed one thousand years. The rapid decomposition of BC in this study could result from a numbers of reasons: (1) High and consistent incubation temperature was applied throughout, facilitating BC oxidation and thereby decomposition. BC may show unusually high increases in mineralization rates as a result of increasing incubation temperature due to its high chemical stability (Davidson and Janssens, 2006). Cheng et al. (2008b) calculated an increase in mineralization of BC produced from hardwood by a factor of 3.4 with every 10°C temperature increase (the so-called Q_{10}), which is at the upper end of Q_{10} values found for uncharred litter. (2) Mixing BC with sand created an oxygen-rich environment, promoting rapid oxidation of BC. (3) BC-protecting mechanisms were unavailable in this study. In soil BC particles were either physically encapsulated into micro-aggregates (Brodowski et al., 2006), or may form interactions with mineral surfaces (Glaser et al., 2000) or may adsorb non–BC organic matter (Liang et al., 2006), thereby reducing decomposition. (4) A significant amount of an easily decomposable fraction of BC used in this study as well as surfaces of BC may have reacted quickly and were completely mineralized to CO_2 soon after the incubation started. Rapid surface oxidation and disappearance of comparatively labile aliphatic C

forms during 4 months of incubation at 30°C were found by Cheng et al. (2006) for hardwood BC.

However, absolute C loss rates in this study were even higher than those from other incubation studies using sand media. In a 60-day incubation Hamer et al. (2004) reported a C loss rate of 0.3% 60 day^{-1} for oak-BC and 0.8% 60 day^{-1} for maize-BC. The incubation temperature of 20°C in their study was significantly lower than that of 30°C used in our study which may explain the difference in C loss rates in addition to the differences in length of incubation. Similar explanations may hold for comparison with data by Baldock and Smernik (2002) who reported a C mineralization rate below 2% of sapwood-BC formed at 200 to 300°C in a 120-day incubation at 25°C.

III.4.c. BC quality

Effects of water regimes largely depended on BC materials, with greater effects observed for the more labile types of BC, produced from corn and at lower temperature. These differences in C loss and oxidation under varying water regimes may be attributed to different physical and chemical properties of BC. Physically, corn-BC was soft, friable and easily broken down; in contrast oak-BC was hard and more resistant to pressure. In general, a lower density in plants corresponds to a lower density in BC as shown by Byrne and Nagle (1997). Consequently, corn residue which has a low density, formed low-density BC materials, while hardwood of oak created high-density BC materials in this study.

Chemically, higher charring temperature increasingly changed O-alkyl C to aryl and O-aryl furan-like structures (Baldock and Smernik, 2002; Masiello, 2004). Consequently we observed lower H/C and O/C ratios in BC produced at 600°C than at 350°C (Table III.1). With respect to the differences between types of BC, Hamer et al.

(2004) attributed a higher C-loss rate of BC produced from corn than from oak to its lower C/N ratio and aryl contents, which mirrors findings in our study.

The lack of a correlation between oxidation or C loss and pH changes (Table III.3) may be the result of two different processes. Oxidation indeed increases carboxyl C groups with significant acidity as seen from the FTIR results and the O/C ratios. The same conclusions were drawn by Cheng et al. (2006) for incubation of BC produced from hardwood. At the same time, however, dissolution of mineral matter originating from high-ash containing biomass increases the pH, as seen for corn-BC, which contained 1.5% alkaline metals such as Na, K, Mg and Ca in comparison to 0.3% in oak. The release of these alkaline metals may compensate for acidification by oxidation, resulting in a net increase in pH with corn-BC, whereas small contents of the alkaline metals in oak-BC were insufficient to compensate for oxidation, resulting in a net pH decrease as shown in Fig. III.4.

III.4.d. Decomposition processes

Although relatively stable compared to uncharred organic matter (Baldock and Smernik, 2002), BC is eventually mineralized in this study, with significant differences depending on moisture conditions and BC properties. Reported BC decomposition likely followed two major processes (i) microbial degradation (Hamer et al., 2004) and (ii) abiotic oxidation (Cheng et al., 2006; Cohen-Ofri et al., 2006). Oxidation may play an important role in controlling BC stability in this study as we observed significant correlation coefficients between O/C ratios and C loss rate (Table III.3). Likewise, Cohen-Ofri et al. (2007) concluded that oxidation processes were the major mechanism degrading fossilized charcoal.

The C loss under waterlogged conditions was significant even though the BC was submerged for the duration of the experiment. Either dissolved oxygen contents in the water were sufficient for microorganisms to oxidize the BC, or other sources of oxygen were present for both biotic and abiotic oxidation. For example, Endo et al. (1996) concluded that oxidation with MnO_2 converted benzyl alcohols into corresponding aldehydes. Moreover, Lequart et al. (1998) reported a decrease in lignin content collected from wheat straws when incubated with Na-oxalate and MnO_2-buffering solution for 20 hrs at room temperature. They concluded that interactions between MnO_2 and oxalate directly oxidized lignin phenolic moieties. In our study Mn was detected in corn-BC, but undetected in oak-BC**.** Formation of Mn species may interact with oxalate from the inoculum or BC decomposition products, serving as an abiotic catalytic reagent in BC oxidation and degradation. In addition, NO_3^- and Mn^{2+} added with the nutrient solution as well as minerals in the BC can serve as electron acceptors, facilitating BC oxidation under oxygen-limited conditions. Under submerged conditions, O/C ratios were significantly correlated with CECp (r^2=0.48, P<0.05) but not significantly correlated with C loss (r^2=0.05, P>0.05), whereas under aerobic conditions O/C ratios were significantly correlated with both CECp (r^2= 0.58, P<005) and C loss (r^2= 0.59, P<005). This indicates that under oxygen-limited conditions, oxidation may significantly decompose BC and thereby enhance CECp, but may not be strong enough to mineralize BC to carbon dioxide to account for significant C loss. Additional mechanisms, such as those using NO_3^- or Mn^{2+} as electron acceptors, may have been responsible for BC mineralization. Such mechanisms require further investigation.

In addition, minerals may also directly influence BC stability in this study. Significant amounts of minerals in corn-BC may cause defects in aromatic structures, reducing

cross links between layers to reduce the stability of an overall structure that is dominated by C links. Because the amounts of added nutrients were small (Table III.2), minerals contained in the BC also indirectly affected BC mineralization through microbial activity. Microbial biomass C was, for example, enhanced with soil K concentration and increased K application (Xiao et al., 2007). As a result, greater mineral content in corn-BC may lead to greater microbial activities and consequent biotic oxidation of BC.

Oxidation again depended on BC quality and the higher recalcitrance of oak-BC than corn-BC resulted in lower surface oxidation and CECp. CECp of the studied BC varied from 230-240 mmole(+)/kg^{-1}C for oak-600-BC, 250-420 mmole(+)/kg^{-1}C for oak-350-BC, 390-620 mmole(+)/kg^{-1}C for corn-600-BC to 860-1390 mmole(+)/kg^{-1}C for corn-350-BC. Theses values are still much smaller than those from soil humus, ranging from 1500-2500 mmole(+)/kg^{-1} (Brady and Weil, 1999, p332), but are estimated to increase over time as seen from aged BC (Cheng et al., 2008a). A number of studies reported BC oxidation and consequent increase in negative surface charge (CECp). Glaser et al. (2002) assumed that formation of carboxylic groups by oxidation on the edges of the aromatic backbone of BC was responsible for increasing CEC. As a result, the high CEC of Amazonian Dark Earths was attributed to BC oxidation (Glaser et al., 2003; Liang et al., 2006). Oxidation was demonstrated to start from surfaces of BC particles and to penetrate to a limited extent into BC particles over long periods of time (Lehmann et al., 2005; Cheng et al., 2006; Nguyen et al., 2008). Consequently, changes were more pronounced for CECp than for oxidized functional groups determined by FTIR, because CECp was quantified based on NH_4^+ exchange, which captures only surface negative charge, in contrast to FTIR analyses of finely ground BC powder, characterizing entire BC particles. Surface oxidation of BC may

therefore explain the comparatively rapid BC losses to a greater extent than oxidation of the bulk BC. This observation agrees well with results showing oxidized functional groups being limited to BC surfaces even after several hundreds (Nguyen et al., 2008) to thousands of years (Lehmann et al., 2005).

III.4.e. Environmental implications

The difference in C loss between moisture conditions was likely related to availability of oxygen. As a result one may expect BC materials to be present in smaller amounts in aerated soils but in high amounts in wetlands. However, a number of reasons contribute to such differences, involving BC production and transport in addition to mineralization (Czimzcik and Masiello, 2007). The differences between aerated and submerged conditions found in our study do not explain estimated differences between mean residence times in soils of hundreds to thousands of years (Skjemstad et al., 1998; Bird et al., 1999; Swift, 2001) and presence in ocean sediments of more than 13,000 of years as reported by Masiello and Druffel (1998). This may be due to extremely oxygen-limiting conditions in deep sea sediments compared to terrestrial environments or due to differential effects of the labile fraction of BC.

III.5. Conclusion

BC mineralization and changes in BC properties such as acidity and negative surface charge significantly depended on water regimes and initial properties of BC materials. Notably, the effects of water regimes greatly differed depending on the initial properties. The more labile BC types such as those produced from corn or at lower temperature were subject to greater change in quantity and quality by different water regimes than more stable BC forms. This may indicate that changes of more stable BC can be more easily predicted than less stable BC. However, predictions enabled by

results from this study are restricted to initial losses of the labile fraction of BC and do not allow extrapolation to longer periods of time without explicit investigation of the relationship between mineralization of labile and stable BC fractions. Changes over time also depended on BC properties, to the extent that increases of pH values in corn-BC contrasted with decreases in oak-BC. Oxidation processes were shown to be a major mechanism responsible for BC change and mineralization. However, mechanism controlling BC decomposition under submerged conditions requires additional research.

REFERENCES

Antal, M.J., Grønli, M., 2003. The art, science, and technology of charcoal production. Industrial & Engineering Chemistry Research 42, 1619-1640.

Baldock, J.A., Smernik, R.J., 2002. Chemical composition and bioavailability of thermally altered Pinus resinosa (Red pine) wood. Organic Geochemistry 33, 1093–1109.

Birch, H.F., 1958. The effect of soil drying on humus decomposition and nitrogen availability. Plant and Soil 10, 9–31.

Bird, M.I., Moyo, C., Veenendaal, E.M., Lloyd, L., Frost, P., 1999. Stability of elemental carbon in a savanna soil. Global Biogeochemical Cycles 13, 923-932.

Braadbaart, F., Boon, J.J., Veld, H., David, P., van Bergen, P.F., 2004. Laboratory simulations of the transformation of peas as a result of heat treatment: changes of the physical and chemical properties. Journal of Archaeological Science 31, 821-833.

Brady, N.C., Weil, R.R., 1999. The Nature and Properties of Soils. Twelfth edition, Prentice-Hall, Inc. 881 pages.

Brodowski, S., Amelung, W., Haumaier, L., Abetz, C., Zech, W., 2005. Morphological and chemical properties of black carbon in physical soil fractions as revealed by scanning electron microscopy and energy-dispersive X-ray spectroscopy. Geoderma 128, 116–129.

Brodowski, S., John, B. H. Flessa, Amelung, W., 2006. Aggregate-occluded black carbon in soil. European Journal of Soil Science 57, 539-546.

Brown, R., 2009. Biochar production technology. In: Lehmann, J., Joseph, S. (eds.) Biochar for Environmental Management: Science and Technology. Earthscan Publ., London, UK, in press.

Byrne, C.E., Nagle, D.C., 1997. Carbonization of wood for advanced materials applications. Carbon 35, 259-266.

Cabrera, M.L., 1993. Modeling the Flush of Nitrogen Mineralization Caused by Drying and Rewetting Soils. Soil Science Society of America Journal 57, 63-66.

Cheng, C.H., Lehmann, J., Thies, J.E., Burton, S.D., Engelhard, M.H., 2006. Oxidation of black carbon by biotic and abiotic processes. Organic Geochemistry 37, 1477-1488.

Cheng, C.H., Lehmann, J., Engelhard, M.H., 2008a. Natural oxidation of black carbon in soils: Changes in molecular form and surface charge along a climosequence. Geochimica et Cosmochimica Acta 72, 1598-1610.

Cheng, C.H., Lehmann, J., Thies, J.E., Burton, S.D., 2008b. Stability of black carbon in soils across a climatic gradient. Journal of Geophysical Research-Biogeosciences 113, G02027.

Chepkwony, C.K., Haynes, R.J., Swift, R.S., Harrison, R., 2001. Mineralization of soil organic P induced by drying and rewetting as a source of plant-available P in limed and unlimed samples of an acid soil. Plant and Soil 234, 83-90.

Cohen-Ofri, I., Boaretto, E., Mintz, G., Weiner, S., Weiner, L., 2006. Modern and fossil charcoal: aspects of structure and diagenesis. Journal of Archaeological Science 33, 428-439.

Czimczik, C.I., Preston, C.M., Schmidt, M.W.I., Werner, R.A., Schulze, E.D., 2002. Effects of charring on mass, organic carbon, and stable carbon isotope composition of wood. Organic Geochemistry 33, 1207-1223.

Czimczik, C.I., Masiello, C.A., 2007. Controls on black carbon storage in soils. Global Biogeochemical Cycles 21, GB3005.

Davidson, E.A., Janssens, I.A., 2006. Temperature sensitivity of soil carbon decomposition and feedbacks to climate change. Nature 440, 165-173.

Denef, K., Six, J., Bossuyt, H., Frey, S.D., Elliott, E.T., Merckx, R., Paustian, K., 2001. Influence of dry-wet cycles on the interrelationship between aggregate, particulate organic matter, and microbial community dynamics. Soil Biology & Biochemistry 33, 1599-1611.

Endo, K., Takahashi, H., Aihara, M., 1996. Neighboring assistance of a hydroxyl group on manganese dioxide oxidation of benzyl alcohols to lactones. Heterocycles 42, 589-596.

Gestel, M.v., Ladd, J.N., Amato. M., 1991. Carbon and nitrogen mineralization from two soils of contrasting texture and microaggregate stability: influence of sequential fumigation, drying and storage. Soil Biology & Biochemistry 23, 313-322.

Gestel, M.v., Merckx, R., Vlassak, K., 1993. Microbial biomass responses to soil drying and rewetting: the fate of fast- and slow-growing microorganisms in soils from different climates. Soil Biology & Biochemistry 25, 109-123.

Gibson, D. J., Hartnett, D.C., Merrill, G.L.S., 1990. Fire temperature heterogeneity in contrasting fire prone habitats: Kansas tallgrass prairie and Florida sandhill. Bulletin of the Torrey Botanical Club 117, 349-356.

Glaser, B., Balashov, E., Haumaier, L., Guggenberger, G., Zech, W., 2000. Black carbon in density fractions of anthropogenic soils of the Brazilian Amazon region. Organic Geochemistry 31, 669-678.

Glaser, B., Lehmann, J., Zech, W., 2002. Ameliorating physical and chemical properties of highly weathered soils in the tropics with charcoal - a review. Biology and Fertility of Soils 35, 219-230.

Goldberg, E.D., 1985. Black Carbon in the Environment, Wiley, New York.

Glaser, B., Guggenberger, G., Zech, W., Ruivo, M.L., 2003. Soil organic matter stability in Amazonian Dark Earths. In: Lehmann, J., Kern, D.C., Glaser, B., Woods, W.I. (Eds.), Amazonian Dark Earths: Origin, Properties, Management. Kluwer Academic Publishers, Dordrecht, The Netherlands, pp.141–158.

Gordon, H., Haygarth, P.M., Bardgett, R.D., 2008. Drying and rewetting effects on soil microbial community composition and nutrient leaching. Soil Biology & Biochemistry 40, 302-311.

Halverson, L.J., Jones, T.M., Firestone, M.K., 2000. Release of intracellular solutes by four soil bacteria exposed to dilution stress. Soil Science Society of America Journal 64, 1630–1637.

Hamer, U., Marschner, B., Brodowski, S., Amelung, W., 2004. Interactive priming of black carbon and glucose mineralization. Organic Geochemistry 35, 823–830.

Hofrichter, M., Ziegenhausen, D., Sorge, S., 1999. Degradation of lignite (low-rank coal) by ligninolytic basidiomycetes and their manganese peroxidase system. Applied Microbiology and Biotechnology 52, 78–84.

Kim, N.H., and Hanna, R.B., 2006. Morphological characteristics of Quercas variabilis charcoal prepared at different temperatures. Wood Science and Technology 40, 392-401.

Kuhlbusch, T.A.J., 1998. Black carbon and the carbon cycle. Science 280, 1903-1904.

Labbe, N., Harper, D., Rials, T., 2006. Chemical structure of wood charcoal by infrared spectroscopy and multivariate analysis. Journal of Agricultural and Food Chemistry 54, 3492-3497.

Lehmann, J., Liang, B.Q., Solomon, D., Lerotic, M., Luizao, F., Kinyangi, J., Schafer, T., Wirick, S., Jacobsen, C., 2005. Near-edge X-ray absorption fine structure (NEXAFS) spectroscopy for mapping nano-scale distribution of organic carbon forms in soil: Application to black carbon particles. Global Biogeochemical Cycles 19, GB1013.

Lequart, C., Kurek, B., Debeire, P., Monties, B., 1998. MnO_2 and oxalate: An abiotic route for the oxidation of aromatic components in wheat straw. Journal of Agricultural and Food Chemistry 46, 3868-3874.

Liang, B., Lehmann, J., Solomon, D., Kinyangi, J., Grossman, J., O'Neill, B., Skjemstad, J. O., Thies, J., Luizão, F. J., Petersen, J., Neves, E. G., 2006. Black Carbon increases cation exchange capacity in soils. Soil Science Society of America Journal 70, 1719-1730.

Masiello, C.A., Druffel, E.R.M., 1998. Black carbon in deep-sea sediments. Science 280, 1911–1913.

Masiello, C.A., 2004. New directions in black carbon organic geochemistry. Marine Chemistry, 92, 201–213.

Mochidzuki, K., Soutric, F., Tadokoro, K., Antal, M.J., Toth, M., Zelei, B., Varhegyi, G., 2003. Electrical and physical properties of carbonized charcoals. Industrial & Engineering Chemistry Research 42, 5140-5151.

Morris, D.R., Gilbert, R.A., Reicosky, D.C., Gesch, R.W., 2004. Oxidation potentials of soil organic matter in histosols under different tillage methods. Soil Science Society of America Journal 68, 817-826.

Nguyen, B.T., Marschner, P., 2005. Effect of drying and rewetting on phosphorus transformations in red brown soils with different soil organic matter content. Soil Biology & Biochemistry 37, 1573-1576.

Nguyen, B.T., Lehmann, J., Kinyangi, J., Smernik R., Engelhard, M. H., 2008. Long-term black carbon dynamics in cultivated soil. Biogeochemistry 89, 295-308.

Nishimiya, K., Hata, T., Imamura, Y., Ishihara, S., 1998. Analysis of chemical structure of wood charcoal by X-ray photoelectron spectroscopy. Journal of Wood Science 44, 56-61.

Schmidt, M.W.I., Skjemstad, J.O., Gehrt, E., Kögel-Knabner, I., 1999. Charred organic carbon in German chernozemic soils. European Journal of Soil Science 50, 351-365.

Schmidt, M.W.I., Noack, A.G., 2000. Black carbon in soils and sediments: Analysis, distribution, implications, and current challenges, Global Biogeochemical Cycles 14, 777-793.

Schmidt, M.W.I., Skjemstad, J.O., Jager, C., 2002. Carbon isotope geochemistry and nanomorphology of soil black carbon: Black chernozemic soils in central Europe originate from ancient biomass burning. Global Biogeochemical Cycles 16, GB1123.

Skjermstad, J.O., Clarke, P., Taylor, J.A., Oades, J.M., McClure, S.G., 1996. The chemistry and nature of protected carbon in soil. Australian Journal of Soil Research 34, 251-271.

Skjemstad, J.O., Janik, L.J., Taylor, J.A., 1998. Non-living soil organic matter: what do we know about it? Australian Journal of Experimental Agriculture 38, 667-680.

Shneour, E.A., 1966. Oxidation of Graphitic Carbon in Certain Soils. Science 15, 991-992.

Soerensen, L.H., 1974. Rate of decomposition of organic matter in soil as influenced by repeated air drying-rewetting and repeated additions of organic material. Soil Biology & Biochemistry 6, 287-292.

Swift, R.S., 2001. Sequestration of carbon by soil. Soil Science 166, 858–871.

Trompowsky, P.M., Benites, V.D., Madari, B.E., Pimenta, A.S., Hockaday, W.C., Hatcher, P.G., 2005. Characterization of humic like substances obtained by chemical oxidation of eucalyptus charcoal. Organic Geochemistry 36, 1480-1489.

Wu, J., Brookes, P.C., 2005. The proportional mineralisation of microbial biomass and organic matter caused by air-drying and rewetting of a grassland soil. Soil Biology & Biochemistry 37, 507-515.

Xiao, C., Stevens, R., Fauci, M., Bolton, R., Lewis, M., McKean, W.T., Bezdicek, D.F., Pan, W.L., 2007. Soil microbial activity, aggregation and nutrient responses to straw pulping liquor in corn cropping. Biology and Fertility of Soils 43, 709-719.

Zhao, M.S., Heinsch, F.A., Nemani, R.R., Running, S.W., 2005. Improvements of the MODIS terrestrial gross and net primary production global data set. Remote Sensing of Environment 95, 164-176.

CHAPTER 4

TEMPERATURE SENSITIVITY OF BLACK CARBON DECOMPOSITION AND OXIDATION

Abstract

Global warming accelerates decomposition of soil organic carbon (SOC) with different rates and sensitivity, depending on the quality of the material. In which way the decomposition of black carbon (BC) materials bearing different structures and properties responds to increasing temperature is little known. Four BC materials, produced by carbonizing corn residue and oak wood at 350 and 600°C (corn-350-BC, corn-600-BC, oak-350-BC and oak-600-BC), were mixed with pure sand and incubated at 4, 10, 20, 30, 45 and 60°C for one year to investigate structure and temperature dependence of decomposition. Corn-BC was more porous than oak-BC as determined by Scanning Electron Microscopy (SEM). Increasing charring temperature led to better orientation of graphene layers as observed by Transmission Electron Microscopy (TEM). Decomposition increased rapidly with increasing incubation temperature, and significantly depended on the type of BC. With a temperature increase from 4 and 60°C, decomposition of corn-350-BC increased from 10 to 20%, corn-600-BC from 4 to 20%, oak-350-BC from 2.3 to 15%, and oak-600-BC from 1.5 to 14% of initial C content, respectively. Temperature sensitivity (Q_{10}) decreased with increasing temperature and was highest in oak-600-BC, followed by oak-350-BC, corn-600-BC and corn-350-BC, indicating decomposition of more stable BC was more sensitive to increased temperature than less stable materials. Carbon loss and potential cation exchange capacity (CECp) significantly correlated with O/C ratios and change in O/C ratios, indicating that oxidative processes were the most important mechanism controlling BC decomposition in this study.

IV.1. Introduction

The temperature sensitivity of the resistant soil C pools to decomposition is still under debate. On the one hand a number of studies reported increasing sensitivity of stable soil organic carbon (SOC) to decomposition, relative to young and labile SOC pools (Agren, 2000; Knorr et al., 2005; Davidson and Janssens, 2006). On the other hand, Liski et al. (1999) concluded that in response to warming, decomposition of the resistant SOC pool was less sensitive than that of young pools and Giardina and Ryan (2000) even reported that decomposition of SOC in forest mineral soil was not influenced by increased temperature. Reichstein et al. (2005a) suggested that it was premature to conclude on a greater temperature sensitivity of stable than of labile SOC.

Black carbon (BC) is an important C form, accounting for a considerable proportion of SOC, for example up to 45% in German Chernozemic soils (Schmidt et al., 1999, 2002). BC is typically considered as a recalcitrant SOC pool, as it was estimated to have mean residence times of 10 thousands of years in soil (Swift, 2001). However, the highest proportion of BC was in some instances found in the light fraction (Glaser et al., 2000), which is commonly described as the labile fraction of SOC. In addition, BC materials greatly differ in chemical, physical and structural properties, depending on production temperature and BC precursors (Labbe et al., 2006). How sensitive BC materials with differing properties respond to a warming environment is poorly known.

Over the next three centuries, the global environment could warm on average by 8 K, as simulated by Bala et al. (2005). The warmer environment likely accelerates decomposition of BC materials. Oxidation, a process influencing structure degradation

of BC (Cohen-Ofri et al., 2007), would be accelerated by the increase in temperature. In a 120-day incubation experiment, Cheng et al. (2006) reported a higher O content when BC particles were incubated at 70°C than at 30°C, indicating that BC oxidation may occur abiotically, and was shown to significantly increase with a rise in temperature. Additionally, the same authors (Cheng et al., 2008a) observed a positive significant correlation between oxidation of BC deposited from charcoal production and increasing mean annual temperature over 130 years.

Oxidation and decomposition is primarily driven by microbial activity, and several authors show a positive effect of microorganisms on BC degradation (Brodowski, 2004; Hamer et al., 2004; Marschner et al., 2008). Microbial activities are greatly sensitive to temperature changes. Qureshi et al. (2003) showed that microbial respiration rates were highest at 28°C, while further increasing temperature to 37°C or lowering temperature down to 16°C resulted in lower respiration rates. Individual microbial communities have their optimum temperature range for decomposition of organic matter. Changing the environmental temperature to above or below the biological optimum likely limits microbial activity and thereby BC decomposition.

In addition to environmental temperature, intrinsic properties of BC apparently control its stability. BC is the product of incomplete combustion of vegetation (Koelmans et al., 2006), possessing high aromaticity (Kuhlbusch, 1995; Haumaier and Zech, 1995) and is most likely present in all terrestrial and aquatic ecosystems as well as in the atmosphere. The defining feature of BC is a high elemental C content from highly condensed aromatic rings (Kima et al., 2004), having both microcrystalline graphitic structure (Bourke et al., 2007) as well as amorphous non-organized structure (Cohen-Ofri et al., 2007). Polyaromatic graphene sheets, composed of basic aromatic units, stack over each other (Schmidt and Noack, 2000), forming three-dimensional

structures and thus porous and light particles. The proportion of aromatic C and the physical characteristics of micro- and nano- structures likely determine BC stability and decomposition. However, such relationship has not yet been reported.

To address these knowledge gaps, an experiment on temperature sensitivity of BC decomposition was set up to test the hypotheses that (a) decomposition rates of BC increase with increased incubation temperature; (b) decomposition of more stable BC materials is more sensitive to increased temperature than that of less stable BC materials.

IV.2. Materials and methods

Methodology and materials used in this study were similar to those described by Nguyen and Lehman (2009). In brief, four BC materials (corn-350-BC, corn-600-BC, oak-350-BC and oak-600-BC) were produced by carbonizing corn residue (*Zea mays* L.) and oak shavings (*Quercus* ssp.) at 350 and 600°C using slow pyrolysis performed by Best Energies, Inc. (Daisy Reactor, WI, USA). The materials were then slightly ground to pass 2 consecutive 0.5-mm and 2-mm sieves and particles remaining on the 0.5mm sieve were collected for this study. Chemical properties of the BC materials are shown in Table IV.1. Water holding capacity was determined and microbial nutrition solution was prepared as described by Nguyen and Lehman (2009).

Table IV.1. Initial properties of BC materials (Nguyen and Lehmann, 2009)

Biomass types	Charring temp. (°C)	Elemental content (%)											C/N	O/C	H/C	CECp[a]	pH[b]
		C	N	O	H	K	Ca	Fe	Si	Mn	Others	Sum					
Corn residue	350	67.5	0.93	25.1	4.74	1.04	0.27	0.05	0.02	0.006	0.50	100.2	73	0.37	0.07	610	5.88
	600	79.0	0.92	16.3	2.52	0.67	0.31	0.08	0.03	0.008	0.49	100.3	86	0.21	0.03	215	6.71
Oak wood	350	75.9	0.10	19.6	4.27	0.11	0.07	0.003	0.02	0.000	0.03	100.1	759	0.26	0.06	131	4.84
	600	88.4	0.12	9.0	2.13	0.22	0.09	0.13	0.01	0.004	0.06	100.2	737	0.10	0.02	89	4.91

[a]CECp = Potential Cation Exchange Capacity in mmole(+)kgC^{-1}

[b]pH in 1:20 w:v water

IV.2.a. Experiment

A completely randomized full factorial experiment with 8 replicates and 3 factors (2 biomass types, 2 charring temperatures and 6 incubation temperature levels) was set up. One gram of ground BC material was added to 30-mL bottles after mixing with 19 g of pure sand material. The sand had been heated at 550°C in a muffle furnace for 24 hours to remove any remaining organic matter. Each bottle received 2 mL of microbial nutrient solution (Nguyen and Lehman, 2009). The BC-sand mixture was then moistened to 60% of water holding capacity which was kept constant over the one-year experiment. The bottles were placed in plastic trays positioned in one of 6 temperature-controlled chambers. The temperature was set to either 4, 10, 20, 30, 45 or 60°C.

The plastic trays were covered with aluminum foil to control water evaporation. Five small holes were created on the covered aluminum foil for gas exchange. Water was added to the tray to maintain a moist environment. The water content of the mixture in the bottle and water level in the plastic trays were monitored weekly by weighing and adding appropriate amounts of distilled water.

IV.2.b. Total elemental analysis

Analyses of elemental contents of C, N, H, O and CECp (Potential Cation Exchange Capacity) were similar to those described in detail by Nguyen and Lehmann (2009). In brief, C, N, and H concentrations of the BC-sand mixture were determined using dry combustion analysis. BC ash and sand material in percent of the mixture were quantified by combusting 50 mg of ball ground BC-sand mixture at 630°C in a muffle

furnace for 24 hours and O contents were calculated by difference from contents of C, N, H and ash-sand mixture.

IV.2.c. Potential Cation Exchange Capacity (CECp)

CECp was quantified by saturating 3.5 g of BC-sand mixture with 40 mL of 1N ammonium acetate at pH = 7 twice. Because BC particles slowly adsorbed ammonium from solution presumably due to the large internal surface area and thus CECp of the mixture, containing 5% BC by weight was low, we increased saturation time to 24 hours for enhanced ammonium adsorption and exchange. The mixture, after ammonium acetate extraction, then received 40 mL of 2N KCl to replace the adsorbed NH_4^+ cation. The extracted NH_4^+ was determined using a continuous flow analyzer (Technicon Auto Analyzer, Chauncey, CT, USA) and calculated as CECp.

IV.2.d. Remaining C (%)

Carbon contents remaining after incubation were determined by calculating the percentage of C concentration (%) after incubation to C concentration (%) before experiment using C contents determined by elemental C analyses, following the formula:

$$remainingC(\%) = \frac{C_{after}}{C_{before}} * 100 . \qquad \text{(Eq. 1)}$$

IV.2.e. X-ray diffraction (XRD)

XRD was performed on a Theta-Theta Diffractometer, Scintag, Inc **(**10040 Bubb Road, Cupertino, CA). The generator was set at 45kV and 40mA. The set of slits for the tube was #1 and #3, and for the detector #0.3 and # 0.5. Scans were run over a 2-theta range from 1.5 degrees to 100 degrees with a step size of 0.03 and preset time of

1.2 s/step. The collected spectra were processed using DMSNT software and exported to Microsoft Excel for plotting.

IV.2.f. Scanning Electron Microscopy (SEM) and Transmission Electron Microscopy (TEM)

Micro-structures of the BC particles were investigated using a LEO (ZEISS) 1550 SEM, which was originally supported by the Keck Foundation at Cornell University. The sample particles were mounted on an aluminum stud and were coated with carbon. Because the particles were thick and long, millimeter scale, the coating material did not interfere with the scanned images.

TEM images of BC particles were collected using a FEI Tecnai T12 Spirit Twin TEM/STEM (20-120kv, 5350 NE Dawson Creek Drive Hillsboro, Oregon, USA) at Cornell University. The materials were finely ground, dissolved in ethanol solution, deposited on a lacey carbon holder and then sonicated for 10s before scanning.

IV.2.g Calculations and statistical analysis

Analysis of variance (ANOVA) was applied as a completely randomized factorial design with 8 replicates and 3 experimental factors. Student test was used to classify any significant difference in means between treatments. Carbon mineralization, oxidation and CECp as a function of incubation temperature were quantified, based on a first order kinetic model (Peterjohn et al., 1994; Holland et al., 2000) with 3 parameters:

$$f = Y_0 + ae^{-bT} \text{ or } f = Y_0 + a(1 - e^{-bT}) \quad \text{(Eq.2),}$$

where the dependent variable is the exponential decay or rise pattern, respectively, f is the content (remaining C, O/C or CECp) at incubation temperature T (°C), Y_o is the initial content, a is a constant and b is a reaction rate constant. A linear model was also used for any observed parameters that were linearly dependent on the incubation temperature. The temperature coefficient (Q_{10}) was calculated using the following formula:

$$Q_{10} = \left[\frac{R_2}{R_1}\right]^{\left(\frac{10}{T2-T1}\right)} \quad \text{(Eq.3)},$$

where R_1 and R_2 are C losses (% of initial C concentration) at 2 temperatures, T1 and T2, of an interval, respectively (Kirschbaum, 1995). All statistical analyses and model fitting were done with a JMP software 6.0, Sigma plot 11 and Microsoft Excel.

IV.3. Results

IV.3.a. Micro-structure of BC

SEM images shown in Fig. IV.1 reflected representative parts of BC from both corn stem and oak wood, used in this study (additional images in Appendix). Figs. IV.1A and IV.1D are images capturing a cross section of corn- and oak-BC particles and Figs. IV.1B and IV.1C are those derived from a longitudinal section of the materials at the same magnification of 1 K. The plant cell structure of the original biomass materials was clearly visible for the BC particles formed at both 350 and 600°C. At the micro-scale, corn-BC appeared more porous than oak-BC and the cell walls of corn-BC were thinner than that of oak-BC.

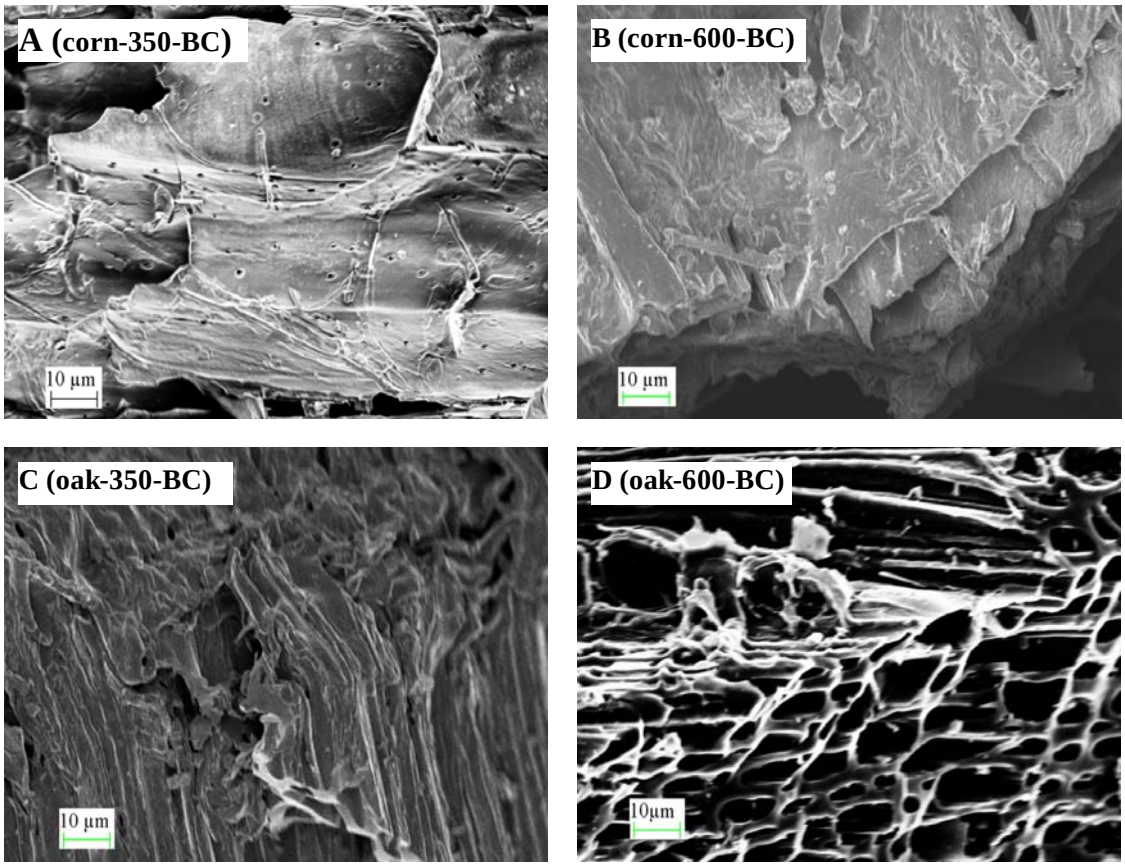

Figure IV.1. Micro-scale morphology of BC materials by SEM capturing. See appendix Figs IV.1a and IV.1b for more SEM images.

IV.3.b. Nano-structure of BC

In general, oak-BC showed slightly more parallel orientation of C layers than corn-BC (Fig. IV.2) at both production temperatures. Increasing carbonization temperature led to better ordered C layers and enhanced the length of C layers for both types of BC. A greater increase in C layer orientation of BC formed at higher temperature was observed in corn-BC than in oak-BC. Corn-350-BC was composed of short C layers, which arranged rather randomly, forming amorphous structure (Fig. IV.2A). In contrast, part of oak-350-BC seemed to be composed of multiple circular C structures with a diameter of less than 1 nm (Fig. IV.2C). Parallel arrangement of 3 to 5 C layers

formed oval shapes in corn-600-BC (Fig. IV.2B) whereas a lattice structure of a number of C sheets was seen in oak-600-BC (Fig. IV.2D).

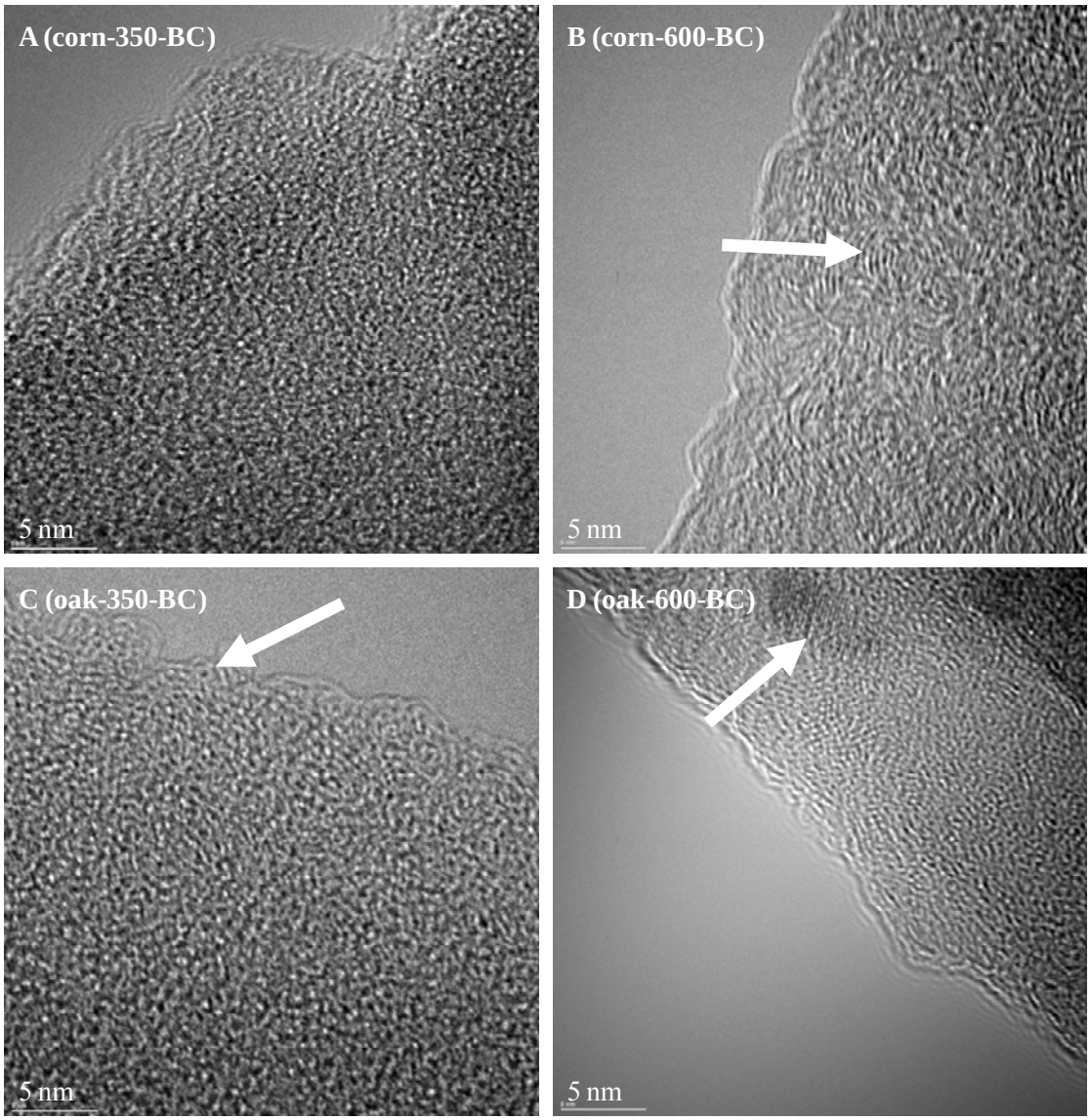

Figure IV.2. TEM images of the BC materials. Arrow in panel B indicates an oval shape of a size of a few nanometers formed by curling of C layers; arrow in panel C indicates a circle of less than one nanometer; and arrow in panel D indicates a lattice structure, formed by parallel arrangement of a number of C layers. See appendix Figs IV.2a and IV.2b for additional images.

IV.3.c. Chemical functional structure of BC materials by Xray-diffraction

The low angle, 2 theta from 5-35 degrees, was deconvoluted and separated into the (002) band and γ band (Fig. IV.3). The former band reflects aromatic structures and the latter represents saturated structures (Lu et al., 2000). Oak-BC had higher intensities of the aromatic (002) band and a broader peak at 44 degrees (2 theta), which reflects hexagonal ring structures, than corn-BC at both production temperatures. Increasing production temperature also led to enhanced intensity of the peak at 44 degrees.

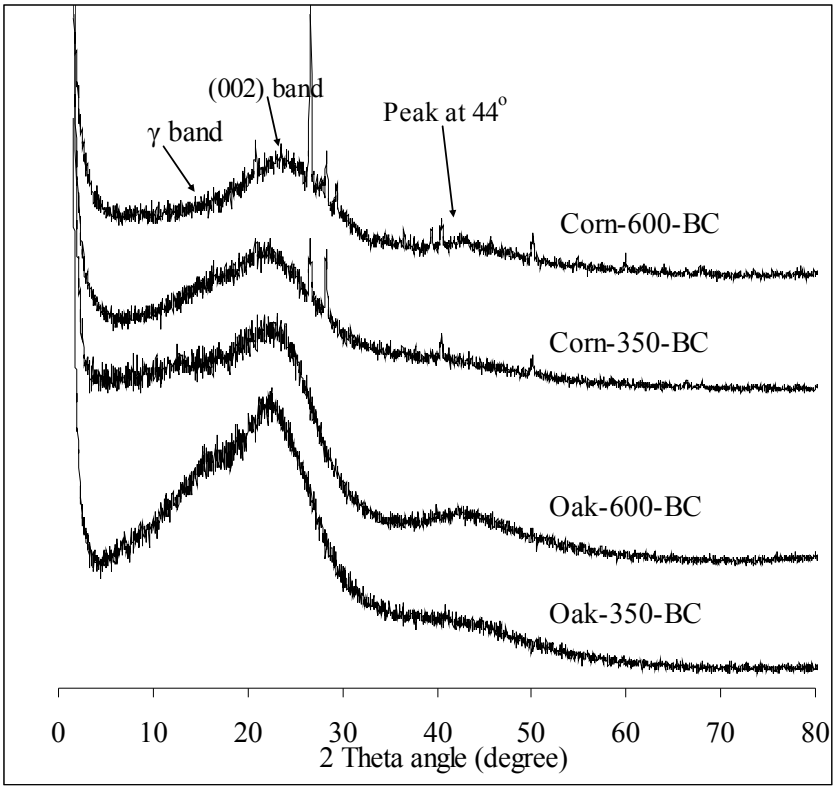

Figure IV.3. Xray diffractograms of the BC materials.

IV.3.d. BC mineralization

BC was mineralized rapidly when incubation temperature was increased from 4 to 30°C, at which, C loss was 4.6% and 14.6% during the first year, respectively (data calculated, based on the fitted model). Remaining C (% of initial C) of corn-BC and 350-BC was significantly lower than that of oak-BC and of 600-BC, respectively, at any incubation temperature (Fig. IV.4B). The dynamics of BC mineralization as a function of incubation temperature significantly depended on BC types. For example, the temperature sensitivity of corn-600-BC from 4°C to 30°C incubation temperature was greater than that of corn-350-BC.

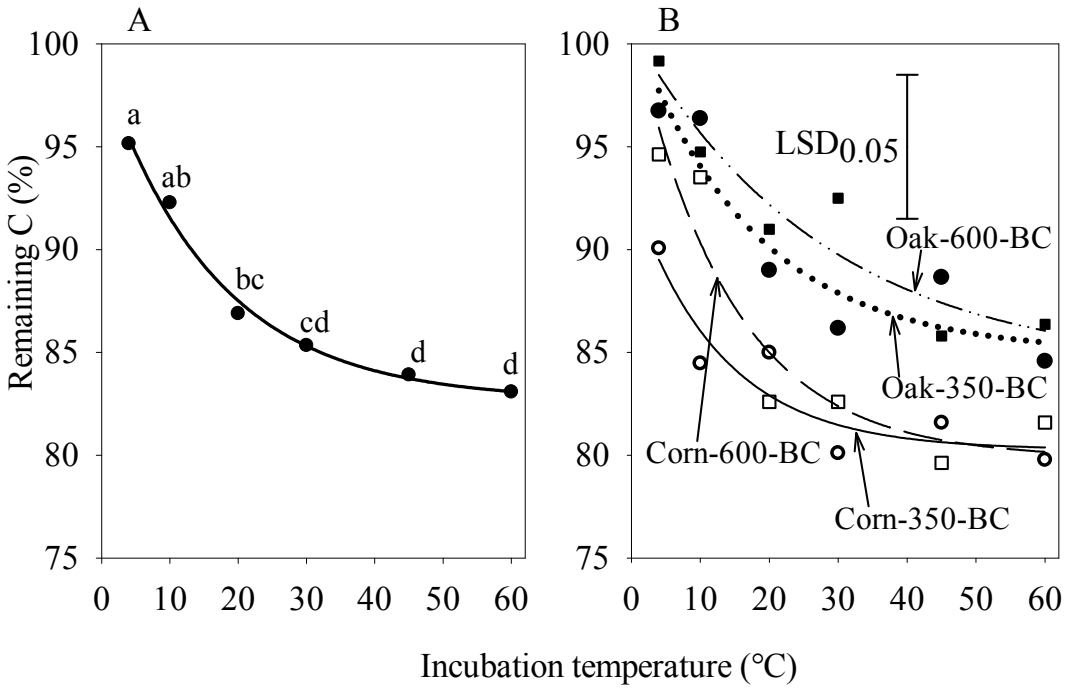

Figure IV.4. Remaining C of overall mean (A) and individual BC materials (B) after the first year of incubation. Within panel A, data points with the same letter were not significantly different. Parameters of the fitted curves were shown in Table IV.2. See appendix Tables IV.1 and IV.2 for individual remaining C values.

The fitted curves of remaining C for both the overall mean of all BC materials and for individual BC materials were significant, with correlation coefficients higher than 0.84 ($P \leq 0.05$) (Table IV.2). Based on the fitted model, the increase in absolute C loss per degree Celsius, parameter b, was lower in oak-BC than in corn-BC, and also decreased with increasing charring temperature. Therefore, temperature increases had a lower effect on absolute C loss of the more stable BC materials such as oak-BC and BC produced at higher charring temperature.

Table IV.2. Parameters of fitted model, $f = Y_0 + ae^{-bT}$, of remaining C as a function of incubation temperature, showed in Figs IV.4D and IV.4E.

BC materials	Y_o	a	b	R^2	P
Overall mean	82.67	16.27	0.061	0.99	0.008
Corn-350-BC	80.26	12.63	0.078	0.84	0.050
Corn-600-BC	79.86	21.35	0.071	0.90	0.031
Oak-350-BC	84.94	16.04	0.057	0.87	0.048
Oak-600-BC	84.15	16.57	0.036	0.90	0.030

The proportions of C loss at different incubation temperatures relative to the C loss at 60°C are shown in Fig. IV.5. Corn-350-BC, incubated at 4°C, lost as much as 53 % of that incubated at 60°C, followed by corn-600-BC (21 %), oak-350-BC (16 %) and then oak-600-BC (11 %). Increasing the incubation temperature resulted in different increases in the proportion of C loss, depending on temperature ranges and BC materials. For example, the highest increase in C loss, about 25-28% was similar for corn-600-BC and oak-350-BC, when increasing the incubation temperature from 4 to

10°C and from 10 to 20°C, whereas oak-600-BC lost 25% C, when incubation temperature was increased from 10 to 20°C.

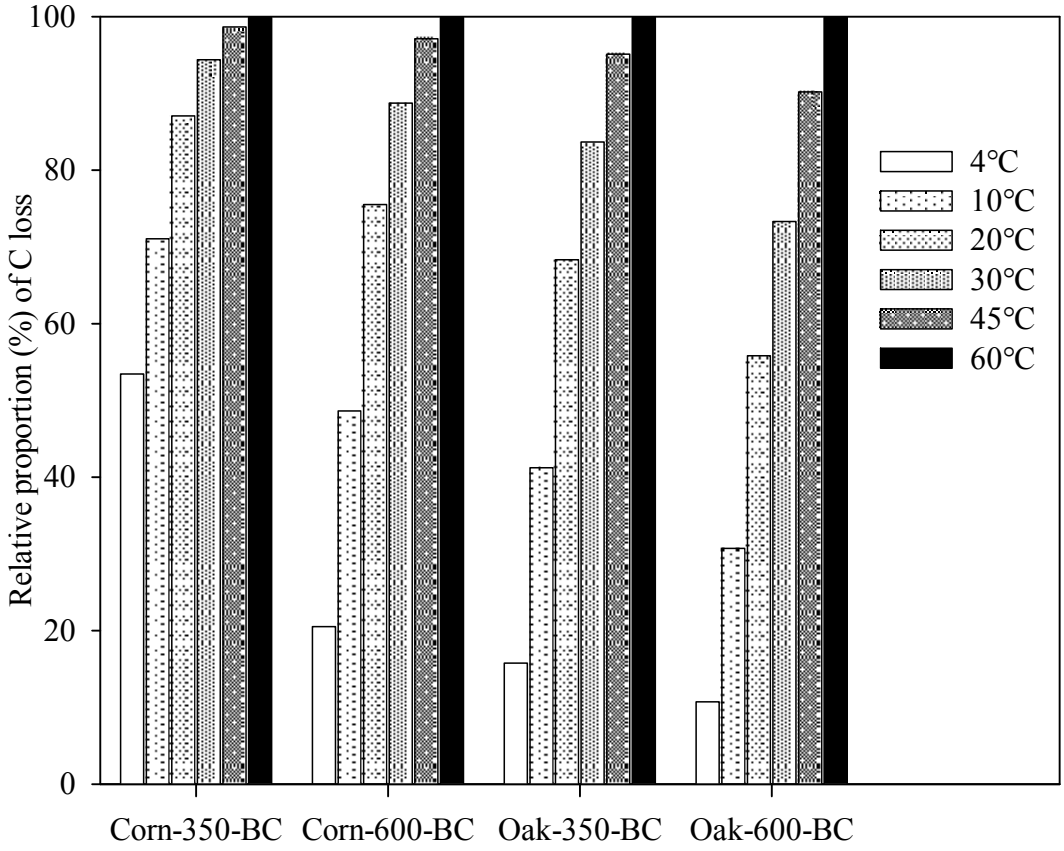

Figure IV.5. Proportion of C loss of the BC materials at different temperatures relative to that at 60°C.

In the lowest temperature range from 4-10°C, the Q_{10} value of corn-350-BC, 1.6, was much smaller than those of the other BC materials, varying from 4.2 to 5.8 (Fig. IV.6A). At higher temperature ranges, the difference in Q_{10} between the four BC materials decreased, varying from 1.01 to 1.82, with corn-350-BC still having the lowest and oak-600-BC the highest Q_{10} values. Relative to the Q_{10} at 4-10°C, the Q_{10}

values of corn-350-BC decreased to a lesser extent with increasing incubation temperature ranges than those of the other materials (Fig. IV.6B).

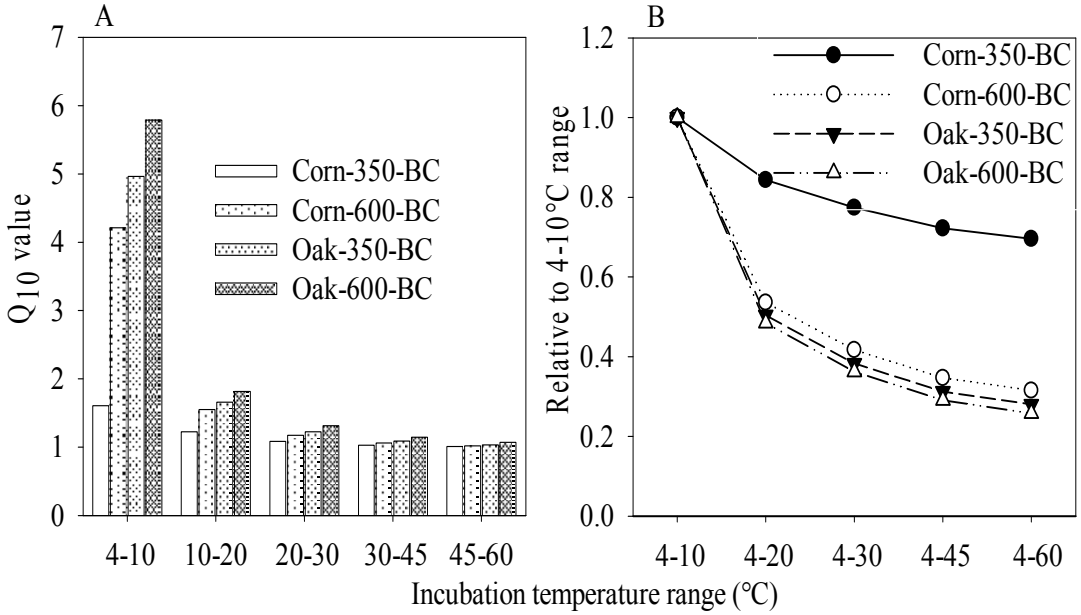

Figure IV.6. Absolute Q_{10} values of BC materials at different ranges of incubation temperature (A) and Q_{10} relative to that at the 4-10^{o}C range (B). These values were calculated based on equation 2 and the fitted curves with parameters are shown in Table IV.2.

IV.3.e. BC oxidation

With increasing incubation temperature, the O/C ratios increased and a first order model was fitted well to the data points (Fig. IV.7A). At temperatures higher than 10°C, the O/C ratios of the 4 BC materials after incubation were significantly greater than before incubation. Increases in O/C ratios as a function of incubation temperature were significant ($P<0.05$) and similar among the four BC materials. However, the absolute values of O/C ratios were highest in corn-350-BC, followed by corn-600-BC, oak-350-BC and oak-600-BC at any incubation temperatures (Fig. IV.7B).

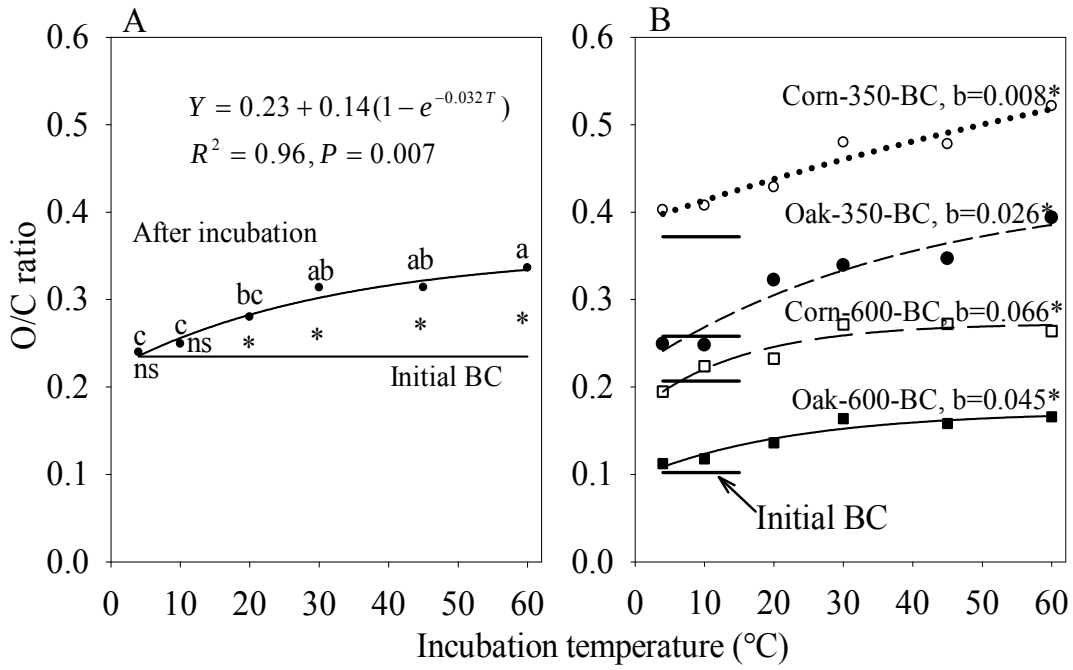

Figure IV.7. O/C ratios of overall means (A) and individual BC materials (B). Within panel A, data points with the same letter are not significantly different. b is the slope of the fitted curve. * and ns indicate whether the slope or the difference in O/C ratios after and before incubation is significant (P<0.05) or non-significant (P>0.05), respectively. See appendix Tables IV.3 and IV.4 for individual O/C values.

IV.3.f. Potential Exchange Capacity (CECp)

CECp of BC materials increased significantly by 165 to 973 mmole kg C^{-1} when the incubation temperature was increased from 4°C to 60°C, respectively (Fig. IV.8A). The increase in CECp as a function of incubation temperature greatly depended on the charring temperatures. For example corn-BC and oak-BC formed at 350°C changed with a rate of 25 and 22 mmole (+) kg C^{-1} $°C^{-1}$, respectively, much more than the BC formed at 600°C with a rate of 6.4 and 4.7 mmole(+)kg C^{-1} $°C^{-1}$ for corn-600-BC and

oak-600-BC, respectively. CECp of corn-BC was significantly greater than that of oak-BC at any charring temperature and incubation temperature.

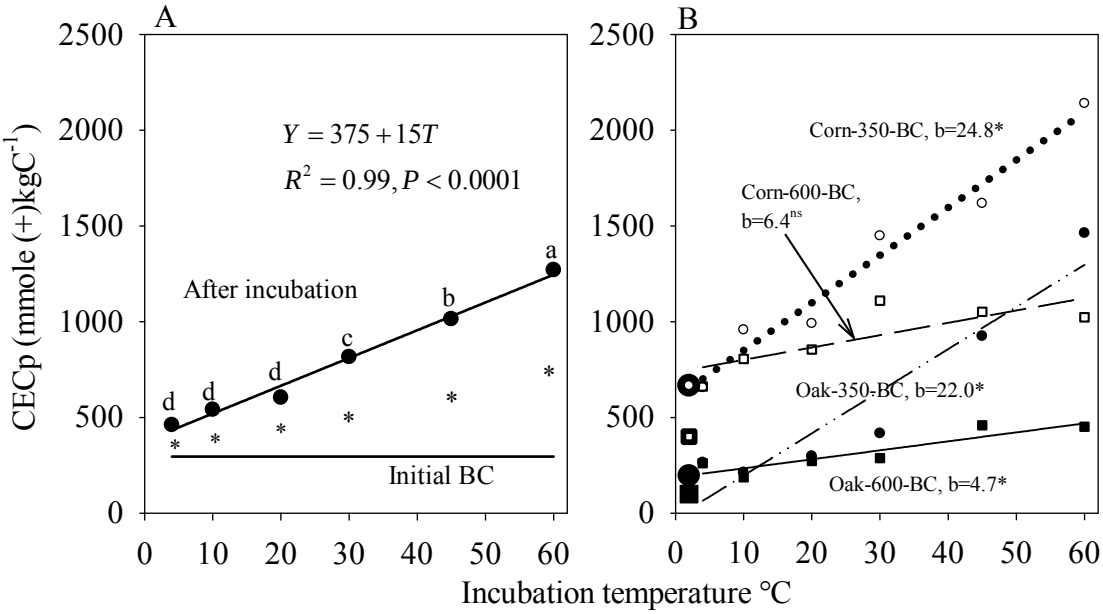

Figure IV.8. Potential CEC of overall mean (A) and individual BC materials (B). Within panel A, data points with the same letters are not significantly different. b is the slope of the fitted curve. * and ns indicate whether the slope or the difference in O/C ratios after and before incubation is significant (P<0.05) or non-significant (P>0.05), respectively. Larger symbols in panel B indicate initial CECp of the materials. See appendix Tables IV.5 and IV.6 for individual CECp values.

IV.3.g. Inter-relationships with O/C ratio

With increasing O/C ratios, the remaining C (%) significantly decreased and CECp (mmole(+)kgC^{-1}) increased (Fig. IV.9). Changes in O/C ratios were also significantly and inversely correlated with the remaining C content and positively with change in CECp.

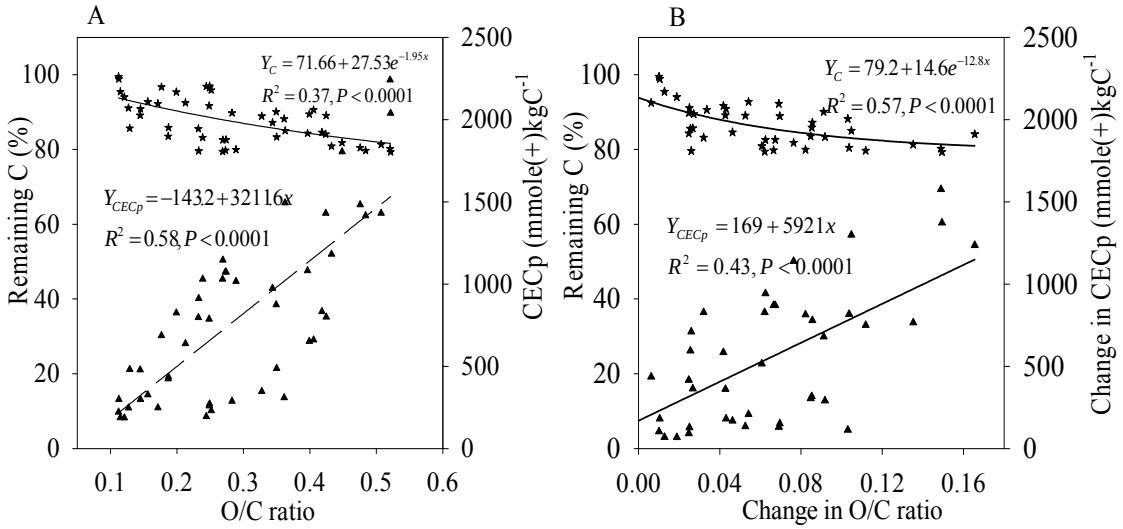

Figure IV.9. Remaining C (Y_c) and CECp (Y_{CECp}) as a function of O/C ratios (A) and change in O/C ratios (B)

IV.4. Discussion

IV.4.a. BC properties

BC properties including chemical, physical and structural properties were greatly influenced by production temperature and biomass type. Such influences on chemical properties were discussed in more detail in our previous paper, and were also addressed by other authors such as Nishimiya et al. (1998), Antal and Grønli (2003) and Mochidzuki et al. (2003). With increasing production temperature, BC materials tended to condense and increase in aromaticity (Lu et al., 2000). Nishimiya et al. (1998) also observed an increase in $A_{(002)}/A_\gamma$ ratio as production temperature was increased to 2000°C due to condensation of aromatic rings.

An important difference between corn-BC and oak-BC was observed in their micro-structure (Fig. IV.1). The SEM images captured from corn and oak materials formed at 350 and 600°C showed that the tissue structure of the original plant biomass was

retained in the BC materials which appeared more rigid in oak than corn. This is in agreement with observations by Brodowski et al. (2005) and Kim and Hanna (2006).

At nano-scale, C layer orientation of BC materials may be characterized with different models, such as a diamond structure (Ishimaru et al., 2001), onion-like structure (Derenne and Largeau, 2001), fullerene structure (Harris et al., 2000), ribbon-like structure (Ban et al., 1975) and randomly ordered strip segment structure (Franklin, 1951), which were proposed based on experimental observations. Although a BC particle may bear various nano-structures, such as an onion-like structure or a diamond structure (Ishimaru et al., 2001), C layer orientation of 600-BC in this study was rather similar to a model by Franklin (1951) for non-graphitizing C, while that of 350-BC was dominantly amorphous in structure. However, graphite-like structures (Fig. IV.2D), onion-like or fullerene-like structures (Fig. IV.2B), and amorphous structures (Figs. IV.2A and IV.2C) were also visible in some areas from TEM images captured from the studied BC materials.

The effect of charring temperature has been reported to include (a) thermal breaking of cross-links connecting crystallite planes and (b) gradual movement of a whole plane or a group of planes (Franklin, 1951) for parallel rearrangement of C layers, resulting in a more parallel arrangement in BC formed at 600°C than at 350°C in this study (Fig. IV.2). Likewise Harris and Tsang (1997) showed an improved ordered structure of Saran carbon when increasing the carbonization temperature. Because the orientation status of C layers in the BC precursor may also influence the rearrangement of C layers upon heating (Franklin, 1951), better arrangement of C layers in oak-350-BC (Fig. IV.2C) than in corn-350-BC (Fig. IV.2) led to better parallel order of C layers in oak-600-BC (Fig. IV.2D) than in corn-600-BC (Fig. IV.2B), respectively. Moreover, TEM images derived from oak-600-BC even showed some well ordered areas at

which a lattice of graphene-like structure was clearly visible. However, as a result of increased charring temperature, a greater change in nano-structures was observed in corn-BC than in oak-BC (Fig. IV.2) due to a less-ordered structure in corn-350-BC than in oak-350-BC.

High production temperatures also increased the length of C layers, appearing in strip segments (Fig. IV.2), which were shorter in corn-350-BC than in any other studied materials. During pyrolysis, the segments of C layers may first be thermally separated (Franklin, 1951) and move closer to each other, forming nano-particles (Harris and Tsang, 1997), or even join together, forming longer C layer segments than before pyrolysis. Consequently, more pronounced parallel structures were visible in 600-BC than in 350-BC (Fig. IV.2), combined with higher C concentrations (Table IV.1).

IV.4.b. BC degradation and temperature coefficient (Q_{10})

The Q_{10} values in this study varied from 1.01 to 5.79 and are consistent with Q_{10} ranges from 1 to 8, calculated through CO_2 evolution and N dynamics from incubated soils (Kirschbaum, 1995). In addition, Q_{10} calculated for the temperature range from 5 to 15°C in this study was comparable to that of about 3.4, reported by Cheng et al. (2008b) for hard wood-derived BC in the eastern United States. For temperatures between 4 and 10°C, Q_{10} values of BC materials in this study ranged from 1.6-5.7, and decreased rapidly with increasing incubation temperature, resulting in less difference in Q_{10} values between materials at high incubation temperatures. The temperature coefficient of organic matter decomposition is not constant, but rather decreases as temperature increases (Kirschbaum, 1995; Townsend et al., 1997; Davidson and Janssens, 2006).

Based on Q_{10} values (Fig. IV.6) decomposition of more stable BC (which decomposed the least), such as oak-BC formed at 600°C increased to a greater extent as a result of increased incubation temperature than that of more labile BC material, such as corn-BC formed at 350°C. This finding is in agreement with other authors such as Agren (2000), Knorr et al. (2005), and Davidson and Janssens (2006), who hypothesized that the degradation of the resistant SOC fraction would be more sensitive to temperature increase than that of labile SOC. Likewise Fierer et al. (2005) concluded that decomposition of poorer-quality litter was more sensitive to temperature increases than that of better-quality matter. Recently Conant et al. (2008) also reported a rise in temperature sensitivity of soil C decomposition upon depletion of soil labile C.

However, other studies demonstrated different result. Fang et al. (2005) and Czimczik and Trumbore (2007) found the same mineralization rates of labile and resistant SOC pools with increased temperature, based on an incubation experiment. Similarly, Reichstein et al. (2005b) showed no difference in Q_{10} values of SOC in organic and mineral horizons. Moreover, other studies report no difference in temperature sensitivity at all (Liski et al., 1999; Giardina and Ryan, 2000). The differences in experiments showing an increased temperature sensitivity with lower C quality were explained by Davidson and Janssens (2006) with resource limitation due to aggregation or organo-mineral interactions, which was not the case in our incubation studies that were conducted in a sand medium.

In contrast to the greater relative temperature sensitivity of the more stable BC especially at lower temperature as shown by the Q_{10}, more labile BC materials, corn-BC, showed a greater response in absolute C loss to a rise in temperature than oak-BC at the same temperature range. The decomposing fraction of corn-350-BC was most sensitive at lowest incubation temperature, while corn-600-BC and oak-350-BC

contained the highest proportion that was most sensitive to temperature changes from 10 to 20°C and oak-600-BC had the highest portion of C loss at 20°C (Fig. IV.5). As a result, it may be assumed that the BC materials may be composed of different fractions, which were different in their response to temperature changes. The least stable fraction, which was mostly decomposable at a low temperature of 4°C, was significantly more abundant in corn-350-BC than in the other materials. This fraction accounted for about 53% of the total C loss of corn-350-BC during the first year of incubation. The fraction that was mostly decomposable at temperatures from 10-20°C was found to the greatest extent in corn-600-BC and oak-350-BC, accounting for around 25-27% of total C loss. The stable fraction, decomposable to the greatest extent at 20°C, was most abundant in oak-600-BC, accounting for 25% of the mineralized fraction of the material. The BC fraction that decomposed at the lowest incubation temperature likely contains the mostly labile compounds, such as aliphatic C of carbohydrates. These compounds constitute an important portion of plant tissues, and the original structure was still visible in BC derived from corn and oak biomass (Fig. IV.1). The fraction that disappeared at higher incubation temperature increasingly contains aromatic compounds, which are highly resistant to decomposition. This has to be considered when interpreting the Q_{10} and absolute decomposition rates at different incubation temperatures.

IV.4.c. BC degradation mechanisms

We observed a significant relationship between O/C ratio or change in O/C ratio and remaining C (Fig. IV.9). This indicates that the major mechanism mineralizing the studied BC greatly involved either abiotic or biotic oxidation or both. This conclusion was also reached for degradation of BC from black locust wood (Cheng et al., 2006), and of fossilized charcoal (Cohen-Ofri et al., 2007).

Continuously increasing C loss in response to higher temperature in our study is equivalent to CO_2 evasion, as no other losses occurred from the incubation vessels. Whereas in our study, CO_2 emissions approached a plateau, Holland et al. (2000) reported an exponential rise of CO_2 respiration from incubated soils as a function of temperature increases to 55°C. These authors attributed the released CO_2 to biological processes by bacteria and fungi. Similar exponential increase in CO_2 was also observed by Peterjohn et al. (1994) for a temperature range from 5 to 30°C. However, Qureshi et al. (2003) observed the highest microbial respiration rate at 28°C, while further increasing the temperature to 38°C resulted in lowered CO_2 released from peat-glucose-yeast extract system. In our study, we observed a slight increase in C loss at incubation temperatures higher than 30°C, indicating that abiotic oxidation likely occurred and may have been dominant at temperatures beyond 30°C and the importance of microbial decay decreased with a rise in incubation temperature.

The micro and nano-structure of BC is likely important for determining BC stability, as decomposition first occurs at active sites such as particle surfaces (Lehmann et al., 2005; Cheng et al., 2006; Nguyen et al., 2008). This may also apply to the edge of individual C layers or to sites of defect structures in C layers. According to Pierson (1993, p63), the reason is the greater energy state at the edges of a layer or at the ends of basal layers than in the basal plane which results in stronger oxidative reaction on edges than on basal planes. Apart from greater mineralization reactions, the materials having more active sites may also interact to a greater extent with soil minerals, resulting in better protection of BC from further oxidation. However, BC in this study was mixed with pure sand material; therefore, such protecting mechanism may be negligible or even be absent.

The chemical recalcitrance of these nano-composites is also a function of the way in which the C-C bonds are arranged. Corn-BC produced at low charring temperature had a less ordered structure resembling amorphous C (Fig. IV.2), which likely had a high quantity of reactive sites, and thereby a low stability. In contrast, the BC produced at higher temperature (especially oak-BC) appeared to show a greater degree of order, which may explain the increased stability by a reduction of active sites. As a consequence, the biomass type (corn or oak) had a greater effect on stability at lower charring temperatures than at higher charring temperatures. Moreover, an increase of internal surface area through a less ordered structure (Harris, 2005) may decrease its stability. In addition, increasing charring temperature typically shows longer crystallite sizes (Lu et al., 2000) which further reduces the number of active sites (Pierson, 1993, p64). According to Harris (2005), perfect layers of graphene sheets in graphite are held together by comparatively weak van-der-Waals forces, whereas unordered turbostratic C or even folded fullerene structures are much more stable, which can increasingly be seen at greater charring temperature.

In addition to the BC structure itself, nutrient contents may also affect BC mineralization as we observed a higher content of N, K and Ca in corn-BC than in oak-BC (Table IV.1). The amount of added minerals was negligible, relative to those contained in the materials (Table III.2). In fact, Fierer et al. (2003) reported a great increase in CO_2 release in subsurface soil but negligible change in surface soil as a consequence of N and P addition and they attributed the influence of N and P addition to an enhanced production of enzymes required for C mineralization in the nutrient-limited environment.

BC oxidation did not only lead to C loss but also to an increase in negative surface charge (CECp) through formation of carboxylic groups by oxidation on the edges of

the aromatic backbone (Glaser et al., 2002). As a result, Liang et al. (2006) showed that oxidation of BC was the main reason for the high CEC of Anthrosols from the Brazilian Amazon. In this study we also observed a significant relationship (R^2= 0.58) between O/C ratios and CECp or between the change in O/C ratios and the change in CECp (Fig. IV.9), indicating the importance of oxidative processes in enhancing total negative charge density of BC materials after one year of incubation.

IV.5. Conclusion

Black C structure and properties were significantly controlled by charring temperature and biomass type. BC produced at high production temperature had better orientation of C layers than from low temperature, and material derived from corn residue was more porous and had higher mineral contents than those derived from oak wood. As a consequence, the mineralization rate of corn residues charred at 350°C was much greater than that formed from oak wood at 600°C. However, the temperature sensitivity of decomposition of the more stable materials (those which mineralized the least) was greater than that of the more labile materials. Both abiotic as well as biotic oxidation was recognized to be an important process in governing BC decomposition. However, the relative importance of the BC structure at micro- and nano-scale in comparison to the role of minerals, such as N and K, for BC mineralization is still poorly understood and requires studies using BC materials controlled for structure and mineral content. Because the studied BC was composed of different fractions differing in stability, determination of Q_{10} values from fresh BC may interfere with the proportion of the fraction between BC types and between different incubation temperatures. Therefore, studies of temperature sensitivity targeting aged BC are needed.

REFERENCES

Agren, G.I., 2000. Temperature dependence of old soil organic matter. Ambio 29, 55-55.

Antal, M.J., and Grønli, M., 2003. The art, science, and technology of charcoal production. Industrial & Engineering Chemistry Research 42, 1619-1640.

Bala, G., Caldeira, K., Mirin, A., Wickett, M., Delire,C., 2005. Multicentury changes to the global climate and carbon cycle: Results from a coupled climate and carbon cycle model. Journal of Climate 18, 4531-4544.

Ban, L.L., Crawford, D., Marsh. H., 1975. Lattice-Resolution Electron-Microscopy in Structural Studies of Non-Graphitizing Carbons from Polyvinylidene Chloride (Pvdc). Journal of Applied Crystallography 8, 415-420.

Bourke, J., Manley-Harris, M., Fushimi, C., Dowaki, K., Nunoura, T., Antal. M.J., 2007. Do all carbonized charcoals have the same chemical structure? 2. A model of the chemical structure of carbonized Charcoal. Industrial & Engineering Chemistry Research 46, 5954-5967.

Brodowski, S. B., 2004. Origin, Function, and Reactivity of Black Carbon in the Arable Soil Environment, PhD thesis, University of Bayreuth, Bayreuth, Germany.

Brodowski, S., Amelung, W., Haumaier, L., Abetz, C., Zech, W., 2005. Morphological and chemical properties of black carbon in physical soil fractions as revealed by scanning electron microscopy and energy-dispersive X-ray spectroscopy. Geoderma 128, 116–129.

Cheng, C.H., Lehmann, J., Engelhard, M.H., 2008a. Natural oxidation of black carbon in soils: Changes in molecular form and surface charge along a climosequence. Geochimica et Cosmochimica Acta 72, 1598-1610.

Cheng, C.H., Lehmann, J., Thies, J.E., Burton, S.D., 2008b. Stability of black carbon in soils across a climatic gradient. Journal of Geophysical Research-Biogeosciences 113, G02027.

Cheng, C.H., Lehmann, J., Thies, J.E., Burton, S.D., Engelhard, M.H., 2006. Oxidation of black carbon by biotic and abiotic processes. Organic Geochemistry 37, 1477-1488.

Cohen-Ofri, I., Popovitz-Biro, R., Weiner, S., 2007. Structural characterization of modern and fossilized charcoal produced in natural fires as determined by using electron energy loss spectroscopy. Chemistry-a European Journal 13, 2306-2310.

Conant, R.T., Steinweg, J.M., Haddix, M.L., Paul, E.A., Plante, A.F., Six, J., 2008. Experimental warming shows that decomposition temperature sensitivity increases with soil organic matter recalcitrance. Ecology 89, 2384-2391.

Czimczik, C. I., Trumbore, S. E., 2007. Short-term controls on the age of microbial carbon sources in boreal forest soils. Journal of Geophysical Research-Biogeosciences 112, G03001.

Davidson E.A., Janssens, I.A., 2006. Temperature sensitivity of soil carbon decomposition and feedbacks to climate change. Nature 440, 165-173.

Derenne, S., Largeau, C., 2001. A review of some important families of refractory macromolecules: Composition, origin, and fate in soils and sediments. Soil Science 166, 833-847.

Fang, C.M., Smith, P., Moncrieff, J.B., Smith, J.U., 2005. Similar response of labile and resistant soil organic matter pools to changes in temperature. Nature 433, 57-59.

Fierer, N., Allen, A.S., Schimel, J.P., Holden, P.A., 2003. Controls on microbial CO_2 production: a comparison of surface and subsurface soil horizons. Global Change Biology 9, 1322-1332.

Fierer, N., Craine, J.M., McLauchlan, K., Schimel, J.P., 2005. Litter quality and the temperature sensitivity of decomposition. Ecology 86, 320-326.

Franklin, R.E., 1951. Crystallite Growth in Graphitizing and Non-Graphitizing Carbons. Proceedings of the Royal Society of London Series A-Mathematical and Physical Sciences 209, 196-217.

Giardina, C.P., Ryan, M.G., 2000. Evidence that decomposition rates of organic carbon in mineral soil do not vary with temperature. Nature 404, 858-861.

Glaser, B., Balashov, E., Haumaier, L., Guggenberger, G., Zech, W., 2000. Black carbon in density fractions of anthropogenic soils of the Brazilian Amazon region. Organic Geochemistry 31, 669-678.

Glaser, B., Lehmann, J., Zech, W., 2002. Ameliorating physical and chemical properties of highly weathered soils in the tropics with charcoal – a review. Biology and Fertility of Soils 35, 219–230.

Hamer, U., Marschner, B., Brodowski, S., Amelung, W., 2004. Interactive priming of black carbon and glucose mineralization. Organic Geochemistry 35, 823–830.

Harris, P.J.F., 2005. New perspectives on the structure of graphitic carbons. Critical Reviews in Solid State and Materials Sciences 30, 235-253.

Harris, P.J.F., Burian, A., Duber, S., 2000. High-resolution electron microscopy of a microporous carbon. Philosophical Magazine Letters 80, 381-386.

Harris, P.J.F., Tsang, S.C., 1997. High-resolution electron microscopy studies of non-graphitizing carbons. Philosophical Magazine A-Physics of Condensed Matter Structure Defects and Mechanical Properties 76, 667-677.

Haumaier, L., Zech, W., 1995. Black carbon - possible source of highly aromatic components of soil humic acids. Organic Geochemistry 23, 191-196.

Holland, E.A., Neff, J.C., Townsend, A.R., McKeown, B., 2000. Uncertainties in the temperature sensitivity of decomposition in tropical and subtropical ecosystems: Implications for models. Global Biogeochemical Cycles 14, 1137-1151.

Ishimaru, K., Vystavel, T., Bronsveld, P., Hata, T., Imamura, Y., De Hosson, J., 2001. Diamond and pore structure observed in wood charcoal. Journal of Wood Science 47, 414-416.

Kim, N.H., Hanna, R.B., 2006. Morphological characteristics of Quercus variabilis charcoal prepared at different temperatures. Wood Science and Technology 40, 392-401.

Kima, S., Kaplanb, L.A., Bennerc, R., Hatcher, P.G., 2004. Hydrogen-deficient molecules in natural riverine water samples—evidence for the existence of black carbon in DOM Marine. Chemistry 92, 225– 234.

Kirschbaum, M.U.F., 1995. The temperature-dependence of soil organic matter decomposition, and the effect of global warming on soil organic-C storage. Soil Biology & Biochemistry 27,753-760.

Knorr, W., Prentice, I.C., House, J.I., Holland, E.A., 2005. Long-term sensitivity of soil carbon turnover to warming. Nature 433, 298-301.

Koelmans, A.A., Jonker, M.T.O., Cornelissen, G., Bucheli, T.D., Van Noort, P.C.M., Gustafsson, O.R., 2006. Black carbon: The reverse of its dark side. Chemosphere 63, 365–377.

Kuhlbusch, T.A.J., 1995. Method for Determining Black Carbon in Residues of Vegetation Fires. Environmental Science & Technology. 29. 2695-2702.

Labbe, N., Harper, D., Rials, T., 2006. Chemical structure of wood charcoal by infrared spectroscopy and multivariate analysis. Journal of Agricultural and Food Chemistry 54, 3492-3497.

Lehmann, J., Liang, B.Q., Solomon, D., Lerotic, M., Luizao, F., Kinyangi, J., Schafer, T., Wirick, S., Jacobsen, C., 2005. Near-edge X-ray absorption fine structure (NEXAFS) spectroscopy for mapping nano-scale distribution of organic carbon forms in soil: Application to black carbon particles. Global Biogeochemical Cycles 19. GB1013.

Liang, B., Lehmann, J., Solomon, D., Kinyangi, J., Grossman, J., O'Neill, B., Skjemstad, J. O., Thies, J., Luiza˜o, F. J., Petersen, J., Neves, E. G., 2006. Black carbon increases cation exchange capacity in soils, Soil Science Society of America Journal 70, 1719–1730.

Liski, J., Ilvesniemi, H., Makela, A., Westman, C.J., 1999. CO_2 emissions from soil in response to climatic warming are overestimated - The decomposition of old soil organic matter is tolerant of temperature, Ambio 28, 171-174.

Lu, L.M., Sahajwalla, V., Harris, D., 2000. Characteristics of chars prepared from various pulverized coals at different temperatures using drop-tube furnace. Energy & Fuels 14, 869-876.

Marschner, B., Brodowski, S., Dreves, A., Gleixner, G., Gude, A., Grootes, P.M., Hamer, U., Heim, A., Jandl, G., Ji, R., Kaiser, K., Kalbitz, K., Kramer, C., Leinweber, P., Rethemeyer, J., Schaeffer, A., Schmidt, M.W.I., Schwark, L., Wiesenberg, G.L.B., 2008. How relevant is recalcitrance for the stabilization of organic matter in soils? Journal of Plant Nutrition and Soil Science-Zeitschrift für Pflanzenernährung und Bodenkunde 171, 91-110.

Mochidzuki, K., Soutric, F., Tadokoro, K., Antal, M.J., Toth, M., Zelei, B., Varhegyi, G., 2003. Electrical and physical properties of carbonized charcoals. Industrial & Engineering Chemistry Research 42, 5140-5151.

Nguyen TB, Lehmann, J., 2009. Black carbon degradation under varying water regimes. Organic Geochemistry, submitted.

Nguyen, B.T., Lehmann, J., Kinyangi, J., Smernik, R., Riha, S.J., Engelhard, M.H., 2008. Long-term black carbon dynamics in cultivated soil. Biogeochemistry 89, 295-308.

Nishimiya, K., Hata, T., Imamura, Y., Ishihara, S., 1998. Analysis of chemical structure of wood charcoal by X-ray photoelectron spectroscopy. Journal of Wood Science 44, 56-61.

Peterjohn, W.T., Melillo, J.M., Steudler, P.A., Newkirk, K.M., Bowles, F.P., Aber, J.D., 1994. Responses of trace gas fluxes and N availability to experimentally elevated soil temperatures. Ecological Applications 4, 617-625.

Pierson, H.O, 1993. Handbook of carbon, graphite, diamond and fullerenes properties, processing and applications, Noyes Publications Park Ridge, New Jersey, U.S.A.

Qureshi, S., Richards, B.K., McBride, M.B., Baveye, P., Steenhuis, T.S., 2003. Temperature and microbial activity effects on trace element leaching from metalliferous peats. Journal of Environmental Quality 32, 2067-2075.

Reichstein, M., Subke, J.A., Angeli, A.C., Tenhunen, J.D., 2005b. Does the temperature sensitivity of decomposition of soil organic matter depend upon water content, soil horizon, or incubation time? Global Change Biology 11, 1754-1767.

Reichstein, M., Katterer, T., Andren, O., Ciais, P., Schulze, E.D., Cramer, W., Papale, D., Valentini, R., 2005a. Temperature sensitivity of decomposition in relation to soil organic matter pools: critique and outlook. Biogeosciences 2, 317-321.

Schmidt, M.W.I., Noack, A.G., 2000. Black carbon in soils and sediments: Analysis, distribution, implications, and current challenges, Global Biogeochemical Cycles 14, 777-793.

Schmidt, M.W.I., Skjemstad, J.O., Jäger, C., 2002. Carbon isotope geochemistry and nanomorphology of soil black carbon: Black chernozemic soils in central Europe originate from ancient biomass burning, Global Biogeochemical Cycles 16, GB1123.

Schmidt, M.W.I., Skjemstad, J.O., Gehrt, E., Kögel-Knabner, I., 1999. Charred organic carbon in German chernozemic soils. European Journal of Soil Science 50, 351-365.

Swift, R.S., 2001. Sequestration of carbon by soil Soil Science 166, 858–871.

Townsend, A.R., Vitousek, P.M., Desmarais, D.J., Tharpe, A., 1997. Soil carbon pool structure and temperature sensitivity inferred using CO_2 and $^{13}CO_2$ incubation fluxes from five Hawaiian soils. Biogeochemistry 38, 1-17.

CHAPTER 5

GENERAL CONCLUSION AND SUGGESTIONS

Conclusions

Black carbon is not a completely inert material; rather it changes over time at varying decomposition rates, depending on its quality and the prevailing environmental conditions. In cultivated soil, both quality and quantity of BC changed at decadal timescale before reaching a steady state. The relatively short mean residence times of BC in cultivated soil may reflect the nature of human activity, which accelerated BC disappearances from the topsoil layer. It is important to notice that the rapid observed BC loss in the 0-0.1m soil layer may also be due to leaching from the topsoil into the subsoil or due to erosion by water and wind in addition to mineralization to CO_2. Additionally, rapid change in BC quantity and quality may also result from high annual temperature and rainfall in south Nandy – western Kenya. These two environmental factors are well known to influence soil microbial activity, community and therefore SOC stability and content. Other soil processes, such as adsorption of non-BC organic matter or interaction with soil minerals may also be important mechanisms prolonging BC stability and residence time in the soil.

The stability of BC was controlled by charring temperature, biomass type and environmental factors, such as water regime and temperature. The first two factors mostly influenced BC properties, such as mineral content, nano- and micro-structure. BC formed by carbonizing corn residue at lower temperature such as 350°C was more labile than that produced from oak wood at higher temperature such as at 600°C.

The major mechanisms controlling BC stability in our studies were both biotic and abiotic oxidation. As a result, availability of oxygen was important in determining BC

stability and decomposition. Oxygen availability was, in turn, largely controlled by water regime, for which aerobic conditions were expected to provide more O than waterlogged conditions. Consequently, mineralization and oxidation were greater under aerobic than from waterlogged conditions. Oxidation was recognized to start from surfaces of BC particles and to penetrate into interior over long periods of time. Because of this slow process during which oxidation penetrated BC particles, in the relative short-term incubation experiments, changes in BC quality characterized by FTIR were not as profound as that in CECp and pH, which reflected surface properties.

BC stability was also significantly determined by environmental temperature. The more stable BC was more sensitive to decomposition under a warmer environment than the more labile material.

Suggestions for further research

The results obtained stimulated recommendations for further research:

- Downward movement of BC particles was recognized to be a potential mechanism responsible for the short mean residence times in topsoils. This mechanism needs to be verified and thus requires more research. In addition, study of BC movement may also reveal potential changes in BC quality in subsoil layers.

- Under waterlogged conditions, BC loss was also observed, but the controlling mechanism is unclear as oxidation by oxygen is likely small. More research is needed to address this question.

- BC quality determined its stability, as shown in Chapters 3 and 4. A number of parameters, such as mineral content, aromaticity and nano- and micro-structure, may be responsible. However, the relative importance of each factor for BC stability remained unclear.

- Increasing charring temperature resulted in enhanced BC stability. The reason for this relationship lies in the nano-structure and aromaticity of BC. Further increasing charring temperature may lead to even better arrangement of C layers and increasing aromaticity, and hence greater stability. This is an important point to be tested.

APPENDIX

Appendix Table III.1. Carbon loss (% for the first year) of 12 cross combinations. Values followed by the same letter were not significantly different (means and standard deviation (SD), N=8)

Biomass types	Charring temp. (°C)	Aerobic		Waterlogged		Cycle	
		%	SD	%	SD	%	SD
Corn residue	350	21.21[a]	6.56	10.90[bcd]	9.18	15.38[ab]	5.70
	600	11.21[bcd]	1.41	9.43[bcd]	7.06	10.37[bcd]	8.01
Oak wood	350	8.08[cd]	4.17	6.15[d]	4.55	13.86[bc]	7.29
	600	8.90[cd]	5.18	8.61[cd]	4.67	9.84[bcd]	6.45

Appendix Table III.2. ANOVA of C loss (* for P<0.05; ns for P>0.05)

Source	DF	Sum of squares	F ratio	Prob. > F	
Water regime	2	396	5.2	0.007	*
Biomass type	1	502	13.2	0.001	*
Water regime*Biomass type	2	288	3.8	0.027	*
Charring Temp.	1	199	5.2	0.025	*
Water regime* Charring Temp.	2	135	1.8	0.177	ns
Biomass type* Charring Temp.	1	165	4.3	0.040	*
Water regime*Biomass type* Charring Temp.	2	102	1.3	0.269	ns
Error	84	3197			

Appendix Table III.3. O/C ratios of 12 cross combinations. Numbers attached by the same letter were not significantly different (means and standard deviation (SD), N=8)

Biomass types	Charring temp. (°C)	Aerobic		Waterlogged		Cycle	
		O/C	SD	O/C	SD	O/C	SD
Corn residue	350	0.50[a]	0.18	0.38[b]	0.06	0.48[a]	0.09
	600	0.24[cd]	0.11	0.20[de]	0.07	0.23[cd]	0.08
Oak wood	350	0.35[b]	0.07	0.31[bc]	0.05	0.35[b]	0.13
	600	0.15[de]	0.04	0.13[e]	0.06	0.14[e]	0.03

Appendix Table III.4. ANOVA of O/C ratios (* for P<0.05; ns for P>0.05)

Source	DF	Sum of squares	F ratio	Prob. > F	
Water regime	2	0.06	3.65	0.030	*
Biomass type	1	0.15	18.67	<.0001	*
Water regime*Biomass type	2	0.01	0.85	0.433	ns
Charring Temp.	1	1.10	134.55	<.0001	*
Water regime* Charring Temp.	2	0.01	0.84	0.437	ns
Biomass type* Charring Temp.	1	0.00	0.57	0.452	ns
Water regime*Biomass type* Charring Temp.	2	0.00	0.20	0.818	ns
Error	84	0.69			

Appendix Table III.5. CECp (mmole (+) $kg^{-1}C$) of 12 cross combinations. Numbers attached by the same letter were not significantly different (means and standard deviation (SD), N=8)

Biomass types	Charring temp. (°C)	Aerobic		Waterlogged		Cycle	
		CECp	SD	CECp	SD	CECp	SD
Corn residue	350	1395[a]	326	856[c]	170	1046[b]	179
	600	616[d]	292	391[efg]	125	555[de]	267
Oak wood	350	251[fg]	54	253[fg]	90	418[ef]	228
	600	235[fg]	62	229[g]	61	241[fg]	120

Appendix Table III.6. ANOVA table of CECp (* for P<0.05; ns for P>0.05)

Source	DF	Sum of squares	F ratio	Prob. > F	
Water regime	2	598650	8.5	0.0005	*
Biomass type	1	7516084	212.3	<.0001	*
Water regime*Biomass type	2	746675	10.5	<.0001	*
Charring Temp.	1	2544759	71.9	<.0001	*
Water regime* Charring Temp.	2	94951	1.3	0.2671	ns
Biomass type* Charring Temp.	1	1533182	43.3	<.0001	*
Water regime*Biomass type* Charring Temp.	2	213764	3.0	0.0542	ns
Error	84	2973422			

Appendix Table III.7. pH (1:20 w/v water) of 12 cross combinations. Numbers attached by the same letter were not significantly different (means and standard deviation (SD), N=8)

Biomass types	Charring temp. (°C)	Aerobic		Waterlogged		Cycle	
		pH	SD	pH	SD	pH	SD
Corn residue	350	6.79[d]	0.37	7.06[c]	0.37	6.64[d]	0.21
	600	8.11[a]	0.29	7.80[b]	0.30	7.59[b]	0.25
Oak wood	350	4.54[e]	0.22	4.66[e]	0.13	4.62[e]	0.18
	600	4.69[e]	0.16	4.66[e]	0.11	4.75[e]	0.11

Appendix Table III.8. ANOVA of pH values (* for P<0.05; ns for P>0.05)

Source	DF	Sum of squares	F ratio	Prob. > F	
Water regime	2	0.49	4.14	0.0192	*
Biomass type	1	59.41	1014.57	<.0001	*
Water regime*Biomass type	2	0.29	2.52	0.0867	ns
Charring Temp.	1	7.25	123.75	<.0001	*
Water regime* Charring Temp.	2	0.53	4.56	0.0132	*
Biomass type* Charring Temp.	1	4.97	84.89	<.0001	*
Water regime*Biomass type* Charring Temp.	2	0.19	1.65	0.1975	ns
Error	84				

Appendix Table III.9. Full data of C loss, O/C ratio, CECp and pH of chapter 3

Replicate	Water regimes	Biomass types	Charring Temp. (°C)	C loss (%)	O/C ratio	CECp (mmole(+)/kg C^{-1})	pH
1	Aerobic	Corn residue	350	27.74	0.53	1153	7.04
			600	12.75	0.28	384	8.33
		Oak wood	350	9.87	0.35	351	4.53
			600	6.12	0.12	207	4.52
	Waterlogged	Corn residue	350	7.47	0.34	611	6.82
			600	6.55	0.20	167	8.16
		Oak wood	350	0.83	0.27	269	4.58
			600	2.99	0.08	185	4.55
	Cycle	Corn residue	350	11.78	0.42	896	6.87
			600	5.67	0.28	336	8.03
		Oak wood	350	2.93	0.24	151	4.92
			600	20.02	0.15	131	4.89
2	Aerobic	Corn residue	350	9.36	0.27	918	7.24
			600	9.08	0.29	181	8.39
		Oak wood	350	6.40	0.28	241	4.53
			600	14.52	0.19	145	4.65
	Waterlogged	Corn residue	350	32.93	0.48	822	7.06
			600	9.65	0.18	338	8.07
		Oak wood	350	0.76	0.25	249	4.48
			600	15.60	0.07	287	4.55
	Cycle	Corn residue	350	18.16	0.48	882	6.78
			600	-1.48	0.18	304	7.54
		Oak wood	350	19.12	0.52	218	4.79
			600	1.14	0.11	171	4.60

Appendix Table III.9. Full data of chapter 3 (Continues)

Replicate	Water regimes	Biomass types	Charring Temp. (°C)	C loss (%)	O/C ratio	CECp (mmole(+)/kg C^{-1})	pH
3	Aerobic	Corn residue	350	22.94	0.64	1383	6.96
			600	10.06	0.22	830	8.27
		Oak wood	350	9.89	0.40	227	4.57
			600	14.88	0.15	188	4.75
	Waterlogged	Corn residue	350	5.35	0.30	761	7.03
			600	-1.38	0.13	504	7.62
		Oak wood	350	14.26	0.38	174	4.71
			600	5.29	0.14	152	4.81
	Cycle	Corn residue	350	15.26	0.64	1194	6.59
			600	9.59	0.25	981	7.62
		Oak wood	350	17.12	0.36	722	4.77
			600	5.45	0.12	392	4.90
4	Aerobic	Corn residue	350	26.33	0.42	1902	6.70
			600	12.00	0.36	718	8.07
		Oak wood	350	11.90	0.45	259	4.57
			600	9.14	0.21	205	4.83
	Waterlogged	Corn residue	350	5.57	0.37	1118	7.06
			600	1.72	0.13	520	7.83
		Oak wood	350	5.84	0.31	168	4.74
			600	9.41	0.21	275	4.75
	Cycle	Corn residue	350	12.79	0.50	1397	6.96
			600	17.22	0.32	880	7.57
		Oak wood	350	9.78	0.21	703	4.46
			600	13.28	0.15	141	4.78

Appendix Table III.9. Full data of chapter 3 (Continues)

Replicate	Water regimes	Biomass types	Charring Temp. (°C)	C loss (%)	O/C ratio	CECp (mmole(+)/kg C^{-1})	pH
5	Aerobic	Corn residue	350	26.07	0.32	1827	6.06
			600	11.67	0.34	473	7.91
		Oak wood	350	-0.38	0.23	280	4.96
			600	14.32	0.19	342	4.63
	Waterlogged	Corn residue	350	12.57	0.43	914	6.94
			600	18.52	0.32	489	7.51
		Oak wood	350	8.95	0.34	232	4.66
			600	11.60	0.14	305	4.58
	Cycle	Corn residue	350	7.94	0.45	1010	6.54
			600	19.62	0.29	484	7.77
		Oak wood	350	25.46	0.44	303	4.54
			600	3.17	0.12	437	4.76
6	Aerobic	Corn residue	350	16.97	0.38	1327	7.09
			600	9.66	0.19	478	8.11
		Oak wood	350	10.69	0.39	239	4.62
			600	2.58	0.11	266	4.85
	Waterlogged	Corn residue	350	6.67	0.37	712	6.56
			600	8.98	0.13	362	7.54
		Oak wood	350	3.15	0.26	424	4.90
			600	2.57	0.06	268	4.62
	Cycle	Corn residue	350	15.55	0.33	1045	6.50
			600	4.93	0.29	512	7.67
		Oak wood	350	6.67	0.22	373	4.45
			600	14.78	0.20	178	4.61

Appendix Table III.9. Full data of chapter 3 (Continues)

Replicate	Water regimes	Biomass types	Charring Temp. (°C)	C loss (%)	O/C ratio	CECp (mmole(+)/kg C^{-1})	pH
7	Aerobic	Corn residue	350	15.38	0.66	1348	6.59
			600	11.73	0.02	1103	8.29
		Oak wood	350	5.02	0.32	158	4.28
			600	7.11	0.14	241	4.46
	Waterlogged	Corn residue	350	8.14	0.34	853	7.85
			600	14.61	0.24	464	8.18
		Oak wood	350	7.22	0.35	335	4.55
			600	12.44	0.20	199	4.62
	Cycle	Corn residue	350	14.23	0.51	881	6.34
			600	6.63	0.08	270	7.20
		Oak wood	350	12.82	0.30	260	4.44
			600	8.10	0.12	305	4.75
8	Aerobic	Corn residue	350	24.86	0.79	1303	6.69
			600	12.70	0.22	762	7.50
		Oak wood	350	11.22	0.42	255	4.26
			600	2.55	0.09	282	4.88
	Waterlogged	Corn residue	350	8.52	0.41	1053	7.16
			600	16.79	0.27	282	7.51
		Oak wood	350	8.16	0.35	174	4.64
			600	8.95	0.16	159	4.78
	Cycle	Corn residue	350	27.34	0.48	1066	6.53
			600	20.83	0.17	673	7.36
		Oak wood	350	16.99	0.51	617	4.59
			600	12.78	0.11	172	4.70

Appendix Figure IV.1a. SEM images of corn-BC formed at 350 and 600°C

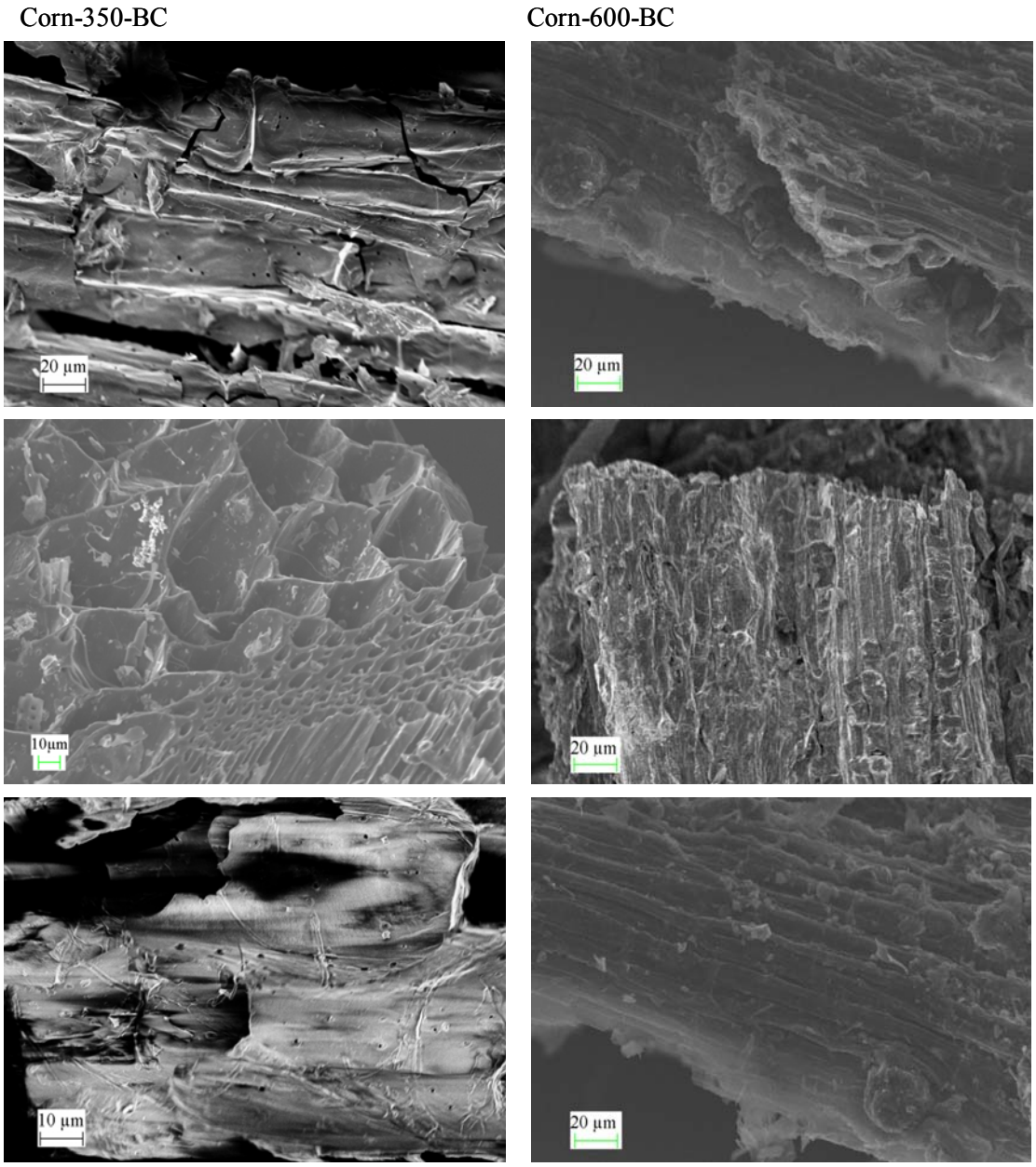

Appendix Figure IV.1b. SEM images of oak-BC formed at 350 and 600°C

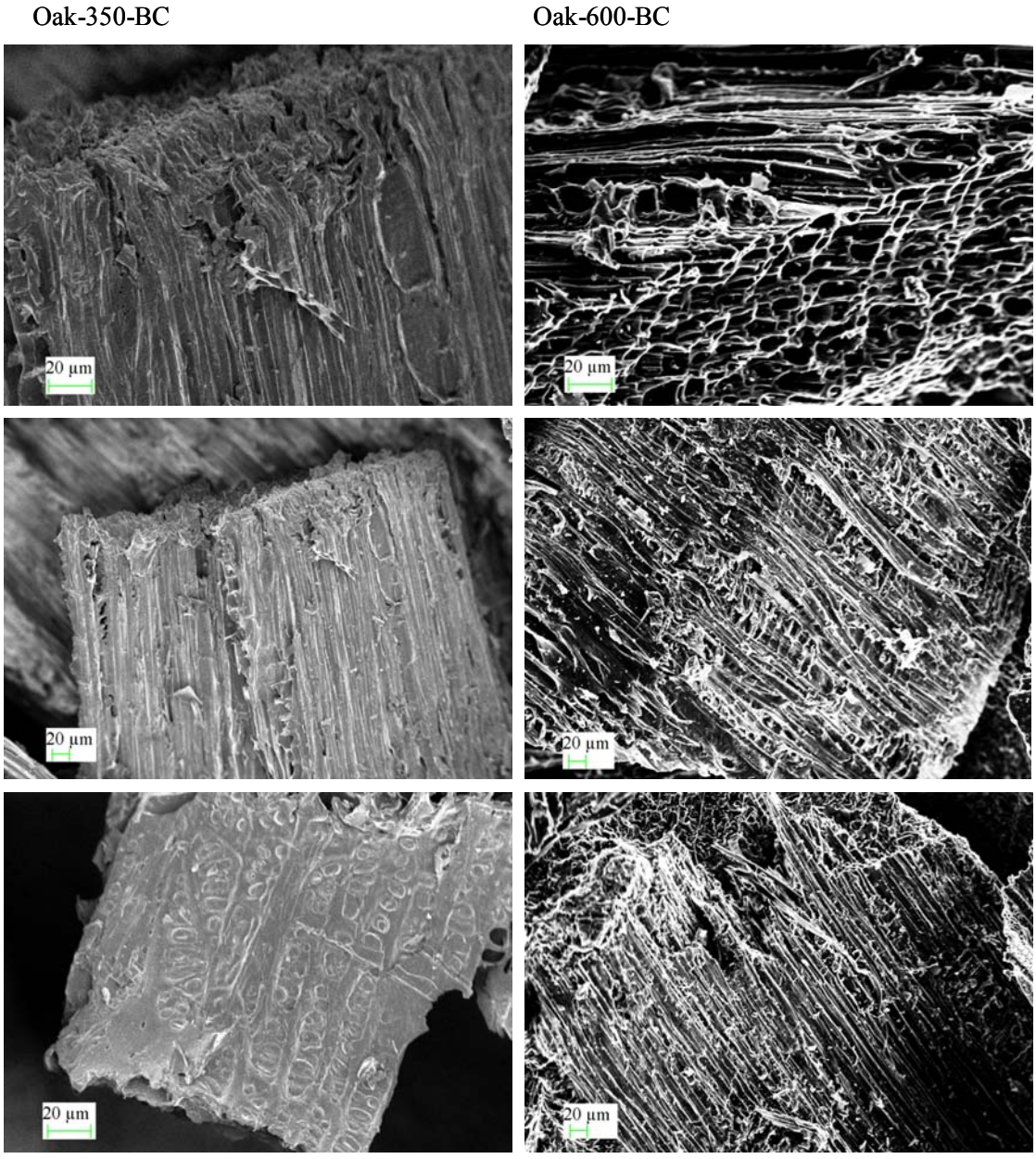

Appendix Figure IV.2a. TEM images of corn-BC formed at 350 and 600 °C

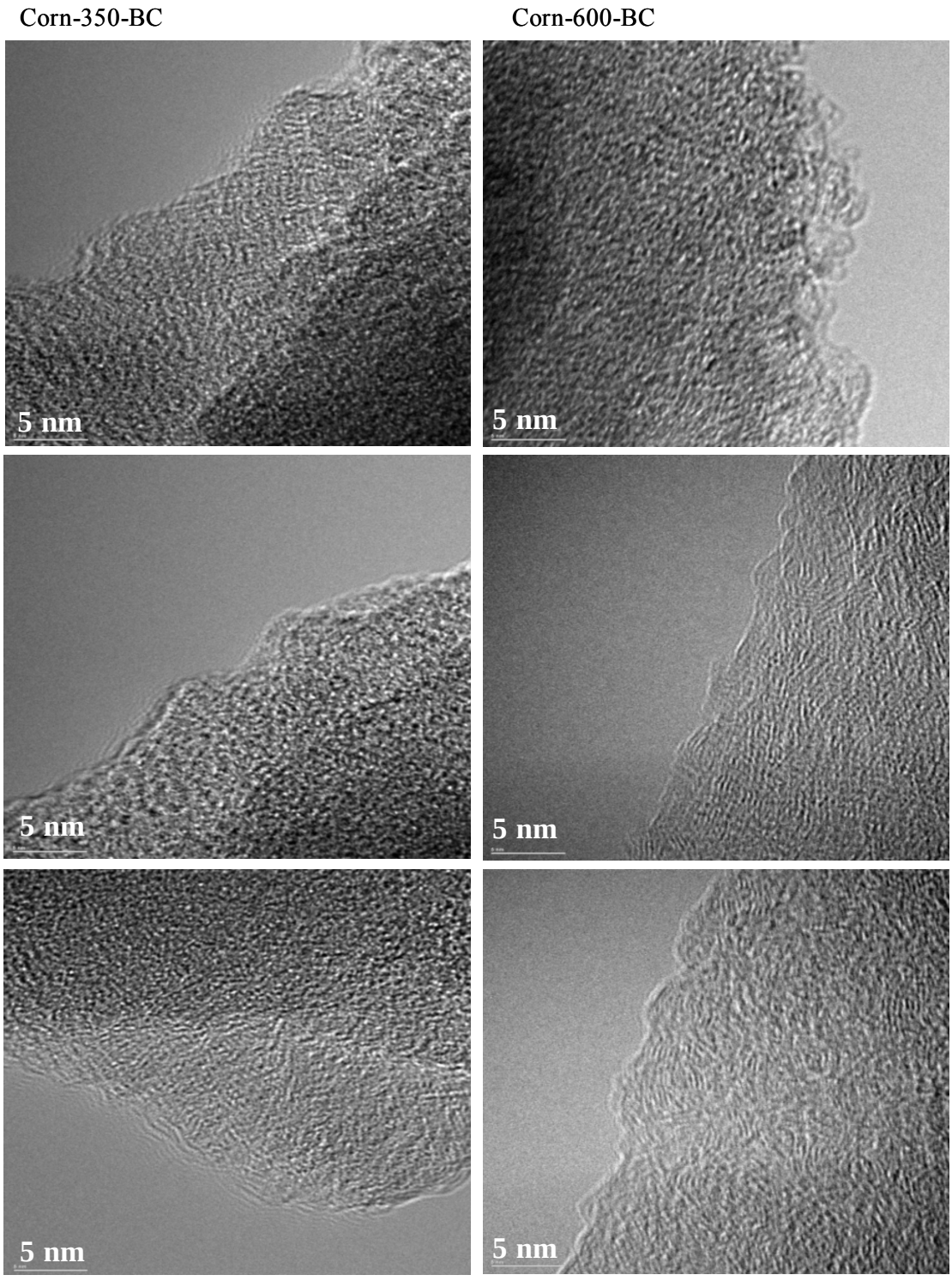

Appendix Figure IV.2b. TEM images of oak-BC formed at 350 and 600 °C

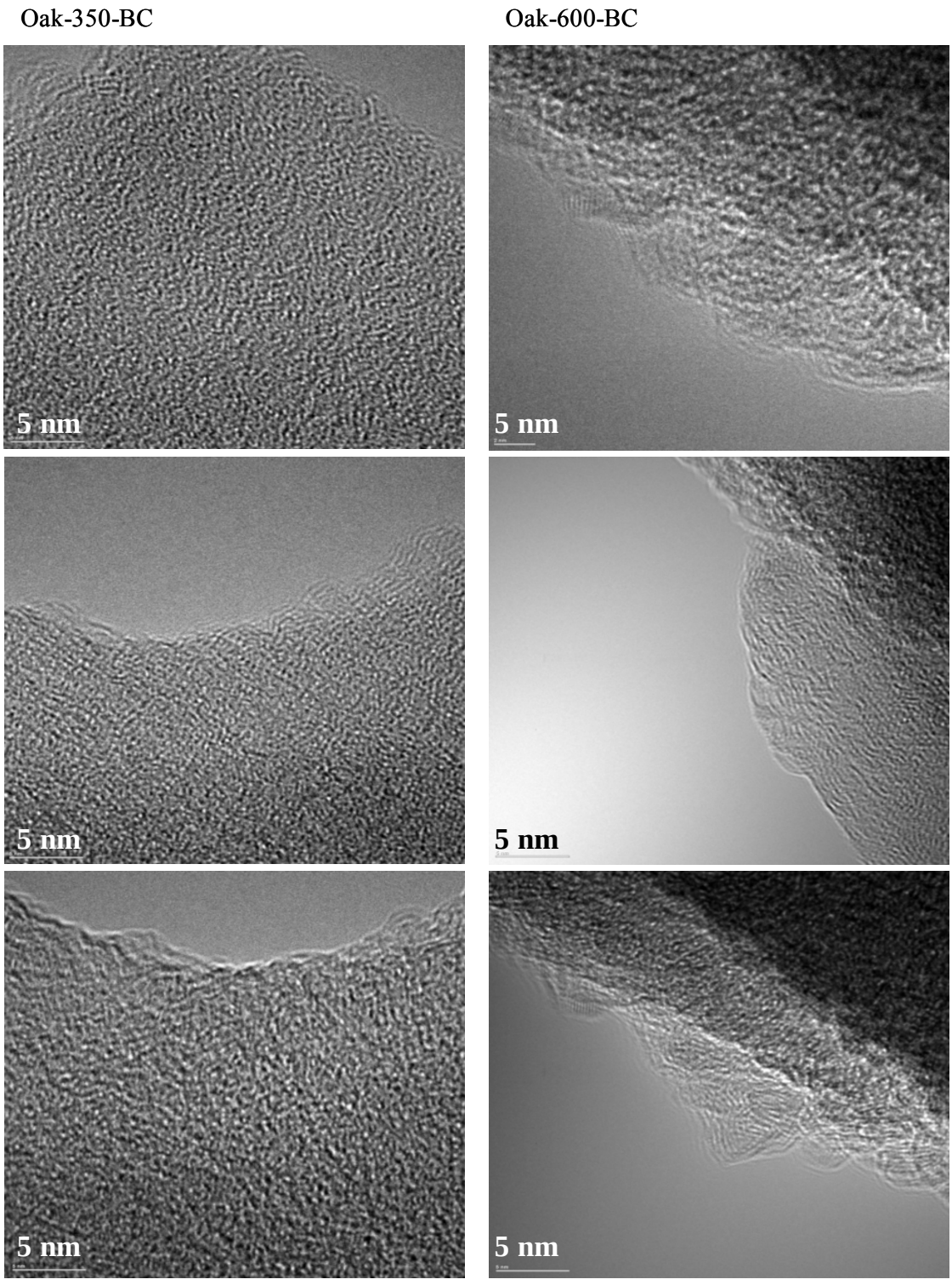

Appendix Table IV.1. Remaining C (%) of 24 cross combinations after 1-year incubation. Numbers attached by the same letter were not significantly different (means and standard deviation-SD, N=8).

Incubation Temp. (°C)	Corn residue				Oak wood			
	350°C		600°C		350°C		600°C	
	%	SD	%	SD	%	SD	%	SD
4	90.1^{cdef}	4.80	94.6^{abc}	7.61	96.7^{ab}	3.29	99.2^{a}	0.81
10	84.5^{ghijk}	2.95	93.5^{bcd}	5.76	96.4^{ab}	3.89	94.7^{abc}	2.92
20	85.0^{ghi}	6.83	82.6^{hijk}	4.67	89.0^{defg}	4.00	91.0^{cde}	6.30
30	80.1^{ijk}	4.99	82.6^{hijk}	1.77	86.2^{efjh}	5.94	92.5^{abc}	6.41
45	81.6^{hijk}	2.42	79.6^{k}	3.62	88.6^{defg}	7.50	85.8^{fgh}	6.32
60	79.8^{jk}	3.86	81.6^{hijk}	5.42	84.6^{ghij}	5.87	86.4^{efgh}	4.23

Appendix Table IV.2. ANOVA of remaining C

Source	DF	Sum of Squares	F ratio	Prob > F	
Incubation Temp.	5	1509	12.10	<.0001	*
Biomass type	1	1094	43.85	<.0001	*
Incubation Temp. * Biomass type	5	155	1.24	0.2915	ns
Charring Temp.	1	157	6.30	0.0130	*
Incubation Temp.*Charring Temp.	5	280	2.24	0.0522	ns
Biomass types*Charring Temp.	1	10	0.40	0.5286	ns
Incubation Temp.*Biomass type*Charring Temp.	5	297	2.38	0.0407	*
Error	168	4190			

Appendix Table IV.3. O/C ratios of 24 cross combinations after 1-year incubation. Numbers attached by the same letter were not significantly different (means and standard deviation –SD, N=8).

Incubation Temp. (°C)	Corn residue				Oak wood			
	350°C		600°C		350°C		600°C	
	O/C	SD	O/C	SD	O/C	SD	O/C	SD
4	0.40^{bcd}	0.07	0.19^{ijk}	0.06	0.25^{hi}	0.05	0.11^{l}	0.04
10	0.41^{bcd}	0.08	0.22^{ij}	0.05	0.25^{hi}	0.05	0.12^{l}	0.04
20	0.43^{bc}	0.03	0.23^{ij}	0.09	0.32^{efgh}	0.08	0.14^{kl}	0.03
30	0.48^{ab}	0.15	0.27^{fghi}	0.10	0.34^{defg}	0.07	0.16^{jkl}	0.08
45	0.48^{ab}	0.12	0.27^{fghi}	0.08	0.35^{def}	0.10	0.16^{jkl}	0.09
60	0.52^{a}	0.08	0.26^{ghi}	0.05	0.39^{cde}	0.10	0.17^{jkl}	0.05

Appendix Table IV.4. ANOVA of O/C ratios

Source	DF	Sum of Squares	F ratio	Prob > F	
Incubation Temp.	5	0.21	7.01	<.0001	*
Biomass type	1	0.44	73.34	<.0001	*
Incubation Temp. * Biomass type	5	0.01	0.28	0.924	ns
Charring Temp.	1	1.77	291.77	<.0001	*
Incubation Temp.*Charring Temp.	5	0.03	1.13	0.349	ns
Biomass types*Charring Temp.	1	0.02	2.60	0.109	ns
Incubation Temp.*Biomass type*Charring Temp.	5	0.01	0.19	0.966	ns
Error	168	1.02			

Appendix Table IV.5. CECp (mmole(+)kgC^{-1}) of 24 cross combinations after incubation. Numbers attached by the same letter were not significantly different (means and standard deviation-SD, N=8).

Incubation Temp. (°C)	Corn residue				Oak wood			
	350°C		600°C		350°C		600°C	
	CECp	SD	CECp	SD	CECp	SD	CECp	SD
4	656^{ef}	129	662^{ef}	181	265^{gh}	180	260^{gh}	159
10	957^{cd}	209	805^{de}	121	212^{gh}	92	187^{h}	85
20	990^{cd}	255	855^{cde}	248	298^{gh}	60	273^{gh}	94
30	1449^{b}	211	1109^{c}	269	416^{fgh}	176	287^{gh}	136
45	1618^{b}	401	1052^{cd}	162	925^{cd}	259	459^{fg}	155
60	2140^{a}	679	1023^{cd}	186	1462^{b}	580	451^{fg}	157

Appendix Table IV.6. ANOVA of CECp

Source	DF	Sum of Squares	F ratio	Prob > F	
Incubation Temp.	5	20713061	61.37	<.0001	*
Biomass type	1	11934931	176.80	<.0001	*
Incubation Temp. * Biomass type	5	833310	2.47	0.0346	*
Charring Temp.	1	5239188	77.61	<.0001	*
Incubation Temp.*Charring Temp.	5	6498700	19.25	<.0001	*
Biomass types*Charring Temp.	1	137499	2.04	0.1554	ns
Incubation Temp.*Biomass type*Charring Temp.	5	50034	0.15	0.9803	ns
Error	168	11340991			

Appendix Table IV.7. Full data of remaining C, O/C ratio and CECp of chapter 4

Replicate	Incubation Temp. (°C)	Biomass types	Charring T (°C)	Remaining C (%)	O/C ratio	CEC (mmole(+)/kgC^{-1})
1	4	Corn residue	350	90.7	0.38	634
			600	88.9	0.22	600
		Oak wood	350	101.1	0.20	519
			600	98.3	0.10	632
	10	Corn residue	350	88.1	0.34	1103
			600	98.0	0.16	947
		Oak wood	350	94.7	0.28	291
			600	95.3	0.11	322
	20	Corn residue	350	87.8	0.48	804
			600	79.3	0.17	479
		Oak wood	350	89.3	0.39	351
			600	88.6	0.18	302
	30	Corn residue	350	76.2	0.44	1571
			600	83.8	0.40	831
		Oak wood	350	79.9	0.33	342
			600	93.7	0.08	217
	45	Corn residue	350	84.9	0.59	1203
			600	83.3	0.23	786
		Oak wood	350	89.6	0.26	663
			600	81.5	0.15	240
	60	Corn residue	350	79.4	0.45	3146
			600	90.4	0.23	1133
		Oak wood	350	91.7	0.24	1165
			600	86.7	0.18	351

Appendix Table IV.7. (Continues)

Replicate	Incubation Temp. (°C)	Biomass types	Charring T (°C)	Remaining C (%)	O/C ratio	CEC (mmole(+)/kgC^{-1})
2	4	Corn residue	350	86.6	0.33	394
			600	95.0	0.24	513
		Oak wood	350	99.2	0.22	577
			600	99.7	0.09	270
	10	Corn residue	350	89.6	0.38	487
			600	88.7	0.27	728
		Oak wood	350	100.9	0.17	394
			600	97.8	0.10	290
	20	Corn residue	350	81.5	0.40	1296
			600	87.0	0.19	496
		Oak wood	350	83.6	0.37	327
			600	91.0	0.12	352
	30	Corn residue	350	85.7	0.44	1105
			600	81.9	0.33	734
		Oak wood	350	89.5	0.29	218
			600	97.4	0.15	177
	45	Corn residue	350	79.8	0.50	1305
			600	79.6	0.27	1018
		Oak wood	350	96.6	0.39	611
			600	77.3	0.33	308
	60	Corn residue	350	74.1	0.52	2103
			600	82.1	0.31	1247
		Oak wood	350	89.8	0.31	1181
			600	85.5	0.18	179

Appendix Table IV.7. (Continues)

Replicate	Incubation Temp. (°C)	Biomass types	Charring T (°C)	Remaining C (%)	O/C ratio	CEC (mmole(+)/kgC^{-1})
3	4	Corn residue	350	90.5	0.39	629
			600	98.7	0.17	549
		Oak wood	350	95.9	0.24	159
			600	99.3	0.07	198
	10	Corn residue	350	82.2	0.29	1017
			600	89.2	0.25	971
		Oak wood	350	95.9	0.24	207
			600	91.4	0.11	177
	20	Corn residue	350	94.3	0.44	533
			600	82.9	0.21	1104
		Oak wood	350	91.6	0.24	358
			600	93.9	0.11	188
	30	Corn residue	350	83.9	0.56	1179
			600	79.6	0.39	1435
		Oak wood	350	76.9	0.49	824
			600	85.1	0.17	520
	45	Corn residue	350	82.4	0.30	1251
			600	78.7	0.39	1181
		Oak wood	350	75.2	0.54	1204
			600	84.3	0.11	732
	60	Corn residue	350	82.8	0.68	2578
			600	77.9	0.23	1164
		Oak wood	350	82.3	0.39	2313
			600	86.6	0.17	622

Appendix Table IV.7. (Continues)

Replicate	Incubation Temp. (°C)	Biomass types	Charring T (°C)	Remaining C (%)	O/C ratio	CEC (mmole(+)/kgC^{-1})
4	4	Corn residue	350	86.1	0.41	854
			600	97.7	0.05	647
		Oak wood	350	91.2	0.35	238
			600	98.5	0.19	122
	10	Corn residue	350	80.8	0.46	991
			600	93.3	0.26	795
		Oak wood	350	93.8	0.27	232
			600	90.8	0.08	108
	20	Corn residue	350	86.2	0.44	1024
			600	87.4	0.15	1024
		Oak wood	350	95.0	0.31	308
			600	92.9	0.13	367
	30	Corn residue	350	73.8	0.74	1570
			600	81.6	0.23	1134
		Oak wood	350	94.7	0.29	371
			600	80.9	0.10	173
	45	Corn residue	350	83.4	0.41	2317
			600	84.3	0.20	1247
		Oak wood	350	79.3	0.39	1240
			600	85.7	0.20	583
	60	Corn residue	350	84.6	0.53	1877
			600	86.9	0.31	1011
		Oak wood	350	76.8	0.47	1307
			600	79.1	0.19	568

Appendix Table IV.7. (Continues)

Replicate	Incubation Temp. (°C)	Biomass types	Charring T (°C)	Remaining C (%)	O/C ratio	CEC (mmole(+)/kgC^{-1})
5	4	Corn residue	350	83.0	0.55	651
			600	85.6	0.25	940
		Oak wood	350	94.5	0.28	150
			600	100.0	0.14	144
	10	Corn residue	350	83.2	0.43	1189
			600	101.9	0.19	665
		Oak wood	350	98.2	0.22	144
			600	95.1	0.08	81
	20	Corn residue	350	81.9	0.41	1019
			600	76.1	0.16	1074
		Oak wood	350	85.2	0.22	222
			600	80.1	0.10	331
	30	Corn residue	350	74.0	0.53	1527
			600	81.9	0.15	1075
		Oak wood	350	86.8	0.31	362
			600	99.4	0.11	161
	45	Corn residue	350	76.9	0.68	1523
			600	82.3	0.24	913
		Oak wood	350	91.7	0.24	807
			600	93.4	0.17	442
	60	Corn residue	350	77.8	0.53	1387
			600	84.3	0.21	769
		Oak wood	350	88.1	0.31	987
			600	92.4	0.08	356

Appendix Table IV.7. (Continues)

Replicate	Incubation Temp. (°C)	Biomass types	Charring T (°C)	Remaining C (%)	O/C ratio	CEC (mmole(+)/kgC^{-1})
6	4	Corn residue	350	91.2	0.44	666
			600	108.2	0.21	652
		Oak wood	350	97.8	0.24	141
			600	99.5	0.09	231
	10	Corn residue	350	83.4	0.45	906
			600	99.3	0.17	713
		Oak wood	350	88.9	0.35	147
			600	99.4	0.13	220
	20	Corn residue	350	72.6	0.43	1239
			600	88.9	0.23	818
		Oak wood	350	88.3	0.30	352
			600	86.2	0.15	343
	30	Corn residue	350	83.6	0.21	1534
			600	84.4	0.24	1482
		Oak wood	350	82.5	0.38	394
			600	93.1	0.12	240
	45	Corn residue	350	81.5	0.39	2062
			600	76.5	0.24	999
		Oak wood	350	89.9	0.29	870
			600	96.8	0.16	409
	60	Corn residue	350	83.5	0.51	1283
			600	74.6	0.21	723
		Oak wood	350	89.5	0.39	854
			600	82.8	0.12	381

Appendix Table IV.7. (Continues)

Replicate	Incubation Temp. (°C)	Biomass types	Charring T (°C)	Remaining C (%)	O/C ratio	CEC (mmole(+)/kgC^{-1})
7	4	Corn residue	350	98.2	0.31	727
			600	96.9	0.22	463
		Oak wood	350	94.6	0.27	209
			600	98.0	0.14	222
	10	Corn residue	350	83.8	0.53	1017
			600	92.3	0.19	712
		Oak wood	350	98.6	0.23	136
			600	94.3	0.19	166
	20	Corn residue	350	92.3	0.37	840
			600	80.2	0.39	993
		Oak wood	350	92.9	0.29	218
			600	101.6	0.13	165
	30	Corn residue	350	84.8	0.40	1384
			600	85.1	0.15	950
		Oak wood	350	89.9	0.27	417
			600	92.8	0.27	408
	45	Corn residue	350	81.2	0.46	1747
			600	73.4	0.22	1239
		Oak wood	350	92.3	0.33	1223
			600	83.7	0.09	514
	60	Corn residue	350	80.9	0.42	1852
			600	80.1	0.28	1054
		Oak wood	350	78.1	0.52	1509
			600	91.0	0.15	586

Appendix Table IV.7. (Continues)

Replicate	Incubation Temp. (°C)	Biomass types	Charring T (°C)	Remaining C (%)	O/C ratio	CEC (mmole(+)/kgC^{-1})
8	4	Corn residue	350	94.1	0.42	691
			600	86.0	0.21	932
		Oak wood	350	99.7	0.19	124
			600	100.2	0.09	261
	10	Corn residue	350	84.5	0.39	947
			600	85.4	0.29	913
		Oak wood	350	99.9	0.22	148
			600	93.8	0.15	133
	20	Corn residue	350	83.2	0.46	1167
			600	79.0	0.35	847
		Oak wood	350	85.8	0.47	247
			600	93.5	0.18	134
	30	Corn residue	350	78.7	0.50	1719
			600	82.4	0.28	1232
		Oak wood	350	89.1	0.35	404
			600	97.5	0.31	402
	45	Corn residue	350	82.6	0.49	1534
			600	78.8	0.39	1029
		Oak wood	350	94.5	0.33	779
			600	83.8	0.05	440
	60	Corn residue	350	75.2	0.52	2892
			600	76.4	0.32	1085
		Oak wood	350	80.2	0.53	2380
			600	86.8	0.26	567